

University of Massachusetts Amherst

ScholarWorks@UMass Amherst

Doctoral Dissertations 1896 - February 2014

1-1-1987

Processing and properties of composite fibers of poly(p-phenylene benzobisthiazole) and poly(ether ether ketone) or nylon 6,6/

Carmen A. Gabriel

University of Massachusetts Amherst

Follow this and additional works at: https://scholarworks.umass.edu/dissertations_1

Recommended Citation

Gabriel, Carmen A., "Processing and properties of composite fibers of poly(p-phenylene benzobisthiazole) and poly(ether ether ketone) or nylon 6,6/" (1987). *Doctoral Dissertations 1896 - February 2014*. 724.
<https://doi.org/10.7275/axsj-by28> https://scholarworks.umass.edu/dissertations_1/724

This Open Access Dissertation is brought to you for free and open access by ScholarWorks@UMass Amherst. It has been accepted for inclusion in Doctoral Dissertations 1896 - February 2014 by an authorized administrator of ScholarWorks@UMass Amherst. For more information, please contact scholarworks@library.umass.edu.

UMASS/AMHERST



312066007782562

PROCESSING AND PROPERTIES OF COMPOSITE FIBERS OF
POLY(P-PHENYLENE BENZOBISTHIAZOLE)
AND POLY(ETHER ETHER KETONE) OR NYLON 6,6

A Dissertation Presented

by

CARMEN A. GABRIEL

Submitted to the Graduate School of the
University of Massachusetts in partial fulfillment
of the requirements for the degree of

DOCTOR OF PHILOSOPHY

September 1987

Polymer Science and Engineering

© Carmen Anoish Gabriel September 1987

All Rights Reserved

AFWAL/MLBP
Contract No.
F-33615-83-K-5001

DuPont Thermoplastic Molecular
Composite Development

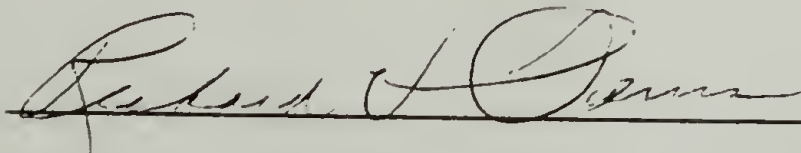
PROCESSING AND PROPERTIES OF COMPOSITE FIBERS OF
POLY(P-PHENYLENE BENZOBISTHIAZOLE)
AND POLY(ETHER ETHER KETONE) OR NYLON 6,6

A Dissertation Presented

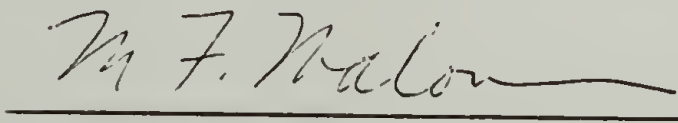
by

CARMEN A. GABRIEL

Approved as to style and content by:



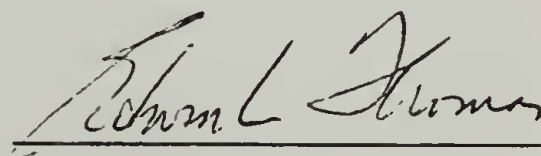
Richard J. Farris, Co-chairman of Committee



Michael F. Malone, Co-chairman of Committee



Henning H. Winter, Member



Edwin L. Thomas, Department Head
Polymer Science and Engineering

To my parents, who have
been a constant source of
encouragement and support.

ACKNOWLEDGEMENTS

I would like to thank my co-advisors, Professors Richard J. Farris and Michael F. Malone for their assistance, advice, and guidance during the course of this research. I am very grateful to both of them for their continued support, and feel that I could not have been more fortunate in my choice of advisors. I would also like to thank Professor H. Henning Winter for serving on my committee, and Professor Mosha Gottlieb for acting as an interim committee member during my data defense.

I am grateful to the students and staff of the Polymer Science Department. Special thanks to Menas Vratsanos and Sam Thomson for their friendship and for many helpful discussion and suggestions. I would also like to thank Robin Hwang, Susan Wickliffe, Olimpia Federico, Ravi Saraf, and Steve DeTeresa, and am grateful to Pat Pierce for determining the intrinsic viscosity. I am very grateful to Brian Devlin for his support, encouragement, and graphic artist expertise during the course of this work and preparation of this document.

I would like to thank the Air Force Wright Aeronautical Laboratories, Materials Laboratory and E. I. DuPont Co., Textile Fibers Department for financial support during the course of this work. I am grateful to Dr. Charles Lee, Dr.

fibers. This is attributed to the fact that methanesulfonic acid, MSA, is a much better solvent for N66 than for PEEK or PPBT; as a result, PPBT will form a fibrillar, network structure during coagulation. The matrix may hinder the formation of a connected structure of this network phase if it solidifies on the same time scale as the PPBT; this is the case with PEEK for higher concentration composite solutions. Sufficient PPBT is required to form microfibrillar domains that span the composite sample, whereupon a continuous phase of PPBT effectively reinforces the composites.

In general, the relative solubilities of solution spun polymer pairs directly effects the tensile properties and morphology of the coagulated product. If one of the polymers has a much lower solubility, it will coagulate first and form its preferred structure which for PPBT is a fibrillar network. If the solubility of the two polymers is similar, the presence of the second polymer may hinder the formation of the preferred structure.

The fibrillar network of PPBT in N66/PPBT and PEEK/PPBT fibers can be perfected by post-processing, i.e., wet-stretching and heat-treatment. The best properties for 50/50 PEEK/PPBT and N66/PPBT are moduli of 44.2 and 49.5 GPa and strengths of 410 and 450 MPa, respectively.

TABLE OF CONTENTS

ACKNOWLEDGEMENTS	v
ABSTRACT	vii
LIST OF TABLES	xii
LIST OF FIGURES	xiii

Chapter

1.	Thesis Overview	1
1.1	Introduction	1
1.2	Properties of Rigid Rod Polymers	2
1.3	Phase Behavior of Rigid Rod Polymers in Solution	6
1.4	Molecular Composites	11
	1.4.1 Processing	13
	1.4.2 Properties	17
1.5	Dissertation Problem	26
1.6	Organization of the Thesis	27
2.	Solution Behavior	29
2.1	Introduction	29
2.2	Materials and Sample Preparation	30
2.3	Solubilities of N66, PEEK, and PPBT	32
2.4	Phase Behavior	37
2.5	Solution Rheology	39
	2.5.1 Results	39
	2.5.2 Discussion	46
2.6	Summary	54
3.	Solution Processing and Fiber Property Relationships	56
3.1	Introduction	56
3.2	Experimental	56

3.2.1	Fiber Spinning.....	56
3.2.2	Post-processing.....	59
3.2.3	Fiber Testing and Experimental Methods.....	60
3.3	Fibers Spun from Isotropic Solutions Close to the Critical Concentration.....	60
3.3.1	Tensile Properties.....	61
3.3.2	Microscopy.....	64
3.3.3	Discussion.....	67
3.4	The Effect of Solution Concentration.....	69
3.4.1	PEEK/PPBT30 Composite Fibers.....	69
3.4.2	N66/PPBT30 Composite Fiber.....	74
3.5	Summary.....	78
4.	PPBT Network Structure.....	80
4.1	Introduction.....	80
4.2	Background.....	80
4.3	Experimental Methods.....	81
4.4	PEEK/PPBT Fiber Spun from 2.0% Solutions.....	82
4.4.1	Results.....	82
4.4.2	Discussion.....	84
4.5	The Effect of PPBT Composition.....	90
4.6	Thermal Characterization.....	95
4.6.1	Differential Scanning Calorimetry....	95
4.6.2	Thermal Mechanical Analysis.....	97
4.6.3	Thermal Removal of the Matrix.....	100
4.7	Fiber Wet Strength.....	101
4.7.1	Results.....	101
4.7.2	Discussion.....	103
4.8	Post-Processing.....	106
4.8.1	Results.....	106
4.8.2	Discussion.....	108
4.9	Summary.....	111

5.	Conclusion and Suggestions for Future Work.....	116
	REFERENCES.....	119
	APPENDIX A	128
	APPENDIX B	130
	BIBLIOGRAPHY.....	139

LIST OF TABLES

Table 1.1	
Articulated Molecular Composite Matrix Polymer.....	14
Table 1.2	
Summary of Molecular Composite Tensile Properties.....	20
Table 2.1	
Maxwell Model Parameters Describing the η^* for PEEK/PPBT and N66/PPBT Composite and 2.0% PPBT Solutions.....	53
Table 3.1	
Concentration of PEEK/PPBT36 Spinning Solutions.....	63
Table 4.1	
Mechanical Properties of 75/25 PEEK/PPBT Heat Treated at 265°C and 425°C.....	89
Table 4.2	
Mechanical Properties of As Spun and Extended Heat-treatment 50/50 N66/PPBT36 Fiber.....	102
Table 4.3	
Tensile Properties of 70/30 PEEK/Graphite and N66/Glass Chopped Fiber Composites.....	112

LIST OF FIGURES

1.1	Specific modulus vs. specific strength for various materials.....	3
1.2	(a) Schematic of rigid rod particle of length x and aligned at an angle of τ . (b) Schematic of idealized rigid rod particle for the lattice model.....	8
1.3	Schematic phase diagram predicted using lattice model. ⁽²⁷⁾ An equilibrium two phase solution of an isotropic, I, and a liquid crystalline, LC, phase is predicted to exist in the chimney region.....	9
1.4	Schematic of phase diagram predicted for a ternary system of solvent (1), rigid rod (2), and flexible coil (3). Above the critical concentration, an isotropic phase, I, is predicted to be in equilibrium with a liquid crystalline phase, LC.....	12
2.1	Illustration of fiber coagulation during the spinning process, depicting the concentration of MSA in the coagulating fiber (dashed line) and the solidification or coagulation line (solid line).....	35
2.2	Solution concentrations of experimentally observed to be isotropic (x) and anisotropic (●) for PEEK/PPBT36/MSA solutions. The solid line represents the prediction ^(47e) for $x_2 = 300$ and $x_3 = 30$	38
2.3	Schematic of experimental set-up for measurement of the rheological solution properties.....	41
2.4	Complex viscosity vs. frequency for 1.0% (O) , 2.0% (●), 3.0% (Δ), and 4.0% (\blacktriangle) 75/25 PEEK/PPBT30 and 2.0% PPBT30 (\square) solutions.....	43
2.5	Tan delta vs. frequency for 1.0% (o), 2.0% (●), 3.0% (Δ), and 4.0% (\blacktriangle) 75/25 PEEK/PPBT30 and 2.0% PPBT30 (\square) solutions.....	44

2.6	Complex viscosity vs. frequency for 1.0% (○), 2.0% (●), 3.0% (Δ), and 4.0% (▲) 75/25 N66/PPBT30 and 2.0% PPBT30 (□) solutions.....	45
2.7	Tan delta vs. frequency for 1.0% (○), 2.0% (●), 3.0% (Δ), and 4.0% (▲) 75/25 N66/PPBT30 and 2.0% PPBT30 (□) solutions.....	47
3.1	Photograph of the fiber spinning apparatus.....	58
3.2	Tensile properties for as-spun (○) and hot-drawn (●) PEEK/PPBT30 fibers, spun close to the critical concentration, (a) modulus, (b) strength. Error bars represent the standard deviation from the average calculated from at least five samples, which appears only if greater than the symbol size.....	62
3.3	Scanning electron micrographs of an (a) as-spun and (b) hot-drawn 70/30 PEEK/PPBT36 fiber spun close to the critical concentration.....	65
3.4	Scanning electron micrographs of an (a) as-spun and (b) hot-drawn PEEK fiber spun from a 4.0% solution.....	66
3.5	Optical micrograph of an as-spun 90/10 PEEK/PPBT36 fiber spun close to the critical concentration, immediately after H ₂ SO ₄ was added.....	68
3.6	Tensile properties for as-spun 75/25 PEEK/PPBT30 fiber vs. the total polymer concentration in the spinning solution, (a) modulus, (b) strength. Error bars represent the standard deviation from the average calculated from at least five samples, which appears only if greater than the symbol size.....	70
3.7	Fiber diameter for as-spun 75/25 PEEK/PPBT30 (□) and as-spun N66/PPBT30 (◇) fiber vs. the concentration of solution. The solid line represents the calculated fiber diameter.....	71
3.8	Scanning electron micrographs of as-spun 75/25 PEEK/PPBT30 fibers spun from (a) 1.0% solution, (b) 2.0% solution, (c) 2.5% solution, (d) 3.0% solution, (e) 4.0% solution.....	73

3.9	Tensile properties for as-spun 75/25 N66/PPBT30 fiber vs. the total polymer concentration in the spinning solution, (a) modulus, (b) strength. Error bars represent the standard deviation from the average calculated from at least five samples, which appears only if greater than the symbol size.....	75
3.10	Scanning electron micrographs of as-spun 75/25 N66/PPBT30 fibers spun from (a) 1.0% solution, (b) 2.0% solution, (c) 3.0% solution, (d) 3.7% solution, (e) 4.0% solution.....	77
4.1	Tensile properties for PEEK/PPBT30 fibers, as-spun (O) and heat treated (●) at 425°C with no tension , spun from 2.0% solution in MSA, (a) modulus, (b) strength. Error bars represent the standard deviation from the average calculated from at least five samples, which appears only if greater than the symbol size.....	83
4.2	Optical micrograph of an (a) as-spun and (b) heat treated at 425°C 90/10 PEEK/PPBT30 fiber spun from a 2.0% concentration solution after being soaked in H ₂ SO ₄ for over four weeks.....	85
4.3	Tensile strain at break for PEEK/PPBT30 fibers, as-spun (O) and heat-treated (●) at 425°C with no tension, spun from a 2.0% solution in MSA. Error bars represent the standard deviation from the average calculated from at least five samples, which appears only if greater than the symbol size.....	87
4.4	Tensile properties for as-spun 75/25 (O), 50/50 (●), 25/75 (Δ) PEEK/PPBT30 fibers vs. the total polymer concentration, (a) modulus, (b) strength. Error bars represent the standard deviation from the average calculated from at least five samples, which appears only if greater than the symbol size.....	92
4.5	Optical micrographs of a single as-spun 75/25 PEEK/PPBT fiber soaked in H ₂ SO ₄ for several weeks (a) spun from a 1.0% solution, (b) spun from a 2.0% solution, (c) spun from a 3.0% solution, (d) spun from a 4.0% solution.....	93

4.6	DSC scans for as-spun 75/25 PEEK/PPBT30 spun from 2.0%, 3.0%, and 4.0% solutions in MSA and for as-spun PEEK fiber spun from a 3.0% solution.....	96
4.7	DSC scans for as-spun first run, AS, as-spun second run, AS2, and heat-treated, HT, at 425°C, 90/10 PEEK/PPBT30 fiber.....	98
4.8	TMA curves for an as-spun fiber of (a) PPBT30 spun from 2.0% solution, (b) 75/25 PEEK/PPBT30 spun from a 2.0% solution.....	99
4.9	Ratio of the dry to wet breaking force for N66/PPBT30 (●) and PEEK/PPBT30 (O) fibers spun from 2.0% solution.....	104
4.10	Tensile properties for as-spun PEEK/PPBT30 (O) and N66/PPBT30 (●) fibers vs. the wt% of PPBT, a) modulus , b) strength. Error bars represent the standard deviation from the average calculated from at least five samples, which appears only if greater than the symbol size.....	107
4.11	Tensile properties for heat-treated PEEK/PPBT30 (O) and N66/PPBT30 (●) fibers vs. the wt% for PPBT, a) modulus, b) strength. Error bars represent the standard deviation from the average calculated from at least five samples, which appears only if greater than the symbol size.....	109
4.12	Typical stress-strain curve for as-spun and heat-treated (a) 90/10 and (b) 50/50 PEEK/PPBT fibers.....	110
4.13	Dependence of composite morphology for ternary solution of flexible coil/rigid rod/solvent on the tc, time for coagulation, tps, time for phase separation, Sm, solubility of the matrix, Sr, solubility of the rigid rod.....	113

CHAPTER 1

THESIS OVERVIEW

1.1 Introduction

Polymer composites are replacing conventionally used materials, such as metals, in many applications. There are several reasons for the rapid increase in applications for polymer composites. For example, the specific strength of polymer composites is often superior to metals, and polymers do not have the corrosion problems associated with many metals. A large complex polymer part may be molded in one piece while a similar metal part often has to be machined piecewise and then assembled. This advantage of "part consolidation" makes processing of polymer composites economically attractive.⁽¹⁾

There is a significant amount of research focused on improving the performance of polymer composites.^(2,3) In general, the composite modulus and strength are improved as the aspect ratio of the reinforcement is increased. An innovative approach for preparing a composite with a high reinforcing aspect ratio is the molecular composite concept.⁽⁴⁻⁷⁾ The premise is to maximize the advantages of the rigid architecture of rod-like molecules by dispersing them throughout a flexible polymer matrix on a *molecular*

level. A molecular composite would be expected to have excellent mechanical properties in comparison to conventional chopped fiber composites, to have good adhesion between the reinforcement and matrix, and to be amenable to melt processing, if the matrix is a thermoplastic.

This dissertation addresses the processing/structure/property relationships for "molecular composite" fibers. The thermoplastic matrices of poly(ether ether ketone) or Nylon 6,6 have been reinforced with rod-like poly(p-phenylene benzobisthiazole). Before discussing the dissertation problem in Section 1.5, some of the relevant research on rigid rod polymers and molecular composites is reviewed.

1.2 Properties of Rigid Rod Polymers

Ultra high modulus/high strength organic fibers^(8,9) have revolutionized the type of materials used for structural applications. These fibers are twice as strong and an order of magnitude stiffer than earlier synthetic fibers such as high strength nylon which has a tensile modulus of 6 GPa and tensile strength of 1.0 GPa.^(8,9) In general, the tensile properties of these ultra high strength/high modulus organic fibers are superior to those of conventional structural materials. Their specific tensile properties are even better; offering substantial weight savings. (Figure 1.1) Since these materials are costly, they are well-suited for

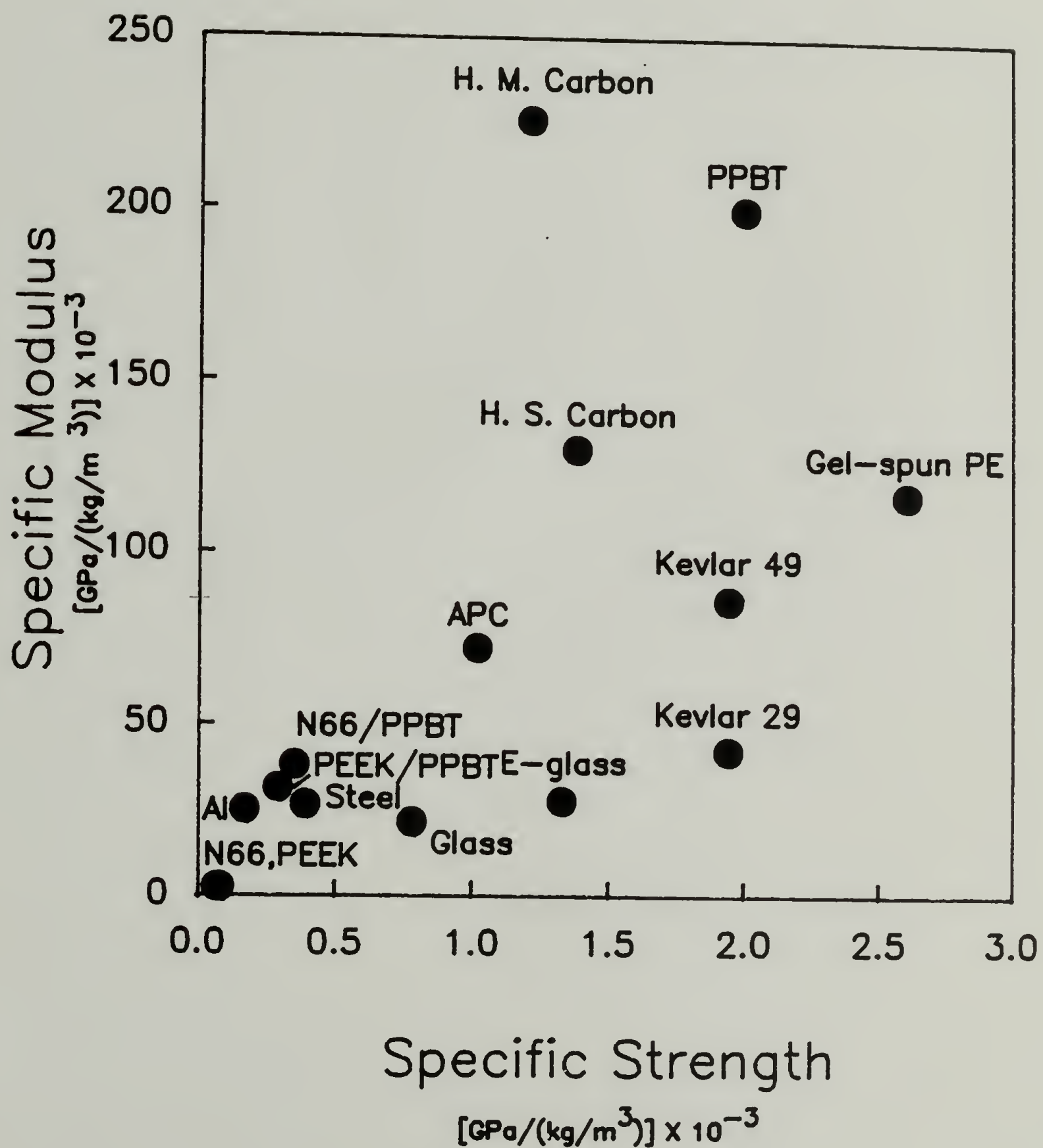


Figure 1.1 Specific modulus vs. specific strength for various materials.

transportation applications, where weight savings is at a premium.

The ultra high modulus/high strength organic fibers can be classified into three categories; flexible chain polymers processed to induce highly oriented extended chain morphology, carbon fibers prepared from polymeric or pitch precursors, and polymeric materials having a rigid molecular structure and a high persistence length.

Flexible chain polymers, primarily polyethylene, have been processed to induce an extended chain conformation. The processing techniques include gel spinning⁽¹⁰⁾, solid state extrusion⁽¹¹⁾ and solid state drawing.⁽¹²⁾ The enhanced properties of the extended flexible chain polymers are of great scientific interest. However, these materials are costly and limited to low temperature use, since polyethylene has a low melting point (about 140°C).⁽⁸⁾

Carbon fibers⁽¹³⁾ have the highest strength (3.1 GPa for Hercules Magnamite AS) and modulus (680 GPa for Union Carbide type P) of the organic fibers. Commercial fibers are prepared from polyacrylonitrile, cellulosic, or pitch precursors by pyrolysis and a high temperature heat treatment (up to 3000°C). These fibers exhibit excellent high temperature stability, but the extensive heat treatment processes significantly increases their price. Also, these fibers are electrically conductive which is not always a desirable property and restricts their usage.

The third class of ultra high modulus/high strength materials are polymers having a rigid, rod-like molecular structure. This molecular architecture insures an extended chain conformation such that these materials exhibit excellent tensile properties. Their elongated molecular shape favors the formation of an ordered liquid crystalline phase that can be processed to give excellent orientation of the molecules in the end product. These liquid crystals are categorized as lyotropic or thermotropic if the mesogenic phase is induced by changing the solution concentration or temperature, respectively.

In general, lyotropic polymers are very thermally stable. In fact, these materials degrade before exhibiting any thermal transitions.⁽⁸⁾ Therefore, thermal processing is prohibited, and lyotropic liquid crystalline polymers must be processed from solution. Strong solvents are required to dissolve the rigid rod molecules, commonly a strong acid. The phase behavior of rigid rods in solution is discussed in section 1.3. DuPont's Kevlar[®]⁽¹⁴⁾, poly(p-phenylene terephthalamide), is a lyotropic polymer of significant commercial importance.^(8,15) The U. S. Air Force^(16,17) has also developed a class of aromatic polymers having excellent tensile properties.

Several thermotropic polymers have been developed and investigated.^(18,19,20) These materials are of commercial interest because they are melt processable, which is more

cost effective than solution processing. To achieve high modulus and strength, however, an extensive heat treatment process is typically required.

1.3 Phase Behavior of Rigid Rod Polymers in Solution

Before reviewing the molecular composite research, it is important to understand the phase behavior of the ternary solution of rigid rod, flexible coil, and solvent, since fibers are spun from such solutions. Since the theory for the ternary system is a modification of the theory for the solution of rigid rod particles, it is essential to understand the phase behavior of rod-like particles in solution.

Molecules having an elongated, stiff architecture tend to form a liquid crystalline phase. The term "liquid crystal" aptly describes this state of matter that has no long range translational order, like a liquid, but which does have long range orientational order, like a crystalline solid. Cellulose,⁽²¹⁾ poly(benzylglutamate),⁽²²⁾ poly(benzamide),⁽²³⁾ PPTA,⁽¹⁴⁾ PPBT,⁽²⁴⁾ and poly(p-phenylene benzobisoxazole)⁽²⁵⁾ are examples of lyotropic polymers. These materials have very high persistence lengths and act as rigid rods in solution.

The phase behavior of rigid rod molecules was described theoretically by Onsager⁽²⁶⁾ and later by Flory⁽²⁷⁾. More recent work on theories for lyotropic systems is reviewed by Grosber and Khokhlov⁽²⁸⁾ and by Odijk⁽²⁹⁾. In Flory's

theory⁽²⁷⁾, the solute molecule is characterized by the length to diameter ratio or aspect ratio, x , that has an orientation angle of θ on a lattice as shown in Figure 1.2a. The polymer is approximated by a set of y submolecules where $y = x \sin\theta$; see Figure 1.2b. The parameter y can be thought of as a "disorder index" which is indicative of the mean orientation of the rods in solution. The limiting values for y are defined as x (complete disorder y and the solution is isotropic) and 1 (perfect order and the solution is highly anisotropic).

The equilibrium phase behavior of the lattice model is a standard calculation. The number of possible configurations for placing the rod-like molecule on a lattice is determined, and the partition function is found. The chemical potential of the anisotropic and isotropic phases can then be evaluated. Setting the chemical potentials of the two phases equal determines the equilibrium phase behavior of the solution, in terms of the aspect ratio, x , of the rigid rod and the volume fraction of rigid rod in solution. A typical phase diagram predicted from this model is shown in Figure 1.3. The critical concentration is the concentration above which the solution is no longer a single isotropic phase, but a biphasic, anisotropic/isotropic solution. At large x , the critical volume fraction approaches $8/x$.

The experimentally observed phase behavior of rod-like molecules in solutions has been found to agree qualitatively

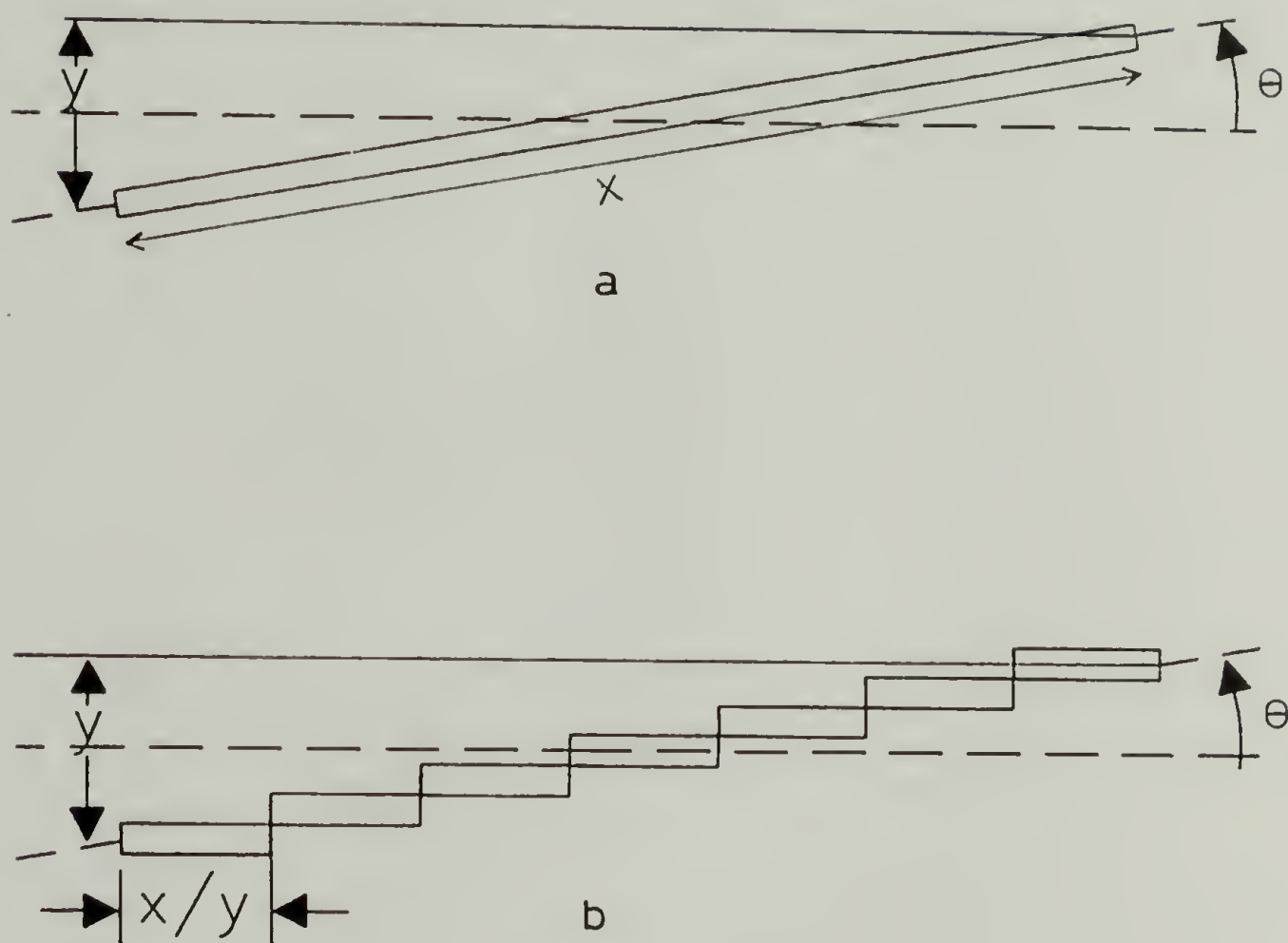


Figure 1.2 (a) Schematic of rigid rod particle of length x and aligned at an angle of θ . (b) Schematic of idealized rigid rod particle for the lattice model.

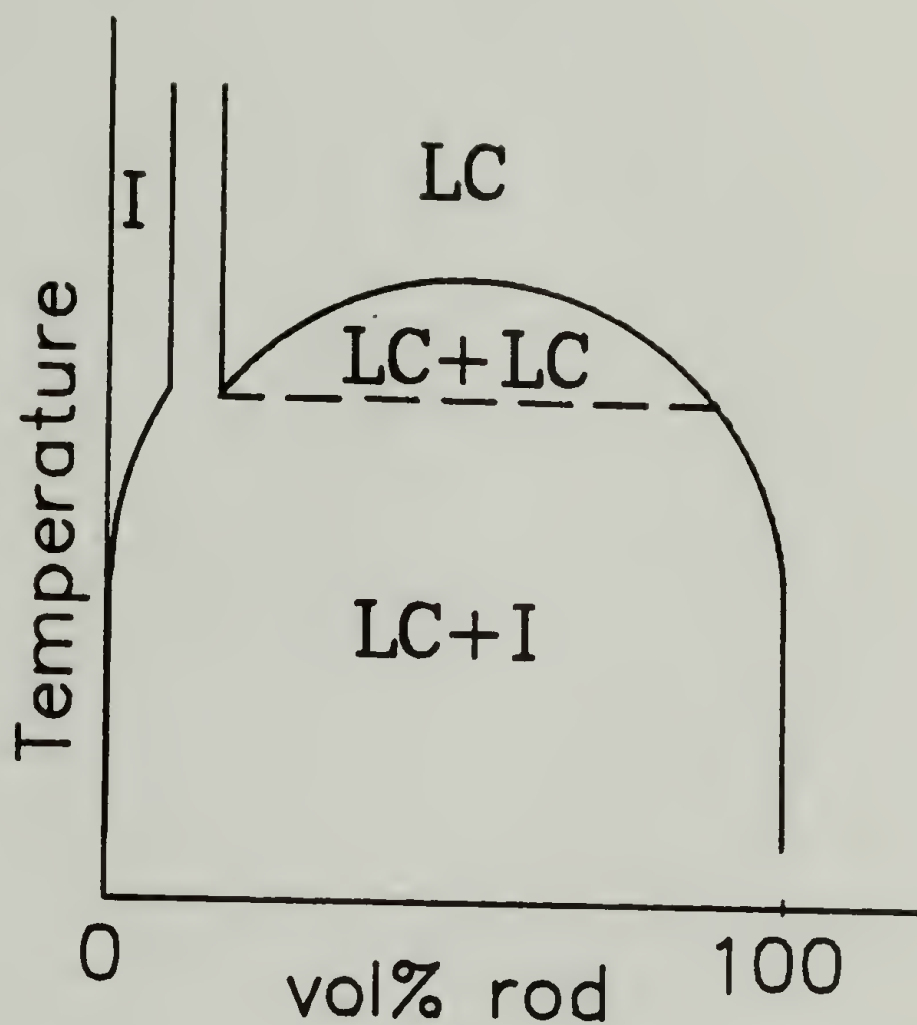


Figure 1.3 Schematic phase diagram predicted using lattice model.⁽²⁷⁾ An equilibrium two phase solution of an isotropic, I, and a liquid crystalline, LC, phase is predicted to exist in the chimney region.

with Flory's predicted phase diagram. (14,28) Of course, since Flory's theory is based on a lattice model, only qualitative agreement would be expected since this model is not exact, even for the case $x \gg 1$.

The phase behavior for PPBT has been thoroughly investigated using optical microscopy and viscometeric methods. (30,31,32,33,34) The phase diagram exhibits a narrow biphasic region, which shifts to higher polymer concentrations with increasing temperature. (30)

Several modifications of the theory for a solution of rigid rod particles have been made. (35a-e) The phase behavior of a ternary solution of solvent(1), rigid rod(2), and flexible coil(3) was treated by Flory. (35e) It is this type of ternary solution from which "molecular composites" are prepared. This theory will, therefore, be reviewed.

The rigid rod component, with an aspect ratio of x_2 , is modeled as shown in Figure 1.2. The aspect ratio for the flexible coil polymer is estimated from the contour length divided by the molecular diameter. The calculation follows the same procedure described for rigid rods in solution. (27)

The theory predicts the existence of an anisotropic nematic liquid crystalline phase that coexists with an isotropic phase. There is almost complete exclusion of the flexible coil polymer from the anisotropic phase, but the flexible coil polymer is more tolerant of the rigid rod polymer in the isotropic phase. A schematic phase diagram

is shown in Figure 1.4. The phase behavior for ternary systems has been found to be in qualitative agreement with the theory. (36,37,38) To predict realistic critical concentrations, however, the aspect ratio, x_3 , of the flexible coil polymer must often be used as an adjustable fitting parameter. (37)

1.4 Molecular Composites

Currently, the major use of the synthetic high modulus fibers is for reinforcing composites. Adhesion problems at the fiber/matrix interface and stress concentrations at discontinuities, such as the fiber ends, limit the strength and stiffness of these composites. Improving adhesion at the interface is an active area of research. (39) The "molecular composite" concept is a promising approach for improving the composite properties. The idealized molecular composite is imagined as a mixture of rigid rod molecules, randomly dispersed throughout a flexible coil polymer matrix. Chemical similarity and increased interfacial area are expected to provide good adhesion and minimize stress concentrations.

The U. S. Air Force has been involved in a research program on aromatic heterocyclic polymers, (16) that has more recently included studies of molecular composites, (4) It was proposed that by using materials of similar molecular composition problems with adhesion and thermal expansion

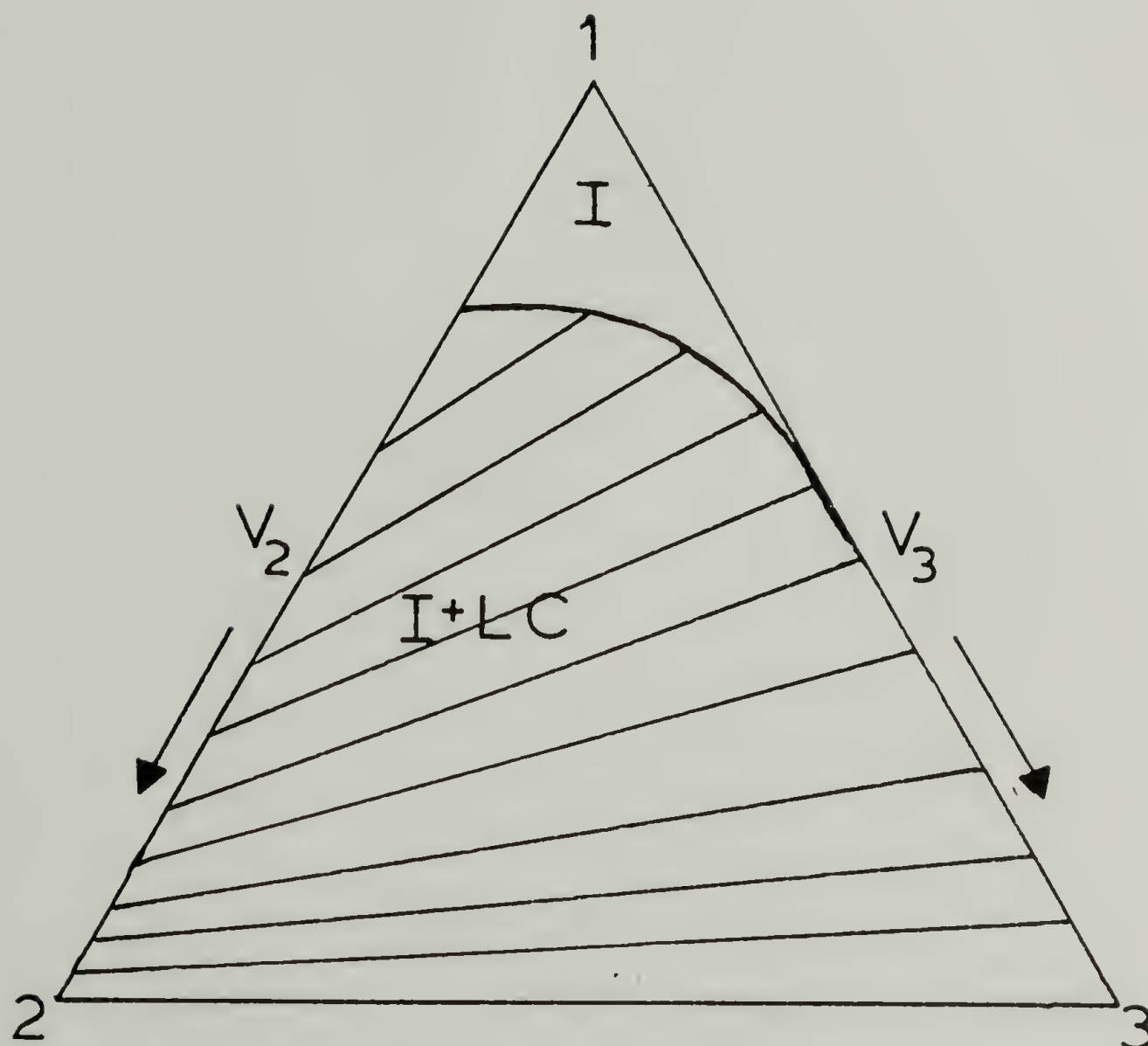
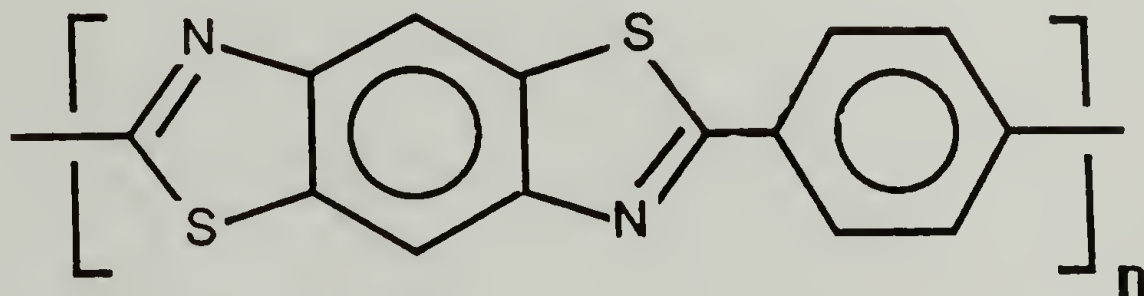


Figure 1.4 Schematic of phase diagram predicted for a ternary system of solvent (1), rigid rod (2), and flexible coil (3). Above the critical concentration, an isotropic phase, I, is predicted to be in equilibrium with a liquid crystalline phase, LC.

present in fiber reinforced composites could be eliminated. Therefore, the articulated polymers in Table 1.1 having similar chemical structure to rigid rod polymer, PPBT which has the structure

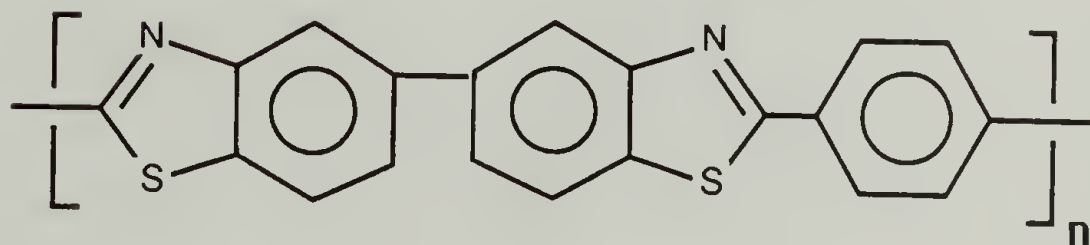
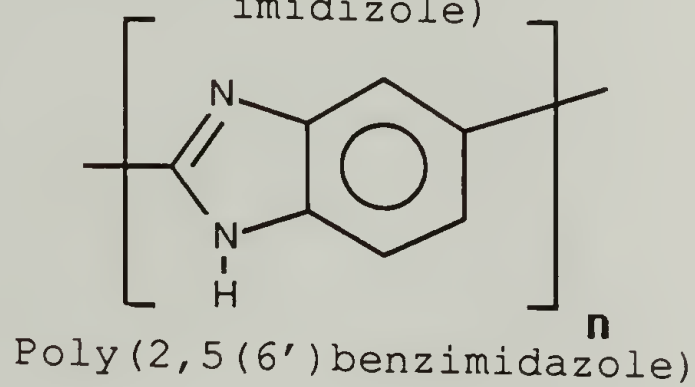
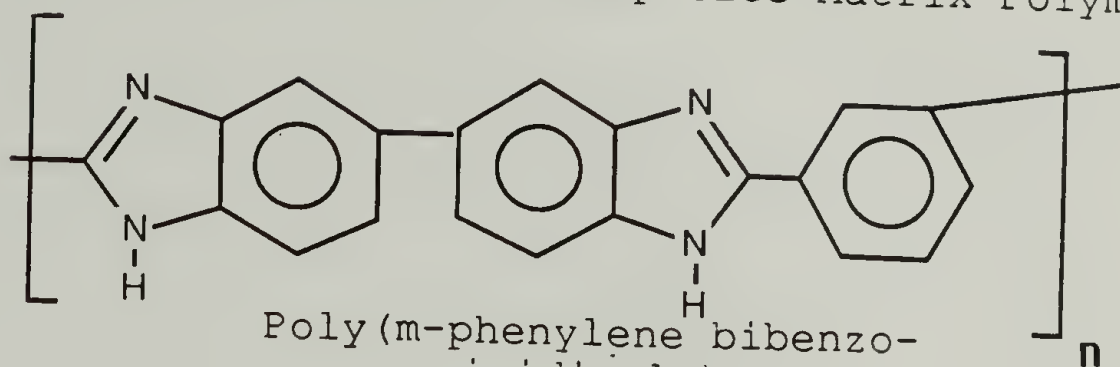


were employed as matrices.

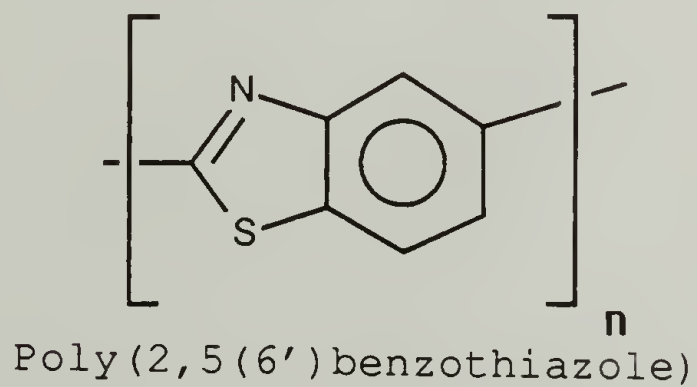
1.4.1 Processing

Preliminary investigators (5,6) studied the feasibility of the molecular composite concept. Various polymer pairs were precipitated into films from dilute methane sulfonic acid, MSA, solutions (1.0 - 2.0 wt.%) by evaporation of the MSA under vacuum. These films were found to be two phase; conglomerates of more than 50% rigid rod component were observed. As the MSA was removed during the process, the effective concentration of the solution was increased above the critical concentration and the structure of the biphasic solution consequently resulted in the final product. It was concluded that this process was too slow to inhibit phase separation of the solution. Rapid coagulation of the ternary solution was hypothesized to result in the random distribution of the PPBT in the resultant composite since no

TABLE 1.1
Articulated Molecular Composite Matrix Polymers



Poly(p-phenylene bibenzothiazole)



agglomerates of PPBT were observed. To produce a homogeneous composite, it is necessary to process from an isotropic solution. It is suggested⁽⁴⁰⁾ that molecular composite fibers be processed just below the critical concentration to maximize the viscosity of the processing solutions, presumably by increased interactions between the molecules in solution. The idea is to freeze in the high dispersity of the rigid rods in solution.

The matrices in Table 1.1 were investigated, but research efforts were focused on the PPBT/ABPBI/MSA system, since the polymerizations of PPBT and ABPBI were the most successful at that time.^(5,41) The phase behavior of this ternary solution was studied, which could be described by the theory of Flory.^(35e) PPBT dissolved in chlorosulfonic acid was reported to exhibit a rigid rod-like conformation in solution,⁽¹⁶⁾ and 640 \AA was reported as a lower bound of its persistence length.⁽⁴²⁾ The length of the repeat unit for PPBT is 12.4 \AA . The persistence length for ABPBI was calculated from chain dimensions to be 87.9 \AA ,⁽⁴³⁾ compared to its repeat unit length of 6.5 \AA , and is expected to be more flexible in solution than PPBT.⁽⁴⁴⁾ Therefore, Flory's theory for rigid rod/flexible coil/solvent should be applicable. If the x_3 calculated for the flexible coil was used in the theory, the critical concentration was overpredicted. Flory's calculated phase diagram was found to be in agreement with that obtained experimentally, when the aspect

ratio of the flexible coil polymer was used as a fitting parameter. It was concluded that this system was described by Flory's theory and could be used as a guideline for future experiments.

A recent investigation⁽⁴⁵⁾ compared the morphology of a 70/30 ABPBI/PPBT composite processed from an isotropic solution close to the critical concentration to that spun from above the critical concentration. The composite spun from an anisotropic solution was found to have ellipsoidal PPBT domains 0.1-4 μm in dimension, while that spun from the isotropic solution had PPBT distributed in fibrils 1-10 μm long and 0.1-0.5 μm in diameter, composed of crystallites no larger than 3 nanometers in diameter. By modifying the definition of a molecular composite to mean a dispersion of components in domains on the scale of a few nanometers, it was concluded that "molecular" composites were spun from isotropic solutions.

Recently, a study using a copolymer of poly(p-phenylene terephthalamide) and poly(3,4'-oxydiphenylene terephthalamide), PPOT, as a matrix for PPBT, reported a novel procedure for preparing a molecular composite.⁽⁴⁶⁾ The PPOT/PPBT/MSA solutions have enough integrity to allow the solution to be dry-jet wet-spun and a 70/30 PPOT/PPBT fiber was spun from a solution close to, but below the critical concentration; in the "ordinary" process. This fiber had a modulus of 52 GPa, which is lower than 60 GPa, the

modulus for the uniaxially drawn matrix material. The ternary solutions of PPOT/PPBT/MSA exhibit thermotropic behavior, as has been observed with other ternary systems⁽³⁷⁾. The temperature for the isotropic to nematic transition was determined for a 70/30 PPOT/PPBT solution in MSA, and was found to range from 25 to 80°C for polymer concentrations in the range of 5.0 to 8.0 wt%. Fibers were dry-jet wet-spun from solutions at 80-90°C, above the isotropic-nematic transition. During the spinning process, the fiber passes through an air gap at room temperature before entering the coagulation bath. This procedure is referred to as the "phase transition" process, and the resulting fiber had a modulus over twice that of the fiber prepared using the ordinary process. This work did investigate the effect of solution concentration to some extent, but the structure of the PPBT within the composite and the effect of PPBT composition were not investigated.

1.4.2 Properties

The mechanical properties of composites are often estimated by using the semi-empirical Halpin-Tsai equations.^(47,48,49) The modulus, E_{11} , for a unidirectional short fiber-reinforced composite is given by;

$$\frac{E_{11}}{E_m} = \frac{(1 + \delta\mu v_f)}{(1 - \mu v_f)} \quad (1.1)$$

$$\delta = 2(L/D) + 40v_f^{10} \cong 2(L/D) \quad (1.2)$$

$$\mu = \frac{(E_f/E_m - 1)}{(E_f/E_m + \delta)} \quad (1.3)$$

The aspect ratio, δ , is twice the length of the fiber, L , divided by its diameter, D , of the fiber. E_m and E_f are the engineering tensile modulus of the matrix and fiber, respectively, and v_f is the volume fraction of fiber.

Equation 1.1 predicts that the composite modulus increases as the aspect ratio of the reinforcing fiber increases. For large δ , we recover the case of a continuous oriented fiber composite

$$E_{11} = E_f v_f + E_m (1 - v_f) \quad (1.4)$$

Equation 1.4 is referred to as the "rule of mixtures", and gives the upper limit for composite properties as estimated by the Halpin-Tsai equations. A molecular composite is expected to result in maximum reinforcement and a very high aspect ratio (on the order of 200-300), therefore the "rule of mixtures" gives a good upper bound for the expected composite modulus.

The majority of the research on molecular composites has focused on using a lyotropic liquid crystalline polymer as a reinforcement for an amorphous or thermoplastic matrix.

A potential advantage of a molecular composite with a thermoplastic matrix is that it may be a melt processable material. Several thermoplastic molecular composite systems have been studied. Poly(p-phenylene terephthalamide), PPTA, has been used with nylon 6 and nylon 6,6 as the matrix.⁽⁷⁾ PPBT has also been used as reinforcement for several nylons^(44,50), poly(p-phenylene-quinoxaline, PPQ⁽²⁶⁾, and an aromatic co-polyamide.⁽⁴⁶⁾ The tensile properties of these molecular composites are summarized in Table 1.2.

"Molecular composites" of nylon 6 and nylon 6,6 reinforced with less than 10% PPTA, or with poly-p-benzamide, PBA, were investigated by Takayanagi et al.⁽⁷⁾ No characterization of the phase behavior of the ternary solutions was reported, but the composites were spun from isotropic solutions of PPTA, nylon, and NaH/DMSO.⁽⁵¹⁾

Electron microscopy of the freeze fractured fiber surface indicated the presence of microfibrils having a diameter of 150-300 \AA . The microfibril diameter was found to increase with increasing PPTA molecular weight for M_η equal to 980, 4500, and 12,300.

The modulus, yield, and breaking stress of the nylon/PPTA composites were greatly improved over that of the matrix alone. The higher molecular weight PPTA was found to provide improved reinforcement.

TABLE 1.2

Summary of Molecular Composite Tensile Properties

<u>Reinforcement/Matrix</u>	<u>E (GPa)</u>	<u>σ (MPa)</u>
ABPBI/PPBT 70/30	120 (115) *	1362
Amorphous Nylon/PPBT (44) 75/25	36	345
PPQ/PPBT (44) 70/30	18	355
Copolyamide/PPBT (46) 70/30	140 (132) *	---
Nylon 6/PPBT (50) 75/25	35 (79) *	319
Nylon 6,6/PPBT (50) 75/25	40 (79) *	342
Nylon 6/PPTA (7) 97/3	3.4 (4.9) *	340

* The prediction for modulus from the rule of mixtures

Samples of 97/3 nylon 6/PPTA were hot drawn at 170°C. A sample having a draw ratio of three had a modulus of 3.35 GPa and a tenacity of 340 MPa. This can be compared to oriented nylon 6, which had a modulus of 1.18 GPa and a tenacity of 220 MPa. Assuming volume additivity for the strength of the composite, the strength of PPTA is estimated to be 4.0 GPa, which is superior to the reported strength for commercial PPTA fibers of 2.7 GPa.⁽¹³⁾ From this, it was inferred that full reinforcement effect of the fibrils had been achieved.

The presence of the rod-like component was found to result in increased crystallinity as shown by wide angle x-ray diffraction, DSC, and isothermal crystallization kinetics. A higher molecular weight of the rigid rod component also resulted in greater crystallinity. It was proposed that the fibrils of rigid rod acted as a nucleating agent for the nylon. A strong interaction between the fibril surface and the matrix was hypothesized, and a shish-kebab type morphology for the nylon was proposed.

In summary, Takayanagi reported full reinforcement from PPTA in nylon/PPTA composites. The reinforcement was provided by a fibrils of PPTA estimated to be 150-300 Å in diameter. It was concluded that blends of rod-like and flexible coil molecules tend to form a fibrillar network of the rod-like reinforcement. However, no evidence was given for the PPTA being dispersed on a molecular level, and the

processing conditions were not investigated. Only low loadings of PPTA or PBA (up to 10%) were reported.

The majority of the molecular composite studies have used PPBT as the reinforcement, the properties for these fibers are summarized in Table 1.2.

A composite of 70/30 PPQ/PPBT spun from an isotropic ternary solution, close to but below the critical concentration, of PPQ/PPBT/MSA was reported to have a tensile modulus of 17.5 GPa and a strength of 355 MPa. The effect of solution concentration and PPBT composition were not investigated. The composite film was assumed to have a higher T_g than neat PPQ ($T_g = 359^\circ\text{C}$) since no T_g was observed up to 450°C (the limit of the instrument).⁽⁴⁴⁾ The alleged increased T_g of the matrix was assumed to be indicative of a molecular dispersion of the PPBT. No direct evidence for a molecular composite of PPQ/PPBT was presented.

PPBT has also been used to reinforce an amorphous nylon (DuPont FE 3303).⁽⁴⁴⁾ The modulus and strength for a 75/25 Nylon/PPBT composite spun from an isotropic solution close to the critical concentration, were reported to be 36 GPa and 345 MPa, respectively. Films of nylon/PPBT composite were compression molded at 250°C . Examination of the freeze fracture laminated sheet with SEM showed cohesive fracture dominated. It was also claimed that no phase separation resulted from the compression molding process. This

investigation concluded that molecular composite films could be consolidated into large parts by compression molding.

A recent investigation⁽⁵²⁾ from the same laboratory contradicted the previous conclusions, stating that phase separation *did* occur during compression molding of N66/PPBT composite films. The phase separation kinetics of N66/PPBT composites were investigated using light scattering. A dramatic increase in scattering intensity was observed as the composite sample was heated. The temperature at which the increased scattering occurred was taken to be the cloud point temperature, which varied with the weight percent of PPBT in the composite. This investigation provides definitive evidence that solution spun N66/PPBT composites phase separate when heated to a temperature at which the matrix molecules have mobility. Phase separation to a more thermodynamically favored structure occurs upon melting of the N66 as the mobility of the N66 chain increases. In light of this investigation, the claim that the amorphous nylon/PPBT composite did not phase separate during compression molding is believed to be unlikely.

Work from our laboratory focused on 70/30 (wt/wt) nylon/PPBT composite fibers.⁽⁵⁰⁾ Nylon 6 and Nylon 6,6 were used as matrix materials. The fibers were spun from an isotropic ternary solution of Nylon/PPBT/MSA. The effect of heat treatment temperature, residence time, and tension were investigated. It was concluded that tensioning the fiber

during heat treatment significantly enhanced the tensile properties. Heat treating the composite fiber at well above the melting temperature of the nylon slightly increased the modulus as compared to heat treatment at the melting temperature.

This study proposed that the structure of the PPBT within the nylon/PPBT composites was distributed, not on a molecular level, but in a continuous network-like structure. Supportive evidence for this hypothesis was that the composite fibers were found to exhibit a melting endotherm associated with the nylon matrix, but despite this observation the composite fibers tolerated heat treatment with high tension well above the melting point of the nylon matrix; the composite did not flow above the melting point of the nylon. When the nylon was washed away with sulfuric acid, a fiber structure was left intact. This residual fiber exhibited no melting endotherm associated with nylon and was presumed to be pure PPBT. This study gave supportive evidence for a PPBT network reinforcing the nylon/PPBT composites, but the investigation was limited to 30% PPBT composition fibers and the effect of solution concentration was not investigated.

A 70/30 ABPBI/PPBT fiber was spun from an isotropic solution close to the critical concentration. An increase in the orientation of the rods was achieved by drawing the wet coagulated fiber. The fiber was subsequently heat

treated at 540°C under tension resulting in a fiber with a modulus of 120 GPa and a strength of 1362 MPa. (44)

Recently thermotropic polymers have been used as blended with a variety of conventional thermoplastics. These blends are so-called *in situ* composites. (53.54.55) The fundamental concept of this research effort is similar to that of the above described molecular composites, and is noteworthy. The size scale of the reinforcing thermotropic is much larger than the molecular level, however these materials have the advantage of being melt processable. The thermotropic polymer can form elongated fibrils during the processing. The size of these fibrils was estimated to be on the order of 1-10 μm from electron micrographs. (53) The thermotropic phase was reported to provide good reinforcement. As the content of the thermotropic was increased, the morphology changed from ellipsoidal particles to rod-like fibrillar network structure. (54) It is interesting to note that the thermotropic composites, like several of the lyotropic composites, tend to form a continuous fibrillar network of the reinforcing phase.

In summary, the concept of a molecular composite of a rigid rod and flexible coil polymer is a novel and promising. Is it, however, realistic? The research to date does not provide any substantial evidence that a true molecular composite has been prepared. However, it has been demonstrated that blends of rigid rod flexible polymers have

excellent mechanical properties when compared to epoxy/carbon fabric composites of tensile modulus ranging from 40 to 98 GPa and strengths of 330 to 630 MPa.⁽¹³⁾ We conclude that these blends of rigid rod polymers have the potential to compete with conventional composite materials.

The processing of molecular composites has only been vaguely addressed. It has been shown that a composite processed above the critical concentration results in a phase separated product, but the effect of isotropic solution concentration has not been addressed. It has been suggested that to prepare a molecular composite it is necessary to quickly coagulate a solution which has an initial concentration just below the critical value.⁽³⁷⁾ An inherent assumption in this suggestion is that the rigid rod and flexible coil polymer will coagulate quickly, at the same time and the same rate. This condition is necessary, but not sufficient for the molecular dispersion of rigid rods present in the solution to be maintained in the solidified (coagulated) fiber, thereby forming the non-equilibrium structure defined as a molecular composite. Also, the effect of PPBT content and matrix material have not been investigated.

1.5 Dissertation Problem

This thesis addresses the processing/structure/property relationship for "molecular composite" fibers prepared from

a ternary solution of rigid rod and flexible coil polymer in a common solvent. The effect of solution concentration, matrix solubility, and PPBT composition on tensile properties and the structure of PPBT within the composite blends is investigated.

This dissertation focuses on poly(p-phenylene benzo-bisthiazole), PPBT, as the reinforcing rod-like polymer and poly(etheretherketone), PEEK, for the thermoplastic. Fibers were prepared from solutions of methane sulfonic acid, MSA. The tensile properties of PEEK/PPBT fibers are also contrasted to those of nylon 6,6, N66, with PPBT. Since the solution behavior and solubility of PEEK are significantly different than those of N66, insight as to the dependence of composite properties on the matrix polymer could be gained. The processing variables of solution concentration and PPBT composition were also considered for both N66/PPBT and PEEK/PPBT. The effect of processing variables on the structure of PPBT within the fiber was also investigated.

1.6 Organization of the Thesis

The dissertation is organized according to the processing procedure. First, a ternary solution is prepared (Chapter 2), from which a fiber is spun (Chapter 3). The fiber is consequently post-processed (Chapter 4). The conclusions are highlighted in Chapter 5.

Chapter 2 discusses the solution behavior of the PEEK/PPBT/MSA and N66/PPBT/MSA mixtures. The conformation of the polymers in solution and the solubility of the polymers is discussed, along with the phase behavior of the PEEK/PPBT/MSA solution. The rheological response of the N66/PPBT and PEEK/PPBT solutions are compared.

In Chapter 3, the processing/property relationships are discussed for the as-spun composite fibers. The dependence of the tensile properties on the concentration of the spinning solution is investigated for the PEEK/PPBT and N66/PPBT fibers.

The structure of the PPBT within the composite fibers is addressed in Chapter 4. The dependence of the as-spun PEEK/PPBT fiber properties on PPBT composition are contrasted to those of N66/PPBT. The effect of post-processing on this PPBT structure and on the resultant fiber properties is discussed. This chapter compares the effect of post-processing on the properties of PEEK/PPBT fibers versus N66/PPBT fibers.

In Chapter 5, the major conclusions are summarized along with suggestions for future work.

CHAPTER 2

SOLUTION BEHAVIOR

2.1 Introduction

This dissertation seeks to define the processing-property relationships for solution-spun composite fibers. In order to fulfill this goal, the behavior of the solutions to be processed are characterized as presented in this chapter. The properties of the fibers prepared from these solutions are studied in Chapter 3, so that insight into processing-property relationships may be gained.

Since composite fibers are prepared by coagulating polymer solutions of methane sulfonic acid, MSA, into water, the solubility of the PEEK, PPBT, and N66 in mixtures of MSA and water are investigated. The conformation of the polymers in MSA is discussed. The implications of the polymer solubility on the spinning process are considered.

In light of the relative solubility and solution conformations, the phase behavior and dynamical mechanical properties of the ternary solutions of PEEK/PPBT/MSA and N66/PPBT/MSA have been measured. The properties of the PEEK/PPBT/MSA solutions are compared to those of N66/PPBT/MSA.

2.2 Materials and Sample Preparation

The rigid rod polymer chosen for the investigation was poly(p-phenylene benzobisthiazole), PPBT. PPBT has excellent thermal stability, and has a degradation temperature below any thermal transitions.⁽¹⁶⁾ Therefore, PPBT may only be processed from solution. The only known solvents for PPBT are very strong acids, such as polyphosphoric acid (PPA), and methane sulfonic acid (MSA).^(56,57)

The PPBT used was synthesized by Dr. J. Wolfe⁽²⁴⁾ at Stanford Research Institute. Two samples were used having intrinsic viscosities of 25 dl/g and 18 dl/g in MSA. The corresponding to weight average molecular weights were calculated with the relations reported by Berry from dilute solution viscometry and light scattering studies⁽⁵⁸⁾

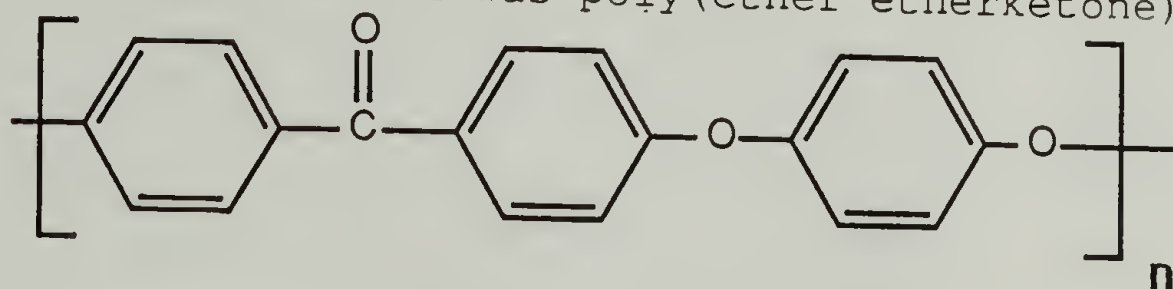
$$\{\eta\} = 4.86 \times 10^{20} [d_H^{0.2}/M_L] [M_\eta/M_L]^{1.8} \quad (2.1)$$

$$M_\eta = M_W (M_Z/M_W)^{4/9} \quad (2.2)$$

Where the hydrodynamic chain diameter, d_H , is taken to be $7 \text{ } \overset{\circ}{\text{A}}$,⁽⁵⁸⁾ and the mass per unit length, M_L , is $22 \text{ daltons}/\overset{\circ}{\text{A}}$,⁽⁵⁹⁾ and M_Z/M_W is 1.3 based on GPC data.⁽⁵⁸⁾ The M_W are calculated to be 36,000 (PPBT36) and 30,000 (PPBT30) for the 25 and 18 IV solutions, respectively.

PPBT36 was received in dope form as polymerized in PPA, and PPBT30 was received in the extracted form. MSA was chosen as the solvent in preference to PPA, since its lower viscosity reduces the dissolution time. MSA was used as received, 98% pure, from Aldrich Chemical Co.

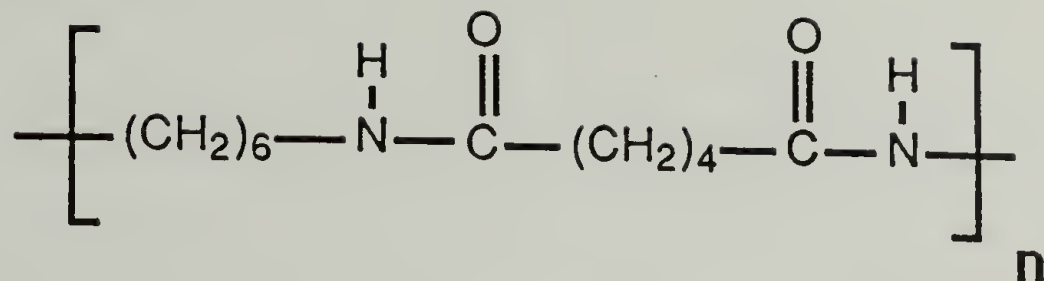
It was necessary for the thermoplastic matrix materials investigated to be soluble in but not degraded in MSA. The primary matrix material was poly(ether etherketone), PEEK,



PEEK has excellent chemical resistance, good thermal stability and mechanical properties in comparison to other engineering plastics. (60-62) It has a glass transition temperature of 143°C and a melting point of 334°C. (63,64) PEEK was generously provided by Dr. P. Staniland at Imperial Chemical Industries; the synthesis is described by Attwood et.al. (65) The PEEK used in this study had a number average molecular weight of 16,000 and weight average molecular weight of 33,000 based on gel permeation chromatography. (66)

Semi-crystalline nylon 6,6, N66, was also used for comparison purposes. N66 was received from DuPont and had a weight average molecular weight of 27,400. The repeat unit

for N66 is



The Nylon 6,6 has a glass transition temperature of 55°C and a melting temperature of 255°C. It has been demonstrated that N66/PPBT composite fibers of substantial stiffness and strength can be processed. (44,50)

PPBT36 was received as a solution in PPA, and extracted by coagulating a film into water. The coagulated film was then cut into strips and boiled in water for several days. After cooling to room temperature, the film was fibrillated in water with a blender. The PPBT was filtered and washed several times with methanol, and then soaked in methanol for several days to remove residual acid.

All of the polymers were dried for one to two days in a vacuum oven at 70°C and 0.5 torr. For solution preparation, the desired amount of polymers were mixed into MSA in a sample jar at room temperature under dry nitrogen, using a magnetic stirrer. The solutions were allowed to mix for at least one week to insure complete dissolution.

2.3 Solubilities of N66, PEEK, and PPBT

It is of interest to compare PEEK/PPBT composites to N66/PPBT since the configuration of the PEEK in solution is somewhat stiff, (67) evident from the persistence length of

PEEK in H_2SO_4 , reported to be 54 \AA , compared to a repeat unit length of 15.25 \AA .⁽⁶⁸⁾ Polyamides are flexible chains if the amide group is separated by at least four methylene groups.⁽⁶⁹⁾ Therefore, N66 has a small persistence length of 6.3 \AA (calculated as discussed in Appendix A)⁽⁷⁰⁾; it is a flexible chain polymer. The chain flexibility of N66 in solution is greater than that for PEEK.

The dissolution process in a strong acid can be thought of as a two step process. First, the molecule is protonated,⁽⁷¹⁾ and then the protonated molecule is dissolved in the solvent. In the case of a long chain molecule the number of protonated sites necessary for the molecule to be soluble depends on the flexibility of the chain. The ability of a chain to configure itself to maximize the interaction of the protonated sites with the solvent increases with increasing chain flexibility.

The solubility of PEEK, PPBT and N66 in MSA/water solutions has been investigated. The amount of water required to coagulate a polymer solution was determined by adding approximately one drop of water per second. The mixture was continuously stirred using a magnetic stir bar and water was added until the solution was observed to be turbid. The polymers precipitate from solutions of 2.0 wt.% polymer in MSA upon dilution with water to 87, 83, and 21 vol. % MSA (which corresponds to 0.15, 0.2, and 3.8 ml. of water/ml of solution) for PEEK, PPBT, N66, respectively. N66 is much

more soluble in MSA/water mixtures as a consequence of its greater chain flexibility in comparison to PEEK or PPBT.

The solubilities of the polymers in MSA/water mixtures have direct consequences in the fiber spinning process. As a filament of composite solution is coagulated, the water will be exchanged for the MSA, as illustrated in Figure 2.1. The dashed line represents the concentration of MSA, scaled from 1 (pure MSA) to 0 (pure water). When the filament enters the water, the MSA concentration within the filament is still very high, and little MSA has diffused into the water bath and little water has diffused into the filament. As the filament passes through the coagulation bath, the acid concentration is decreased within the thread. As the MSA and water exchange proceeds, a point is reached when the MSA/water mixture within the filament is no longer a solvent for the polymer; the polymer precipitates and a fiber is formed. After this point in the coagulation process, the filament is a solid. The solid line in Figure 2.1 represents this solidification or coagulation line, illustrating that the "skin" of the fiber coagulates before the "core." (83)

If the polymer is fairly soluble in a mixture of MSA and water mixture, such as N66, the spinning process becomes more complex. The more soluble the polymer is in MSA/water mixtures, the longer it will take for enough water to be exchanged with MSA to result in the precipitation of

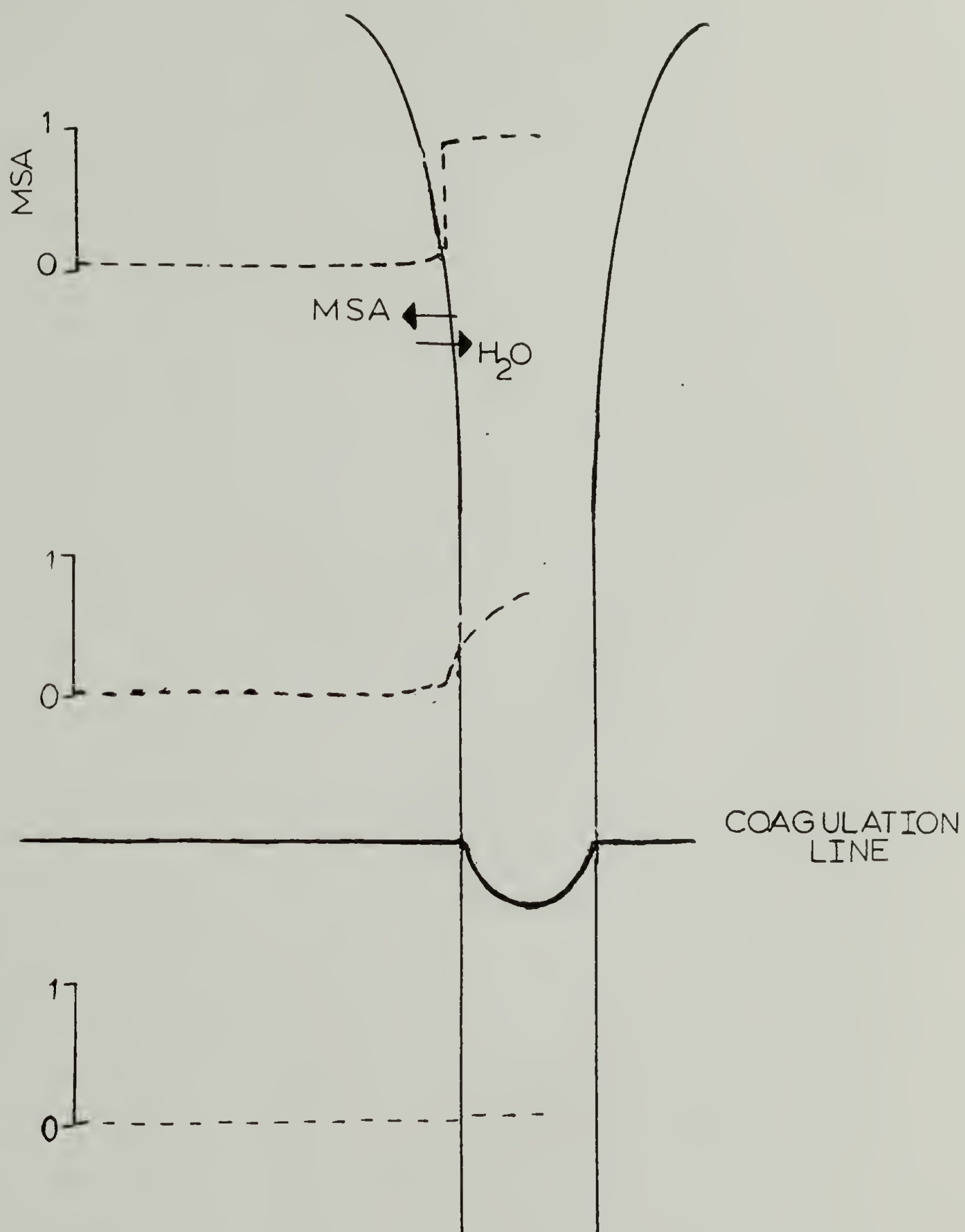


Figure 2.1 Illustration of fiber coagulation during the spinning process, depicting the concentration of MSA in the coagulating fiber (dashed line) and the solidification or coagulation line (solid line).

polymer. The concentration of MSA at the surface of the thread decreases during the coagulation process. If the N66 is soluble in the MSA/water mixture at the surface, it will diffuse into the coagulation bath. In fact, the N66 may not solidify into fiber form, depending on the concentration.

This concept is demonstrated when fibers of either PPBT or nylon 6,6 are spun. Dilute solutions of PPBT can be spun into fibers at concentrations as low as 0.05 wt% in MSA. In contrast, dilute solutions of N66 in MSA cannot be spun into fibers when coagulated into water. The solution forms a loose fibrillar dispersion. To spin a N66 fiber from an MSA solution, the concentration must be greater than about 15% N66.

From these solubility observations, some of the differences in the coagulation process for a ternary solution of N66/PPBT/MSA versus PEEK/PPBT/MSA can be anticipated. For the case of PEEK/PPBT/MSA, both polymers can be expected to precipitate at about the same dilution of MSA. However, for the N66/PPBT/MSA solutions the PPBT is expected to precipitate first, followed by N66 when the MSA is further diluted. The consequence of the relative solubilities of N66/PPBT and PEEK/PPBT on the processing-property relationships is considered in Chapter 3. The influence of chain flexibility on the phase behavior of composite solutions is considered in the next section.

2.4 Phase Behavior

The phase behavior of the solutions was studied by placing a drop of the solution between a microscope slide and a thin coverslip. The edges were sealed with ParafilmTM to exclude moisture and the slide was examined under polarized light with a Vickers No. M70/2/334 optical microscope to test for birefringence, indicative of a nematic/liquid crystalline phase. Birefringent solutions were diluted with MSA and mixed for at least three days. This process was repeated until the birefringence was no longer observed, indicating that the solution was isotropic. The phase diagram is shown in Figure 2.2.

The theory of Flory (35e) for a ternary solution of rigid rod/flexible coil/solvent was fit to the experimental phase diagram, using the aspect ratio for the flexible coil polymer, x_3 , as an adjustable parameter. The iterative procedure described by Flory (35e) was followed. The curve shown in Figure 2.2 is the theoretical prediction for $x_2 = 300$ and $x_3 = 30$. This curve fits the data fairly well. However, the value of $x_3 = 30$ is much lower than 180 estimated for PEEK of $M_n = 16,000$ using a molecular diameter of 6.91 \AA and a repeat length of 15.25 \AA from the crystal dimensions reported by Wakelyn (68).

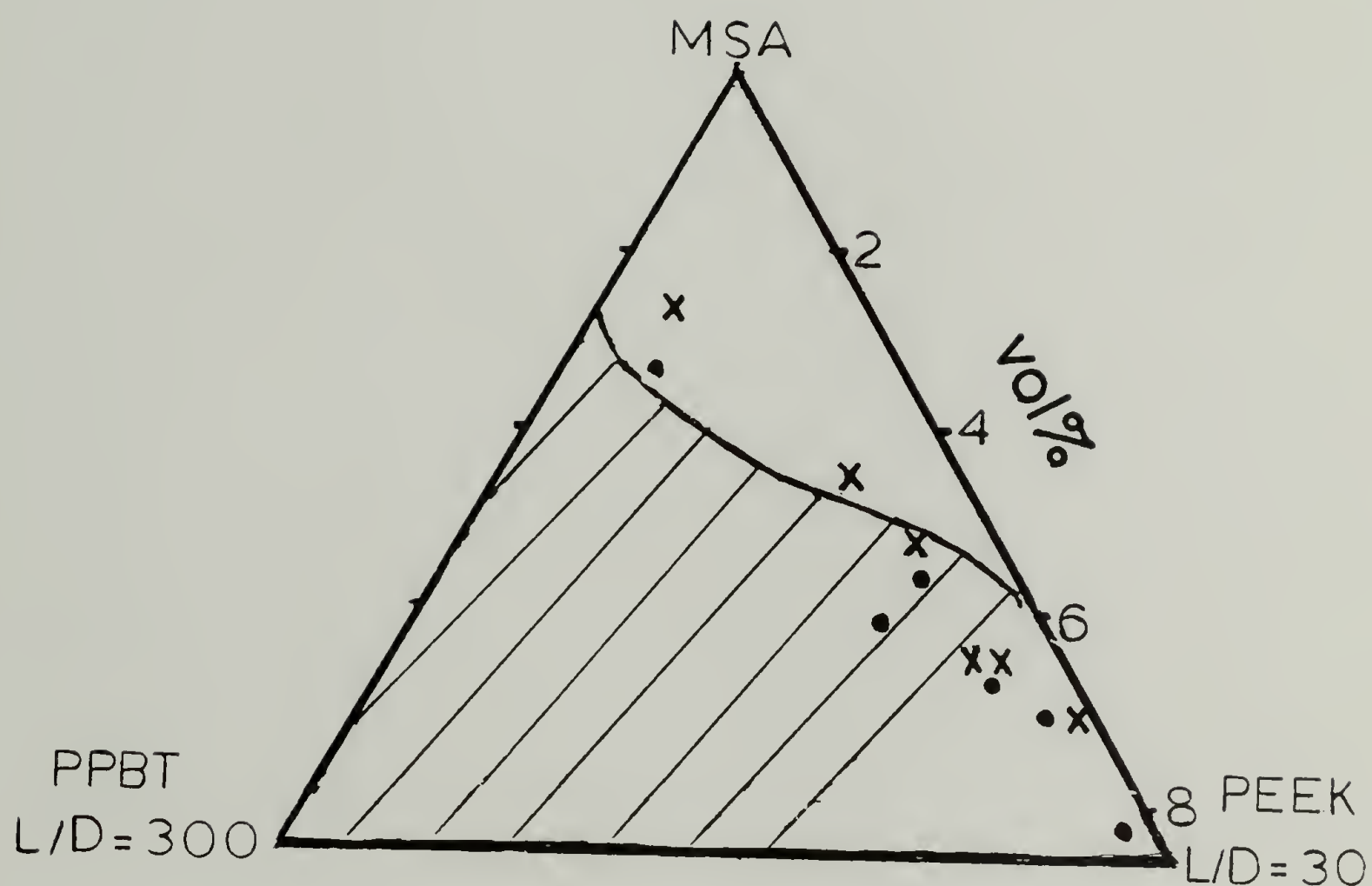


Figure 2.2 Solution concentrations of experimentally observed to be isotropic (x) and anisotropic (•) for PEEK/PPBT36/MSA solutions. The solid line represents the prediction^(47e) for $x_2 = 300$ and $x_3 = 30$.

As discussed in Chapter 1, it has been observed that Flory's theory for the solution of rigid rod, flexible coil and solvent underestimates the critical concentration for ternary solution of a rigid rod, not-so-flexible coil and solvent.⁽³⁷⁾ Flory has also described the solution for a mixture of two rigid rod polymers in a solvent.^(35b) Comparison of the predicted phase behavior of these two systems reveals that the rigid rod polymer is more tolerant of a rigid second component than of a flexible one. Therefore, as the stiffness of the second component is increased, the critical concentration increases.

The phase behavior for the N66/PPBT/MSA system has not been experimentally determined. However, Wickliffe⁽⁵⁰⁾ found the critical concentration for a solution of 70/30 (wt/wt) N66/PPBT25 composition to be 3.7 wt %. The estimates for the aspect ratios in Flory's theory are $x_2 = 325$ and $x_3 = 193$. Based on these values the critical concentration is predicted to be 2.9 wt% (3.5 vol%), which is in fairly good agreement with the measured value.

2.5 Solution Rheology

2.5.1 Results

The dynamic mechanical behavior of PEEK/PPBT/MSA and N66/PPBT/MSA solutions at several concentrations has been measured at 22°C with a Rheometrics Dynamical Spectrometer. The force transducer was rated for torques ranging from 1000 to 1 gr-cm. As a consequence of the low viscosity of

the solutions, it was necessary to use a cone and plate with a 10 cm. diameter to have the measured torque be within the sensitivity of the instrument. A glass cup was fabricated for the bottom plate to prevent spillage of the solution during testing. The experimental set up is depicted in Figure 2.3. The viscosity of 2.0% N66 or PEEK solutions was too low to be measured accurately with the available equipment.

Inertial effects provided the criterion for the validity of the high frequency data points. To insure that inertial effects could be ignored, and viscous effects dominate, it can be shown that

$$R\theta(\rho\omega/2R)^{1/2} < 0.2 \quad (2.3)$$

where, ρ is the density of the solution, R is the radius of the cone, θ is the cone angle, and ω is the frequency. The viscosity of the solutions was tested at strains ranging from 3% to 250% to identify the region where the material displayed a linear response. The viscosities were measured at 10% strain, which was well within the linear region for all of the solutions. To check the validity of the viscosity measurements made with the 10 cm diameter cone and plate fixture, a Brookfield 5,000 viscosity standard was also tested and the response was independent of strain (ranging

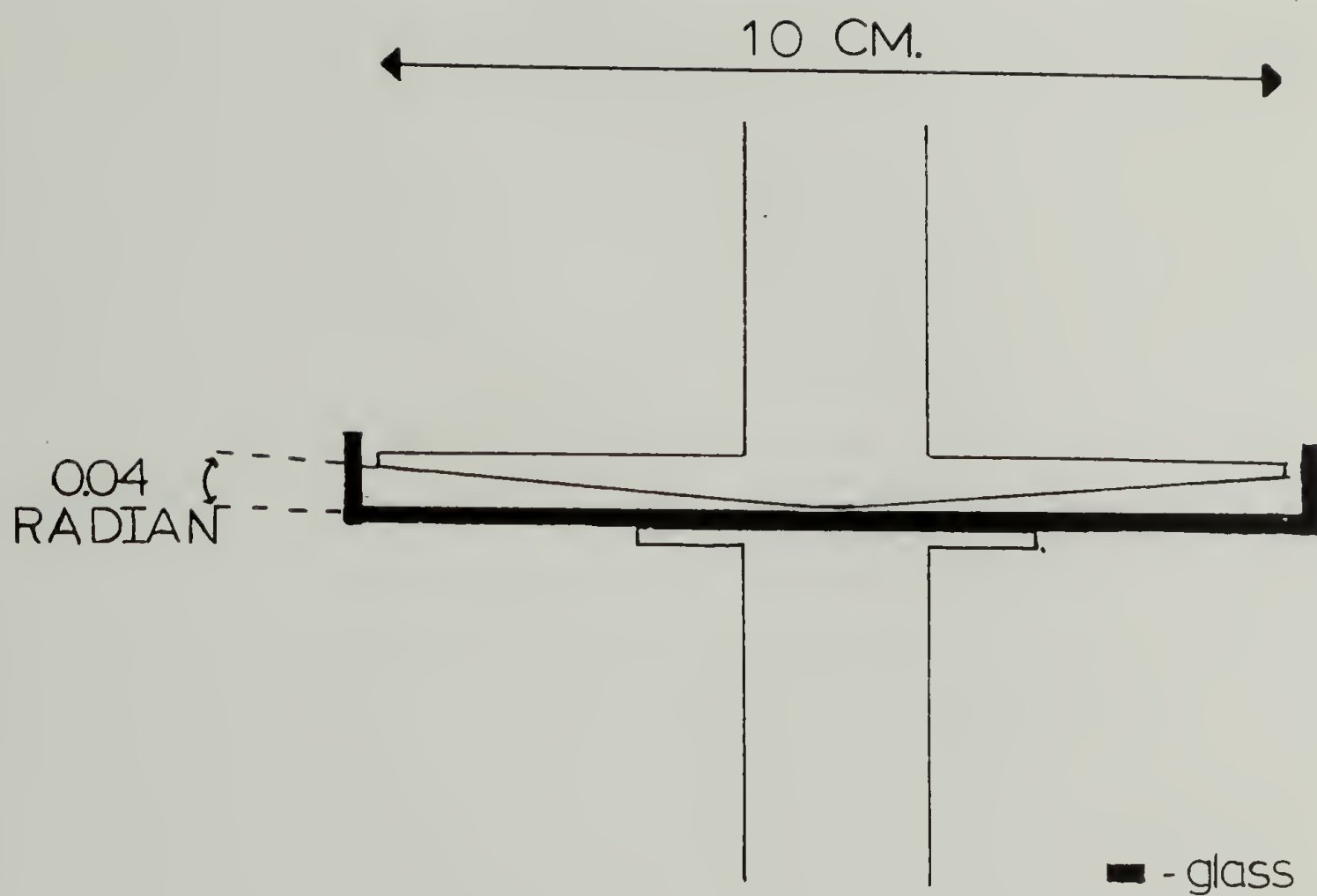


Figure 2.3 Schematic of experimental set-up for measurement of the rheological solution properties.

from 1% to 240%); the measured viscosity of the standard at 24°C was 6.2 Pas (6200 cp), which is in good agreement with 5.7 Pas (5700 cp) measured using a Cannon-Fenske Routine Capillary Viscometer.

The complex viscosity is an increasing function of the total polymer concentration for the PEEK/PPBT30/MSA solutions, as shown in Figure 2.4. The viscosities of all the composite solutions are significantly lower than that for the 2.0% PPBT solution.

For the 1.0, 2.0, 3.0 % PEEK/PPBT30 solutions (Figure 2.5), the real part of the dynamic viscosity is independent of the testing frequency and is several times greater than the imaginary part at low frequencies. The imaginary part increases with increasing frequency, indicating a more elastic material response at higher testing frequencies; these solutions exhibit a decrease in loss tangent as the test frequency is increased. In contrast, the loss tangent for the 4.0% PEEK/PPBT solution is relatively independent of frequency and the elastic response for the 4.0% PEEK/PPBT solution is substantial. The loss tangent for the 2.0% PPBT solution is also relatively independent of frequency. For the PPBT solution, the elastic response is almost equal the viscous response.

The complex viscosity for 1.0, 2.0 and 3.0% 75/25 N66/PPBT solutions, shown in Figure 2.6, increases with increasing concentration. Comparison with Figure 2.4

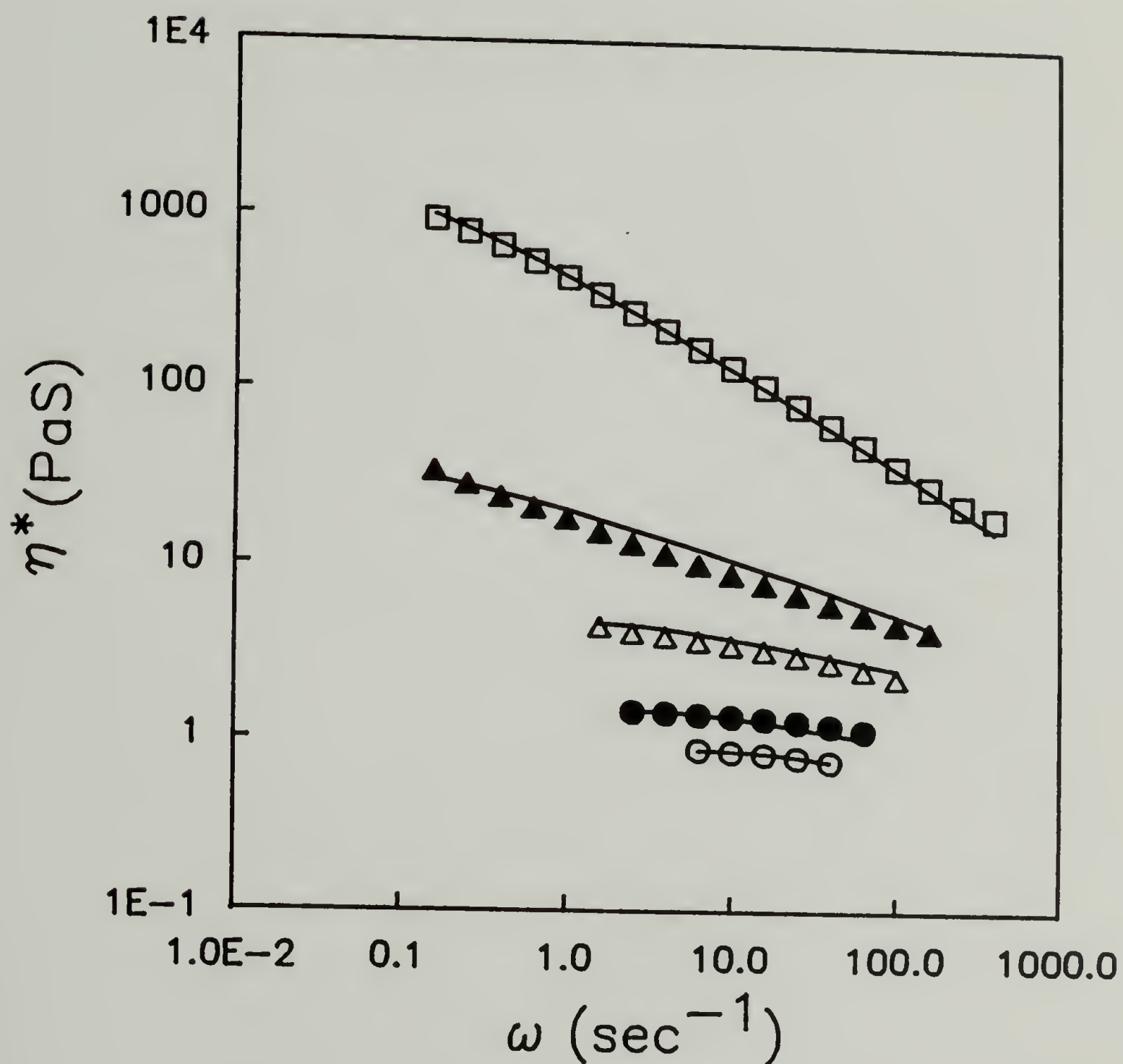


Figure 2.4 Complex viscosity vs. frequency for 1.0% (○), 2.0% (●), 3.0% (△), and 4.0% (▲) 75/25 PEEK/PPBT30 and 2.0% PPBT30 (□) solutions. The solid line is the viscosity predicted from a seven element Maxwell model.

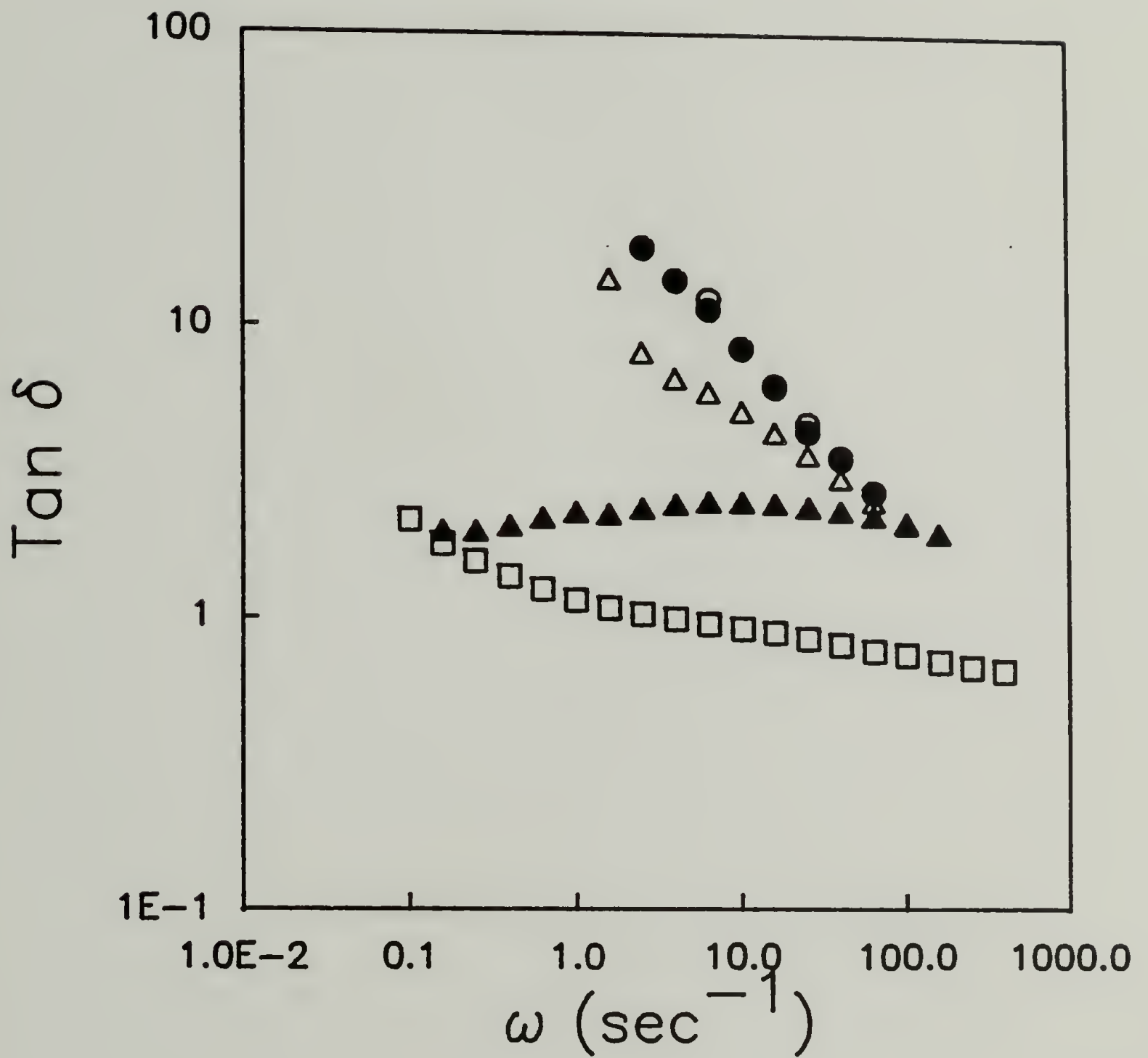


Figure 2.5 Tan delta vs. frequency for 1.0% (○), 2.0% (●), 3.0% (△), and 4.0% (▲) 75/25 PEEK/PPBT30 and 2.0% PPBT30 (□) solutions.

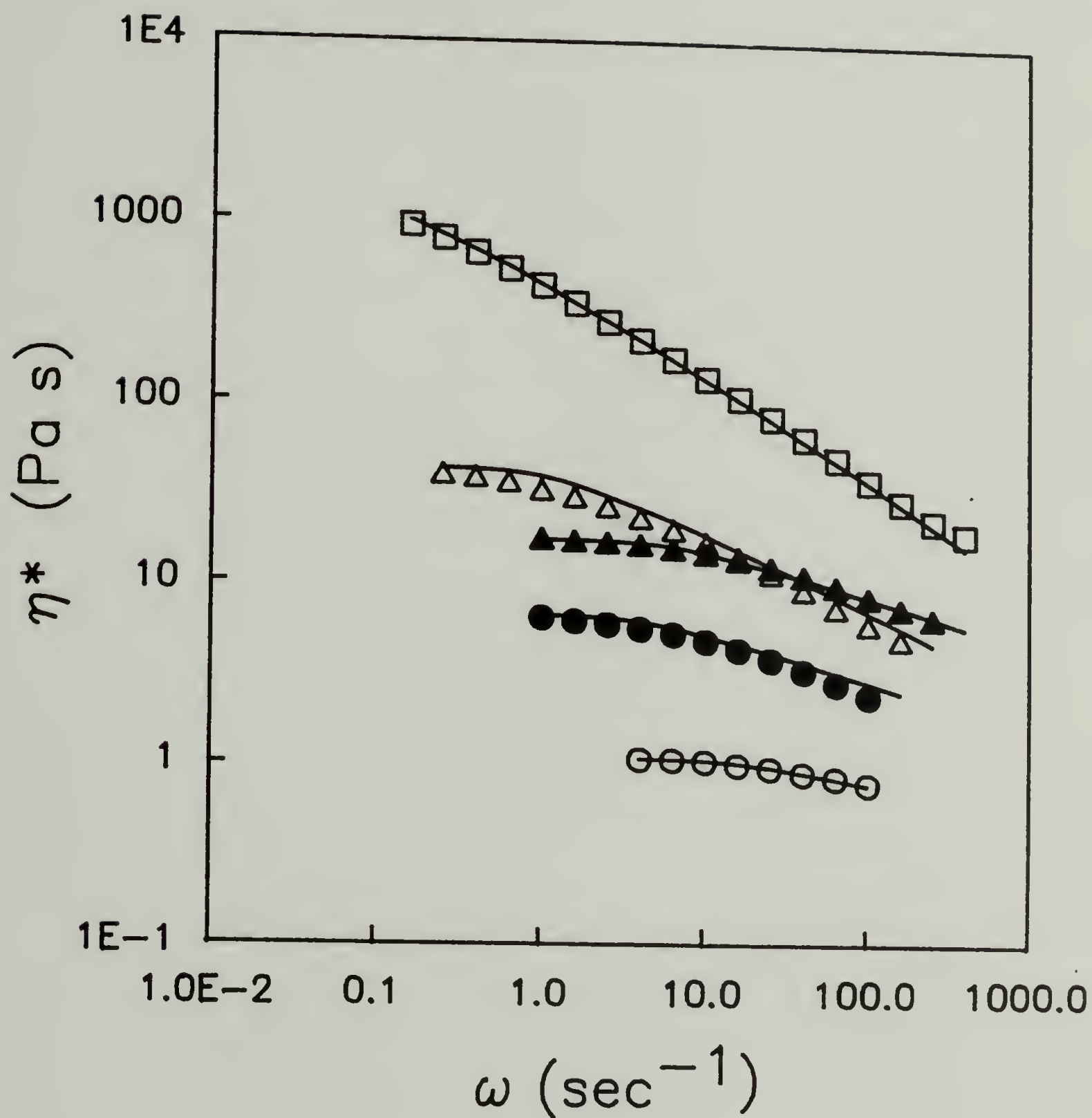


Figure 2.6 Complex viscosity vs. frequency for 1.0% (○), 2.0% (●), 3.0% (△), and 4.0% (▲) 75/25 N66/PPBT30 and 2.0% PPBT30 (□) solutions. The solid line is the viscosity predicted from a seven element Maxwell model.

reveals that these N66/PPBT solutions have higher complex viscosities than the corresponding PEEK/PPBT solutions. The apparent viscosity of the biphasic 4.0% N66/PPBT solution is lower than the viscosity 3.0% N66/PPBT solution for frequencies less than 30 rad/sec. At higher frequencies, the biphasic 4.0% solution exhibits a higher viscosity than the isotropic 3.0% solution.

The real part of the viscosity decreases with increasing frequency for all of the N66/PPBT solutions. This trend is evident from the decrease in $\tan \delta$ with increasing frequency shown in Figure 2.7. The elastic response of these materials increases at higher frequencies.

2.5.2 Discussion

It is useful to consider the entanglement molecular weights of the solute polymers when discussing the viscosity data. Graessley and Edwards⁽⁷²⁾ give an estimate for the entanglement molecular weight, M_e , for a linear polymer in solution from

$$\frac{1}{M_C} \Big|_{v=1} = \frac{K(N_a r)^{a-1} L^2 (1)^{2a-3}}{M^a} \quad (2.4)$$

$$M_C \cong 2 M_e \quad (2.5)$$

$$M_e \Big|_v = M_e \Big|_{v=1} v^{1-a} \quad (2.6)$$

where v is the volume fraction of polymer in solution, N_a is Avagadro's number, M_C is the characteristic molecular

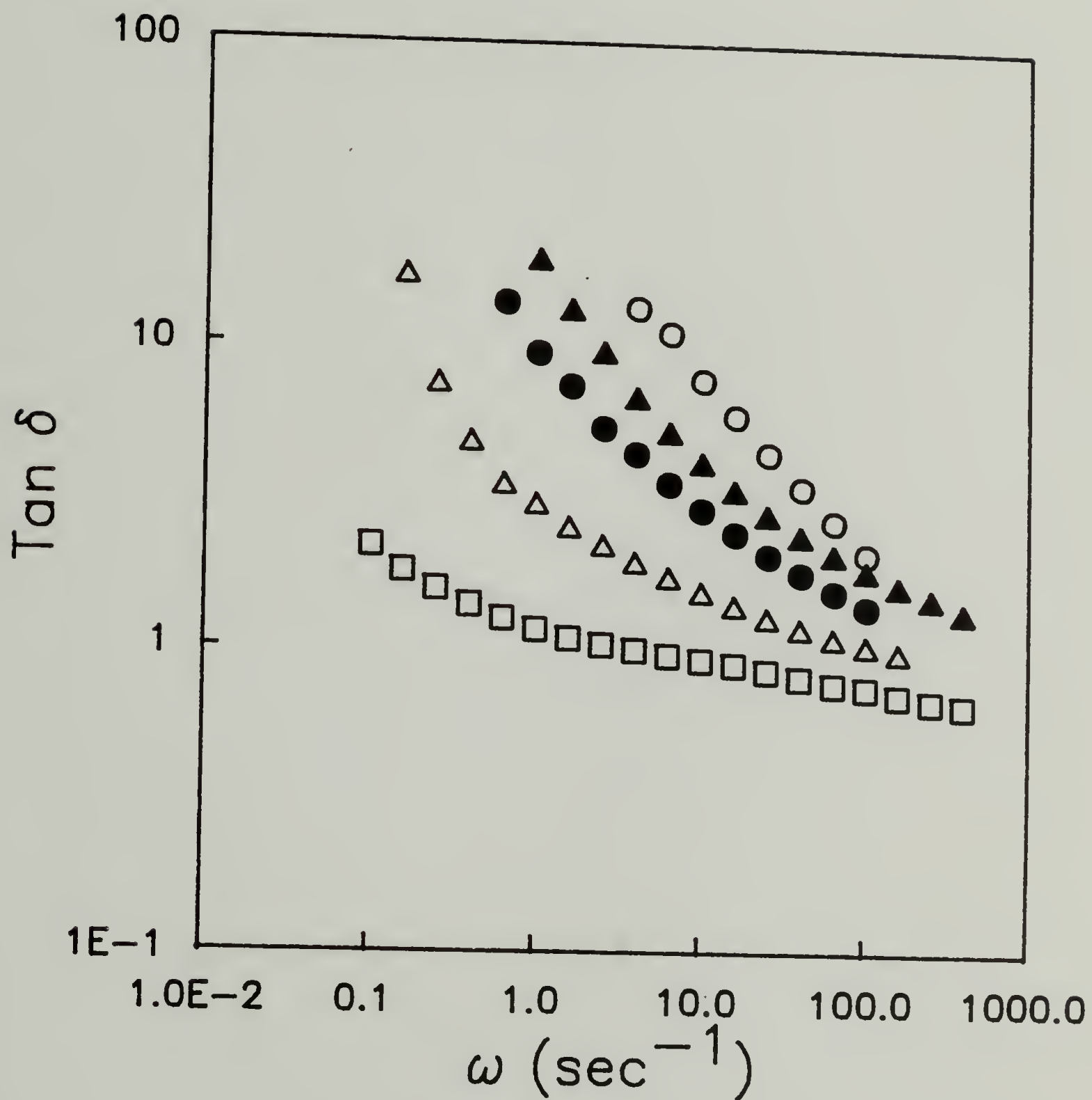


Figure 2.7 Tan delta vs. frequency for 1.0% (○), 2.0% (●), 3.0% (△), and 4.0% (▲) 75/25 N66/PPBT30 and 2.0% PPBT30 (□) solutions.

weight, ρ is the density of the undiluted polymer, L is the chain length, M is the molecular weight of the repeat unit, l is the Kuhn step length, K is a dimensionless constant equal to 0.0049, and the exponent a is in the range of 2.0 to 2.3. For $a = 2.0$, equations 2.4 - 2.6 reduce to

$$M_e|_v = (M/L)^2 (1/2KN\rho l) v^{-1} \quad (2.7)$$

For PEEK, molar mass of a repeat unit is 288, the length for a repeat is $15.2 \text{ \AA}^{(68)}$, the Kuhn length is $108 \text{ \AA}^{(60)}$, and the density is taken as $1.29 \text{ g/cm}^3^{(73)}$. For N66, these values are 226, $17.2 \text{ \AA}^{(74)}$, $12.6 \text{ \AA}^{(70)}$ (see Appendix A), $1.14 \text{ g/cm}^3^{(75)}$. The concentration of N66 or PEEK, for the molecular weights used here, required for an entangled solution is estimated to be 10.7 vol% and 5.2 vol% respectively. None of the composite solutions have concentrations of matrix corresponding to an entangled solution according to this estimate.

The entanglement molecular weight for PPBT has been determined experimentally in a recent paper⁽⁷⁶⁾ from a log log plot η_0 vs. ϕM_w , where ϕ is the concentration of polymer in the solution in g/cm^3 . The point at which the slope of the line changed from 1 to 4.2 was found to correspond to a value of ϕM_w equal to 770. The entanglement molecular weight can be determined as a function of solution concentration, since $\phi M_w|_e$ is a constant. The concentration of

PPBT30 required for an entangled solution is estimated to be 1.7 vol%. All of the composite solutions have a concentration of PPBT30 less than this. Only the 2.0% PPBT30 solutions would be expected to have the PPBT entangled in solution.

These calculations ignore the presence of the second polymer in solution, but probably provide a conservative estimate for the entanglement molecular weight in the composite solutions. The loss tangent and complex viscosity for the 2.0% PPBT30 solution support the prediction that this solution is entangled and suggest that the 4.0% 75/25 PEEK/PPBT30 solution is entangled. The constant value for loss tangent (approximately 2 for the 4.0% PEEK/PPBT30 solution and 1 for the 2.0% PPBT30 solution) are indicates the presence of entanglements.⁽⁷⁷⁾ Also, these solutions have much larger relaxation times than the other composite solutions evidenced by the complex viscosities approaching a constant value at low frequencies.

An entangled matrix in the composite solution would be expected to be desirable for the preparation of a "molecular composite" since the mobility of the rigid rod would be restricted during coagulation step, potentially resulting in the isotropic distribution of the rigid rod polymer, and this higher viscosity solution may be spin drawn. This concept will be considered in Chapter 3 when the dependence

of the composite fiber's mechanical properties on the solution concentration is discussed.

The viscosities of the composite solutions were less than those for the 2.0% PPBT solution. This trend differs with the steady state results reported by Wiff⁽⁷⁶⁾, where the steady state viscosities at shear rates less than 1000 sec^{-1} of 2.0% N66/PPBT solutions of various compositions were found to be greater than those of a 2.0% solution of PPBT, only at higher shear rates is the viscosity of the PPBT solution is greater than that of the composite solutions. Berry⁽⁷⁸⁾ reports the transient and steady state relaxation times and viscosities N66/PPBT solutions to be about two orders of magnitude higher than we measured. However, the N66 used by Wiff⁽⁷⁶⁾ and Berry⁽⁷⁸⁾ had $M_w = 70,000$ and the PPBT had $M_w = 45,000$. The increase in N66 and PPBT molecular weights result in an increase of the viscosity and relaxation times of the composite solutions by approximately two orders of magnitude.

An effort was made to fit the dynamic mechanical data with a simple linear viscoelastic model, the generalized Maxwell model. The model gives a fair fit for the real portion of the viscosity, η' , of the N66/PPBT solutions and the 2.0% and 3.0% PEEK/PPBT solutions, but in general could not effectively describe the behavior of real and imaginary portion of the solution viscosities. However, the magnitude

complex viscosity could be described by a generalized seven element Maxwell model,

$$\eta' = \sum_{k=1}^7 \eta_k / (1 + (\omega\tau_k)^2) \quad (2.8a)$$

$$\eta'' = \sum_{k=1}^7 \eta_k \tau_k / (1 + (\omega\tau_k)^2) \quad (2.8b)$$

$$\eta^* = [\eta'^2 + \eta''^2]^{1/2} \quad (2.8c)$$

even though the model does not describe the imaginary and real portions of the viscosity. To minimize the number of fitting parameters, the relaxation times, τ_k , and viscosities, η_k , are described by the equations,

$$\tau_k = \tau_{k-1} / \alpha \quad (2.9a)$$

$$\eta_k = \eta_{k-1} / \beta \quad (2.9b)$$

was fit to the complex viscosity, η^* , by minimizing the squared error shown by the solid lines in Figure 2.4 and 2.6 and the parameters are reported in Table 2.1. The largest relaxation time, τ_1 , and viscosity, η_1 , follow the same general trends as the characteristic relaxation times estimated from the inverse of the frequency at which the complex viscosity of the solution begins to decrease with increasing

frequency and the estimated plateau viscosity. The relaxation times and viscosities increase with increasing concentration for isotropic solutions, 1.0 -3.0% N66/PPBT30 and 1.0% - 4.0% 75/25 PEEK/PPBT30. However, the anisotropic 4.0% 75/25 N66/PPBT solution has a smaller relaxation time than that of the isotropic 3.0% 75/25 N66/PPBT solution. In fact, the relaxation time for the anisotropic 4.0% N66/PPBT solution is nearly equivalent to that of the 2.0% N66/PPBT solution.

In comparison to the 2.0% and 3.0% N66/PPBT solutions, the 2.0% and 3.0% PEEK/PPBT solutions have lower viscosities and relaxation times. The higher viscosities and greater relaxation times for the N66/PPBT system are probably a consequence of the more expanded N66 molecule hindering the motion of the PPBT molecules more than PEEK. This hypothesis was also suggested by Berry⁽⁷⁸⁾, and is conceivable since MSA is a better solvent for N66 than for PEEK. Thus, the N66 molecule would be expected to be more expanded in solution than the PEEK molecule; and could hinder the motion of the PPBT in solution. The maximum relaxation time and viscosity for the 2.0% PPBT30 and 4.0% 75/25 PEEK/PPBT30 solution are nearly an order of magnitude larger than those of the other solutions which is consistent with these solutions being entangled.

Table 2.1

Maxwell Model Parameters Describing the η^* for PEEK/PPBT
and N66/PPBT Composite and 2.0% PPBT Solutions

	<u>τ_1(sec)</u>	<u>η_1(Pas)</u>	<u>α</u>	<u>β</u>	<u>Err(%)</u>
<u>75/25 N66/PPBT</u>					
1.0%	0.035	0.27	1.2	5	0.01
2.0%	0.15	2.33	1.2	5	0.10
3.0%	0.6	21.5	2	5	0.47
4.0%	0.10	6.0	1.5	5	0.08
<u>75/25 PEEK/PPBT</u>					
1.0%	0.03	0.22	1.2	5	0.01
2.0%	0.03	0.33	1.2	5	0.04
3.0%	0.20	1.08	1.2	5	0.07
4.0%	4.0	11.67	1.5	5	0.45
<u>PPBT</u>					
2.0%	7.0	800	2.5	5	0.11

2.6 Summary

In this chapter, the solution behavior of PEEK, PPBT, and N66 in MSA are considered. The solubility data shows that N66 is much more soluble in MSA/water solutions than either PEEK or PPBT which are each of comparable solubility. This greater solubility of N66 is a consequence of higher chain flexibility in solution, relative to either PEEK or PPBT.

The relative solubility of the materials is expected to strongly effect the spinning process. In the case of a N66/PPBT/MSA solution the PPBT is expected to precipitate before N66. In contrast, PEEK and PPBT are expected to precipitate at about the same conditions from MSA solutions on exposure to water. This concept is discussed further in Chapter 3, where the processing of composite fibers is considered.

The phase behavior of the PEEK/PPBT36/MSA system has been experimentally determined and fit using Flory's theory for rigid rod/flexible coil/solvent. The theory agrees qualitatively with the data, if the value for the aspect ratio of the flexible coil polymer used is much smaller than the estimate based on the contour length, a consequence of the fact that PEEK is somewhat stiff and does not act as a flexible coil in solution. By reducing the effective aspect ratio (the contour length divided by the chain diameter) the theory gives a fair quantitative fit of the data. The

artificially low molar volume for the flexible coil is necessary because PEEK is not a true flexible coil in solution. In contrast to the PEEK/PPBT/MSA solution, the phase behavior of the N66/PPBT/MSA solution is apparently more closely predicted by the theory, without artificially adjusting any parameters. The flexibility of the N66 chain in solution approximates the idealized flexible coil polymer that is assumed in Flory's theory.

The viscosity for isotropic solutions of N66/PPBT/MSA were found be greater than corresponding PEEK/PPBT/MSA solutions. The maximum relaxation time for the isotropic 2.0%, and 3.0% N66/PPBT/MSA solutions was found to be several times those for corresponding PEEK/PPBT/MSA solutions. These observations are interpreted as a result of the well-solvated N66 molecule hindering the motion of the PPBT molecules more than PEEK. The relaxation times for 2.0% PPBT30 and 4.0% 75/25 PEEK/PPBT30 solutions were found to be almost an order of magnitude greater than the other solutions; these solutions are apparently entangled. The consequences of 4.0% PEEK/PPBT possibly being entangled on the properties of a fiber spun from a 4.0% 75/25 PEEK/PPBT30 solution are considered in Chapter 3.

CHAPTER 3

SOLUTION PROCESSING AND FIBER PROPERTY RELATIONSHIPS

3.1 Introduction

In this chapter the effect of solution concentration and matrix solubility are considered as processing variables. The tensile properties for PEEK/PPBT and N66/PPBT composite fibers are studied and contrasted.

The dependence of the mechanical properties of PEEK/PPBT and N66/PPBT fibers on the concentration of the processing solution is investigated. The effect of the relative solubilities of N66, PEEK, and PPBT in MSA/water mixtures is considered.

3.2 Experimental

3.2.1 Fiber Spinning

Fibers were spun from solutions that were prepared as described in Chapter 2. The spinning dope was loaded into a Teflon[®] barrel and ram extruder. The spinnerette pack consisted of a 330 micron wire drawing die (Plymouth Wire and Die) and a disposable 20 micron mesh filter (7X Dynalloy micromesh). Initially, the extruder was inverted and the ram pushed upwards to expel excess gas. If the solutions were highly viscous, like the 2.0% PPBT solution, trapped gas was a problem since such solutions could not be spun

into a continuous length of fiber, as gas bubbles resulted in breaking of the spinning line. To alleviate this problem, the extruder was placed into a vacuum oven approximately 40°C and 0.5 psi for several hours.

A lab scale spinning apparatus was designed in our laboratory. (Figure 3.1) The ram is pushed down at a constant speed of 1.5 cm/hr by a screw driven crosshead. The crosshead speed can be reduced with a ten speed gear box. The fiber is extruded with no air gap, and taken up with little or no draw. The fiber is allowed to coagulate in the water bath overnight.

The fiber may consequently be air-dried on the take up wheel. Fibers of less than 25% PPBT content shortened considerably upon drying. A 90/10 PEEK/PPBT fiber allowed to dry freely shrunk about 50% in length, while a 50/50 PEEK/PPBT fiber shrunk only about 12%. The lower content PPBT fibers could not be air dried on the take up wheel, because the shrinkage force resulting from drying at constant length was greater than the breaking force of the fiber. Also, the fibers adhered to the take up wheel and to one another. Fibers of PPBT content less than 25% were dried while slowly unwinding the wet fiber from an immersed take-up wheel; these fibers are referred to as as-spun fibers.



Figure 3.1 Photograph of the fiber spinning apparatus.

3.2.2 Post-processing

Several post-processes were employed to improve the orientation of PPBT in the composite fiber, thereby increasing the fiber's strength and stiffness.

If the wet fiber had enough tenacity, it was stretched between the two take-up wheels under water. This fiber may be air-dried and is referred to as a wet-stretched fiber. A draw ratio for this process is the ratio of the cross-sectional area of the undrawn fiber to that of the drawn fiber.

The air dried fiber may be hot-drawn by stretching it between two rollers while it is passed over a hot plate set at 265°C , well above the PEEK's T_g of 143°C . A draw ratio can also be calculated for this process from the cross-sectional area of the undrawn fiber divided by that of the drawn fiber. The fibers were hot-drawn only if they were not strong enough to be heat-treated.

Fibers were heat-treated using a constant temperature oven under nitrogen atmosphere. A dynamometer, calibrated with dead weights, was used to control the tension on the fiber during heat-treatment. The residence time is controlled with a 10 speed transmission. A detailed description of the heat-treatment oven is given elsewhere. (79,80)

3.2.3 Fiber Testing and Experimental Methods

Single filaments were mounted with epoxy onto 3 cm gauge length paper tabs. The fibers were tensile tested with a floor model Instron Universal Testing Machine at a strain rate of 0.0033 min^{-1} . The fiber diameters were measured by optical microscopy. Some of the tensile tested fibers were also sputtered with gold using a Polaron E5100 coating unit. These fibers were then examined with an ETEC Autoscan SEM.

Some PEEK/PPBT composite fibers were allowed to soak in sample vials filled with approximately 10 cm^3 of H_2SO_4 for about 3-5 weeks. Since sulfuric acid is a solvent for PEEK, but not for PPBT, the PEEK is dissolved and presumably the microstructure of the PPBT is left intact. A yellow color is associated with the dissolution of PEEK. The residual "fiber" was then removed with a disposable glass pipette and placed on a microscope slide. A glass coverslip was then placed over the fiber, and the fiber was pressed slightly between the glass slides to enhance the visibility and viewed with an optical microscope.

3.3 Fibers Spun from Isotropic Solutions Close to the Critical Concentration

Following the Hwang's⁽⁵¹⁾ suggestions for preparing molecular composite fibers, PEEK/PPBT fibers were spun from solutions with concentrations close to but below the

critical concentration. (The phase behavior of PEEK/PPBT36/MSA solutions was described in Chapter 2.)

Composite fibers with proportions of PEEK/PPBT36 ranging from 100/0 to 70/30 were wet spun from solution concentrations as summarized in Table 3.1. These fibers were too weak to be drawn in the wet state, but the air dried fibers were hot-drawn and subsequently tensile tested.

3.3.1 Tensile Properties

Figure 3.2a shows the tensile modulus for PEEK/PPBT36 fibers spun from the solutions listed in Table 3.1. The composite fiber moduli are low in comparison to the modulus of melt-processed PEEK, which is approximately 3 GPa.⁽⁶⁴⁾ The fact that we are processing from dilute solution is undoubtedly one important factor, since the as-spun modulus for PEEK is only 0.17 GPa. In fact, the as-received PEEK and PEEK extracted from MSA had intrinsic viscosities of 0.90 and 0.66 dl/g in H_2SO_4 , respectively, which is indicative of a reduction in molecular weight as a result of dissolution in MSA. Hot-drawing, however, increases the modulus of the PEEK fiber by almost an order of magnitude. From Figure 3.2a, the tensile modulus for the as-spun composite fibers is approximately the same as the modulus for as-spun PEEK. Hot-drawing the composite fibers was found to improve the tensile modulus significantly.

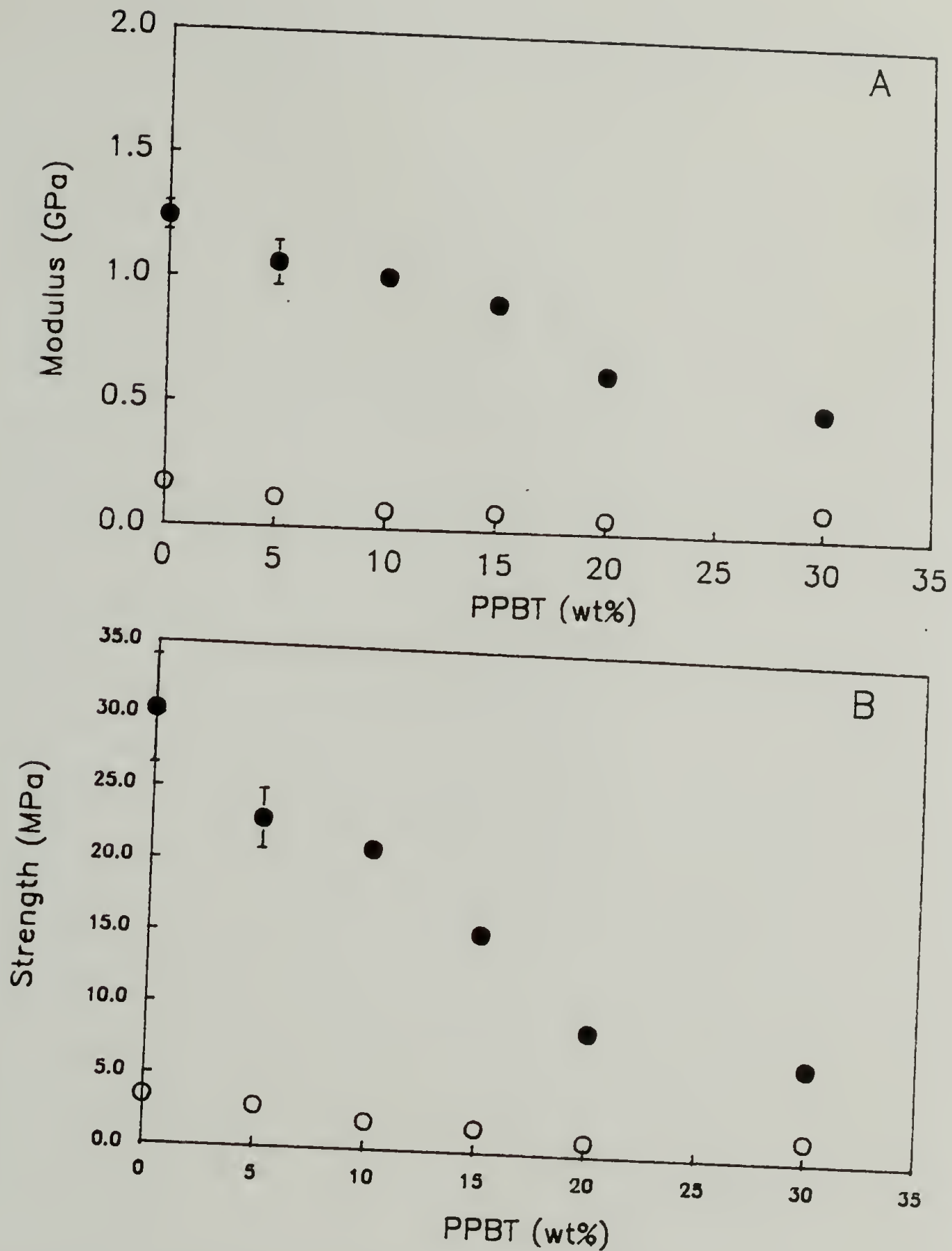


Figure 3.2 Tensile properties for as-spun (○) and hot-drawn (●) PEEK/PPBT30 fibers, spun close to the critical concentration, (a) modulus, (b) strength. Error bars represent the standard deviation from the average calculated from at least five samples, which appears only if greater than the symbol size.

TABLE 3.1

Concentration of PEEK/PPBT36 Spinning Solutions

<u>Amount of PEEK to PPBT (wt%)</u>	<u>Total Polymer Conc. (wt%)</u>
95/5	6.2
90/10	5.6
85/15	5.6
80/20	4.7
70/30	4.0

Nevertheless, the hot-drawn composite fibers had lower moduli than hot-drawn PEEK and there is no effective reinforcement from PPBT.

The same trends are evident for the tensile strength for these fibers shown in Figure 3.2b. These strengths are low in comparison to that of 100 MPa reported for melt processed PEEK.⁽⁶⁵⁾ From the mechanical properties, it is clear that no effective reinforcement has been achieved from the PPBT.

3.3.2 Microscopy

Scanning electron microscopy of the composite fibers was used to examine the fiber surface. The microscopy showed the presence of significant voids on the surface of all of the PEEK/PPBT36 fibers. Although hot-drawing resulted in a more fibrillar appearance and break, the voids were still present and were elongated in the direction of draw. Figure 3.3 shows typical SEM pictures for a 70/30 PEEK/PPBT (a) as-spun and (b) hot-drawn fiber. In contrast, Figure 3.4 shows that the surface of the as-spun PEEK fiber has no significant voids. Upon hot-drawing, the PEEK fiber had fibrillar surface and break as shown in Figure 3.4b.

The PEEK may be selectively removed from the fiber by soaking in H_2SO_4 , which is a solvent for PEEK but not for PPBT. Using this technique, some of the interesting features of the structure of PPBT within the composite fiber

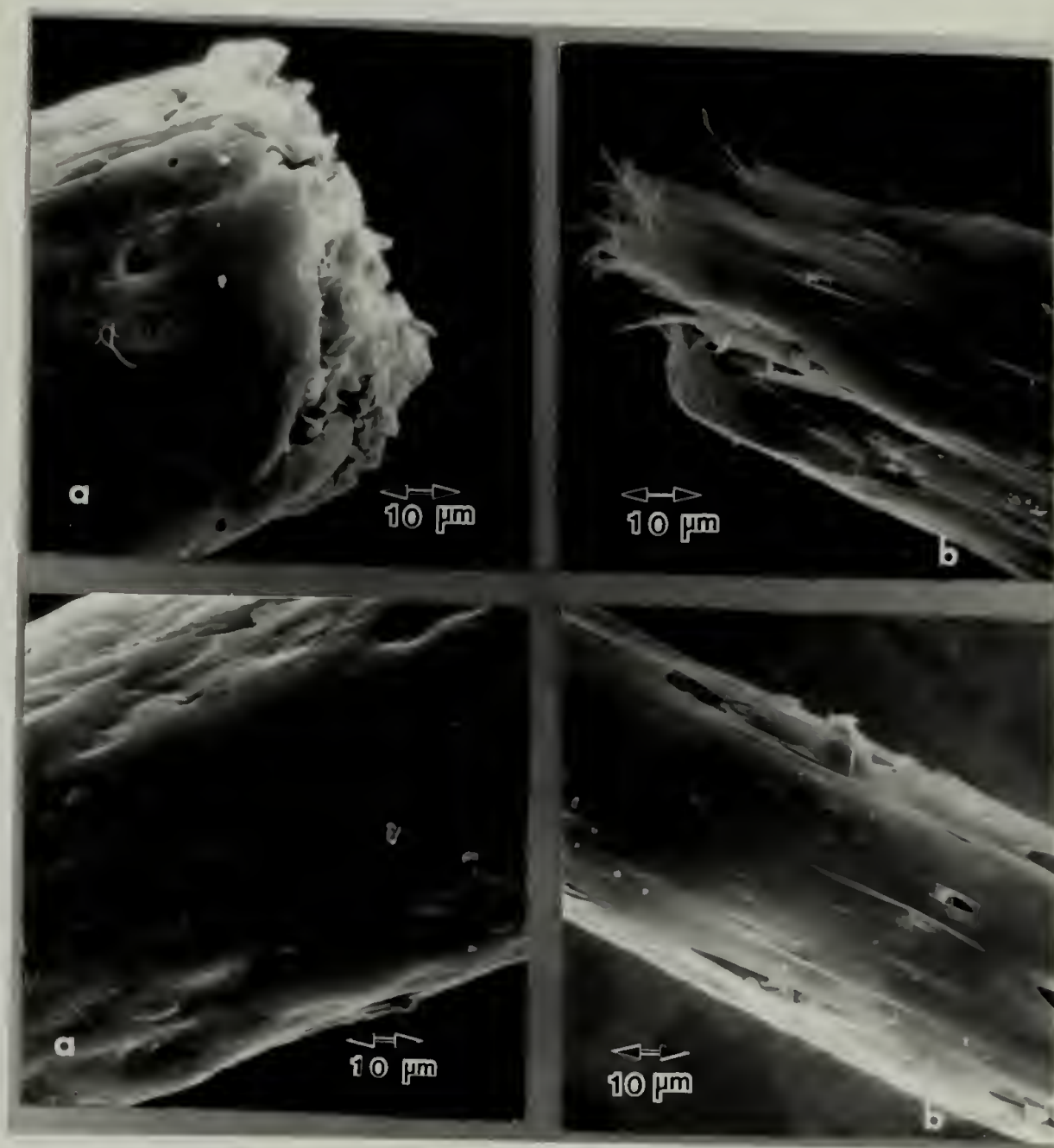


Figure 3.3 Scanning electron micrographs of an (a) as-spun and (b) hot-drawn 70/30 PEEK/PPBT36 fiber spun close to the critical concentration.

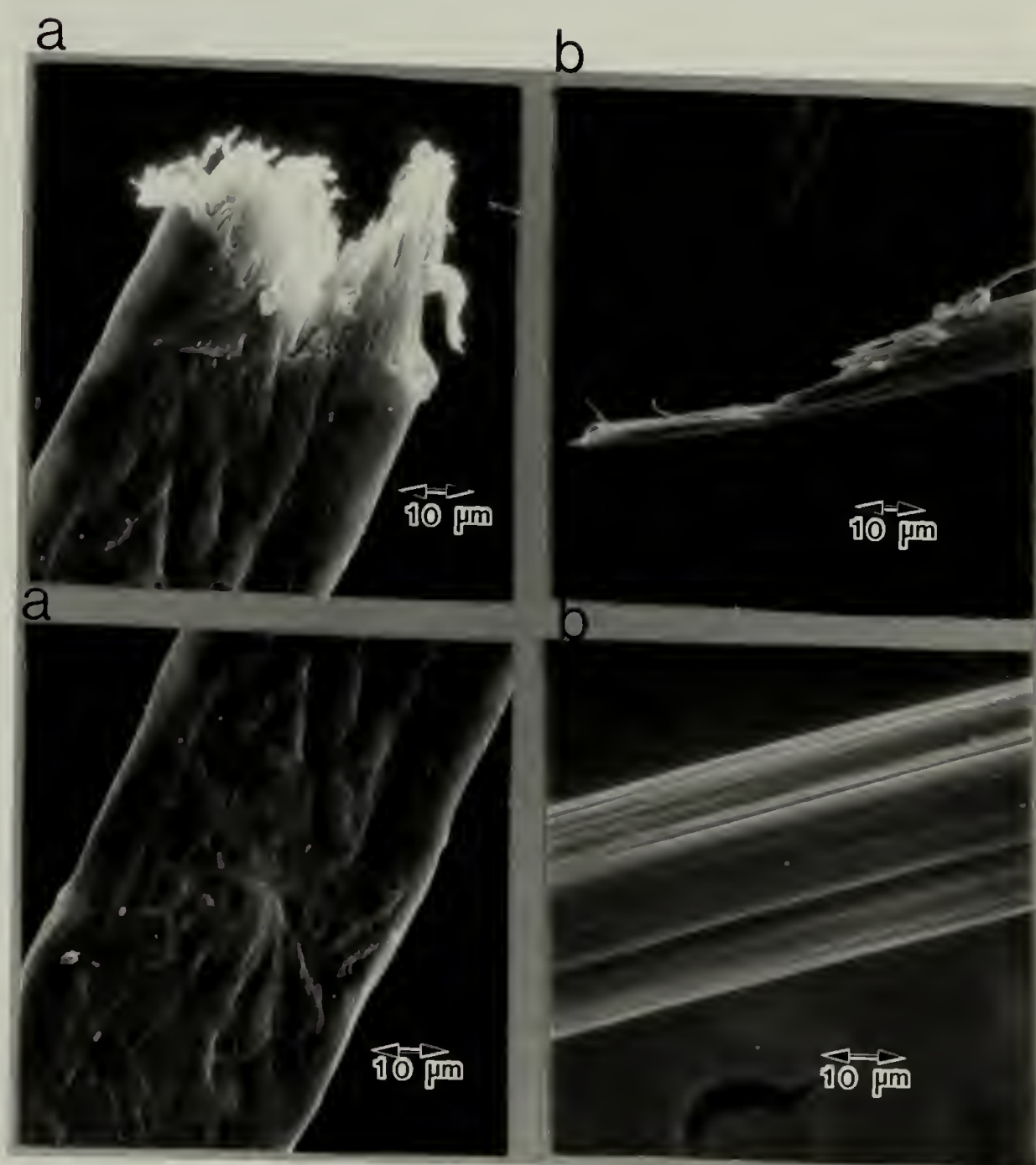


Figure 3.4 Scanning electron micrographs of an (a) as-spun and (b) hot-drawn PEEK fiber spun from a 4.0% solution.

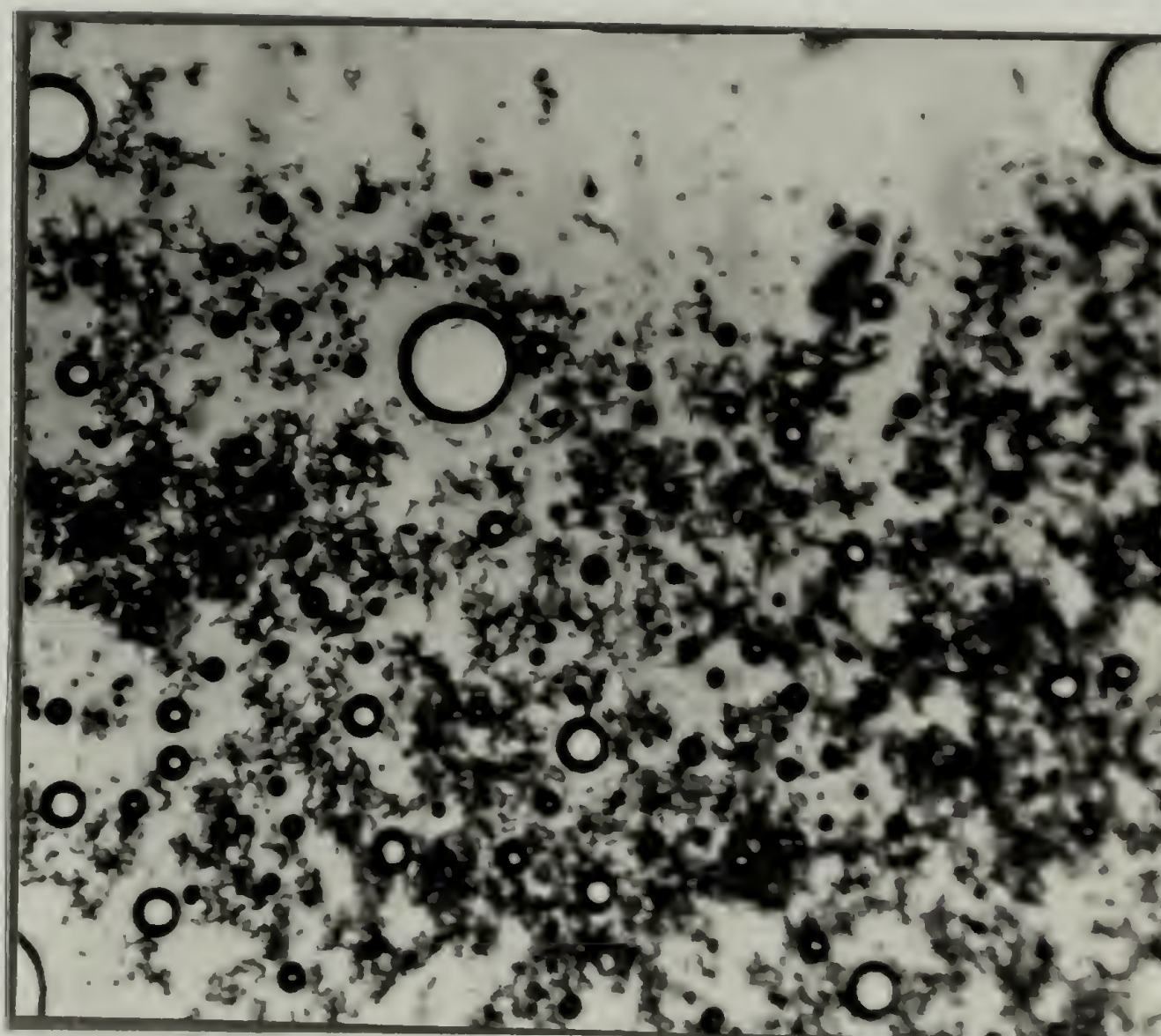
can be examined with an optical microscope. Similar procedures of selectively removing one component in a polymer blend have been used by other investigators. (81,82)

This procedure revealed that PPBT was distributed in discrete domains for fibers at all compositions. Figure 3.5 is a typical optical micrograph of a 90/10 PEEK/PPBT30 fiber. These domains were observed to be birefringent which is indicative of PPBT. Obviously, no reinforcement of the fiber would be expected from isolated domains of PPBT.

3.3.3 Discussion

Isolated domains of PPBT would be expected if these fibers had been spun from an anisotropic solution, above the critical concentration. However, these fibers were spun from solutions having concentrations close to but below the critical concentration with the expectation that the coagulation process would be fast enough to "freeze" in the isotropic distribution of rigid rod molecules.

Apparently, phase separation has occurred on a time scale comparable to coagulation for these fibers. One way to increase the time required for phase separation of the coagulating solution, is to decrease the amount of total polymer in solution. This approach is discussed in the next section.





100 μm

Figure 3.5 Optical micrograph of an as-spun 90/10 PEEK/PPBT36 fiber spun close to the critical concentration, immediately after H_2SO_4 was added. The domains of PPBT are indicated with the arrows; the circles are air pockets.

3.4 The Effect of Solution Concentration

3.4.1 PEEK/PPBT30 Composite Fibers

To examine the effect of concentration, fibers of 75/25 PEEK/PPBT composition were wet-spun from isotropic solutions of 1.0, 2.0, 2.5, 3.0, and 4.0 wt. % concentration. The tensile modulus for the as-spun fibers is given in Figure 3.6a. A significant increase in modulus is realized when the processing concentration is reduced from 4.0%. The tensile strengths of these fibers, shown in Figure 3.6b, exhibits a similar dependence upon solution concentration. The stiffness and strength of the 75/25 PEEK/PPBT fiber increases with decreasing concentration of the spinning solution, down to 2.0%. The drop in modulus and strength at lower concentrations will be discussed in Chapter 4, when the structure of PPBT reinforcing the fibers is considered.

From Figure 3.6, it is seen that approximately 2 wt.% is an optimum processing concentration for a 75/25 PEEK/PPBT as-spun fiber. The most dramatic increase in the as-spun fiber properties occurs when the processing concentration is decreased from 3.0 wt.% to 2.5 wt.%.

The diameter of the as-spun fibers increases with increasing solution concentration as shown in Figure 3.7. The solid line represents the calculated fiber diameter assuming that there is no die swell and that there is a negligible volume change on mixing for the solutions. The fiber diameter expected, D is then

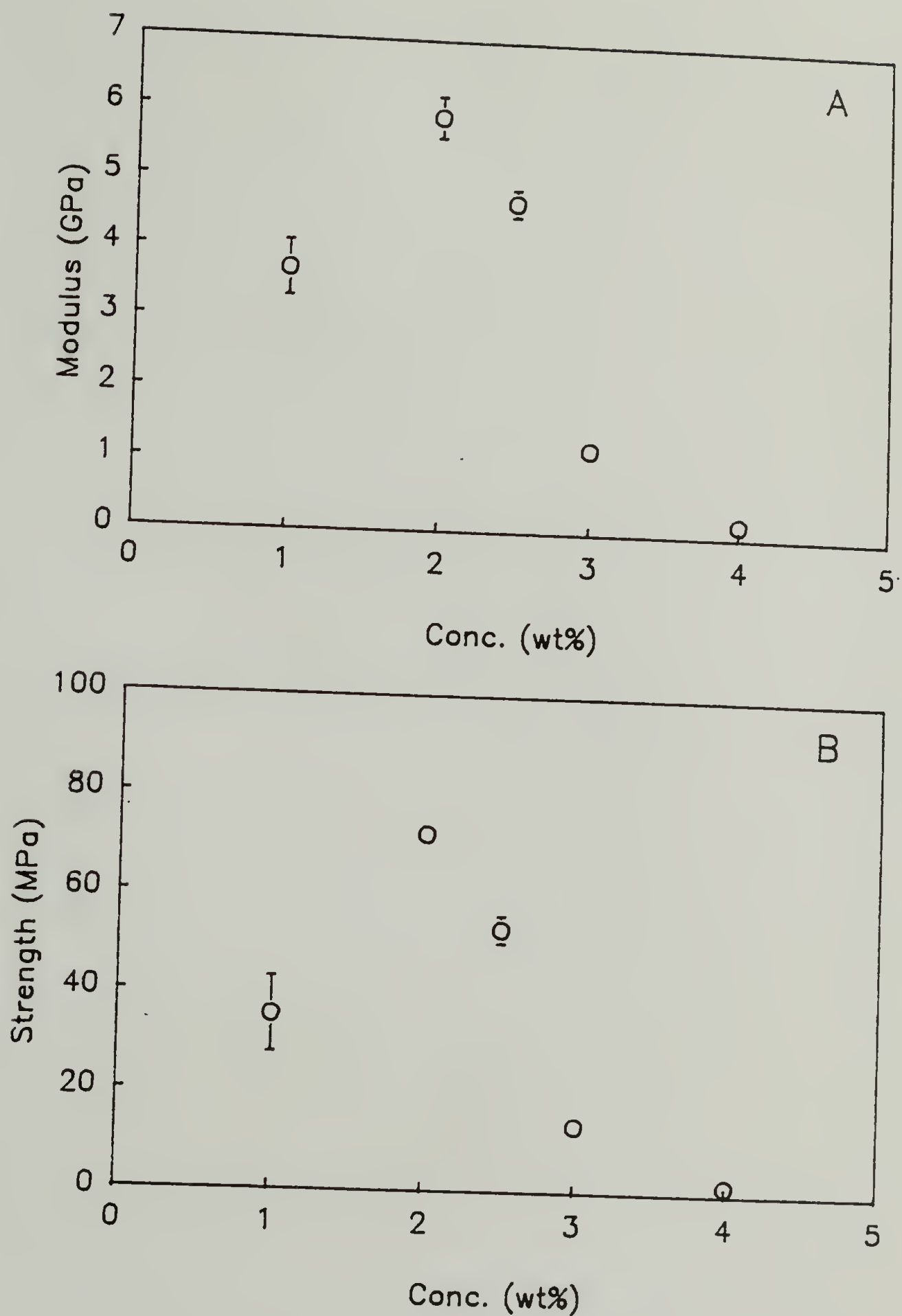


Figure 3.6 Tensile properties for as-spun 75/25 PEEK/PPBT30 fiber vs. the total polymer concentration in the spinning solution, (a) modulus, (b) strength. Error bars represent the standard deviation from the average calculated from at least five samples, which appears only if greater than the symbol size.

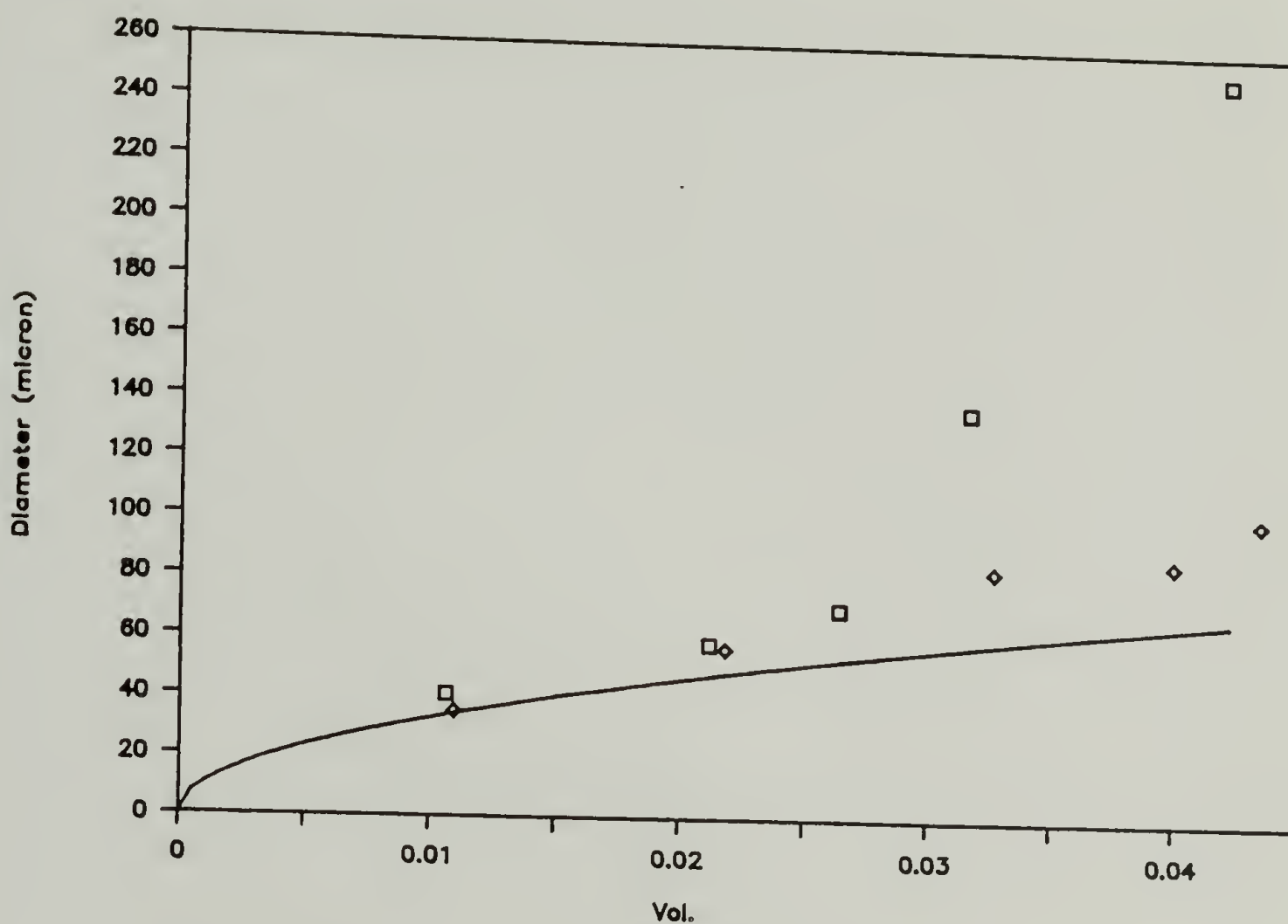


Figure 3.7 Fiber diameter for as-spun 75/25 PEEK/PPBT30 (□) and as-spun N66/PPBT30 (◇) fiber vs. the concentration of solution. The solid line represents the calculated fiber diameter.

$$D/d = v_f^{1/2} \quad (3.1)$$

where, d is the die diameter (330 microns) and v_f is the volume fraction of solute. The unexpectedly large diameter for the fibers spun from 3.0 and 4.0 wt % solutions indicates the presence of voids, and coincides with the drop-off in strength and stiffness. Scanning electron micrographs of these fibers, e.g., Figure 3.8 shows that voids are present on the fiber surface of the 4.0% 75/25 PEEK/PPBT30 fiber.

A strong dependence of the tensile properties on the total polymer concentration was observed for 75/25 PEEK/PPBT fibers. Isotropic solutions close to the critical concentration apparently undergo phase separation during coagulation. The resultant fiber has poor mechanical properties because the PPBT is distributed in discrete domains that provide no reinforcement. The phase separation during coagulation also causes voids in these fibers that also reduce the tensile properties.

The effect of the PEEK being entangled in the 4.0% 75/25 PEEK/PPBT30 solution, as discussed in Chapter 3, was thought to potentially aid the isotropic distribution of the rigid rod molecules. However, it is apparent from the mechanical properties that the phase separated product has been formed.

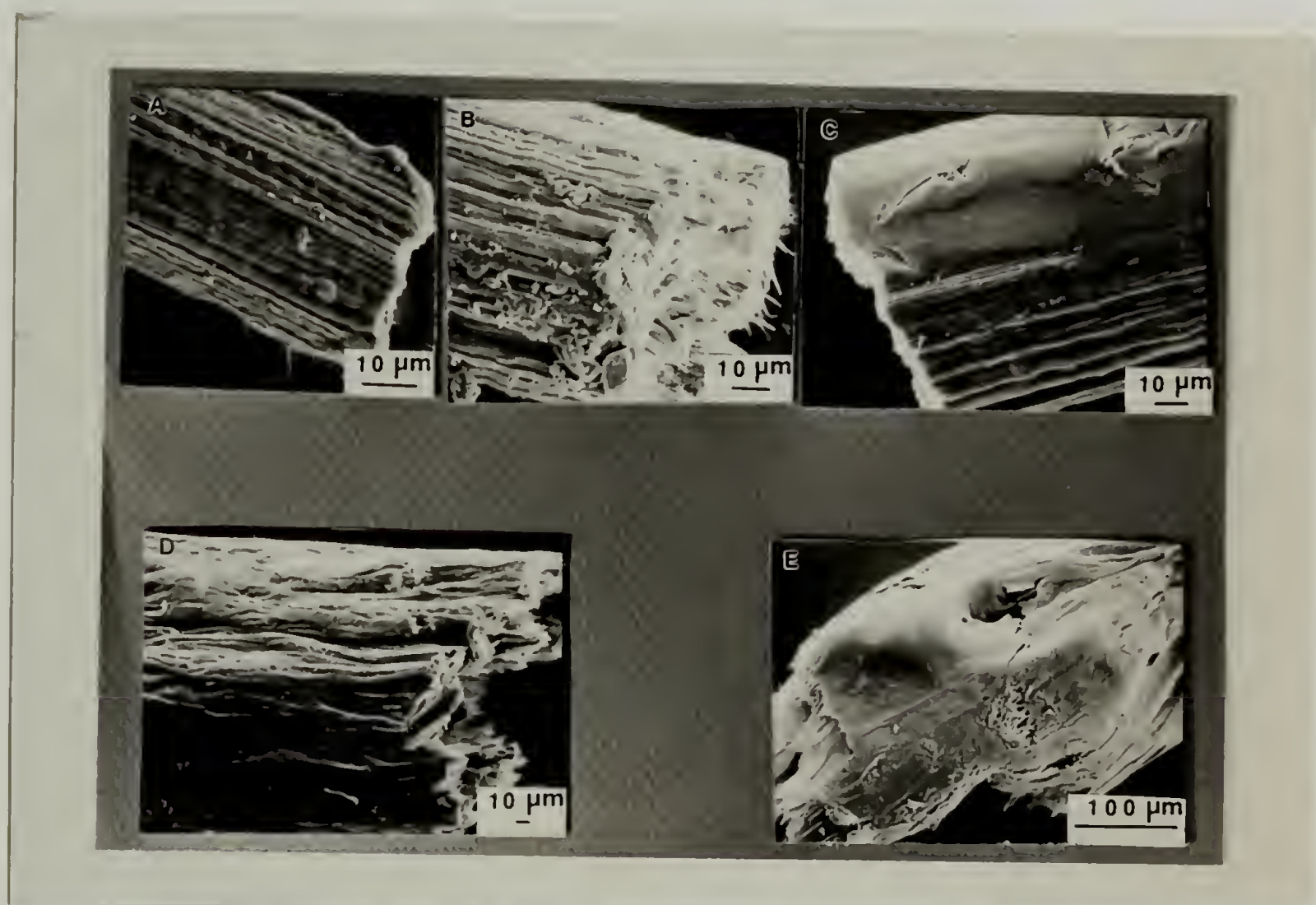


Figure 3.8 Scanning electron micrographs of as-spun 75/25 PEEK/PPBT30 fibers spun from (a) 1.0% solution, (b) 2.0% solution, (c) 2.5% solution, (d) 3.0% solution, (e) 4.0% solution.

By processing from a solution well below the critical concentration, a composite fiber with good strength and stiffness was prepared. Such fibers are fibrillar in their surface appearance and at the fracture surface upon break in tension. Apparently, these solutions are not passing through the phase transition during coagulation step. The question of the how PPBT reinforces these composite fibers is addressed in Chapter 4.

3.4.2 N66/PPBT30 Composite Fibers

In Chapter 2, the solubility of N66 in MSA was shown to be much greater than that of either PEEK or PPBT. Therefore, it is of interest to compare the processing - property relations of PEEK/PPBT to those of N66/PPBT. Thus, the effect of solution concentration was also investigated for 75/25 N66/PPBT fibers.

The tensile properties for fibers spun from isotropic solutions of 1.0, 2.0, 3.0, 3.7 wt % and a fiber spun from an anisotropic solution of 4.0 wt % are shown in Figure 3.9. The tensile modulus and strength for N66/PPBT fibers spun from isotropic solution above 1.0 wt.% are essentially independent of solution concentration. (The behavior for lower concentrations is discussed in Chapter 4.) The critical concentration for 70/30 N66/PPBT36 solution is approximately 3.7%. (50)

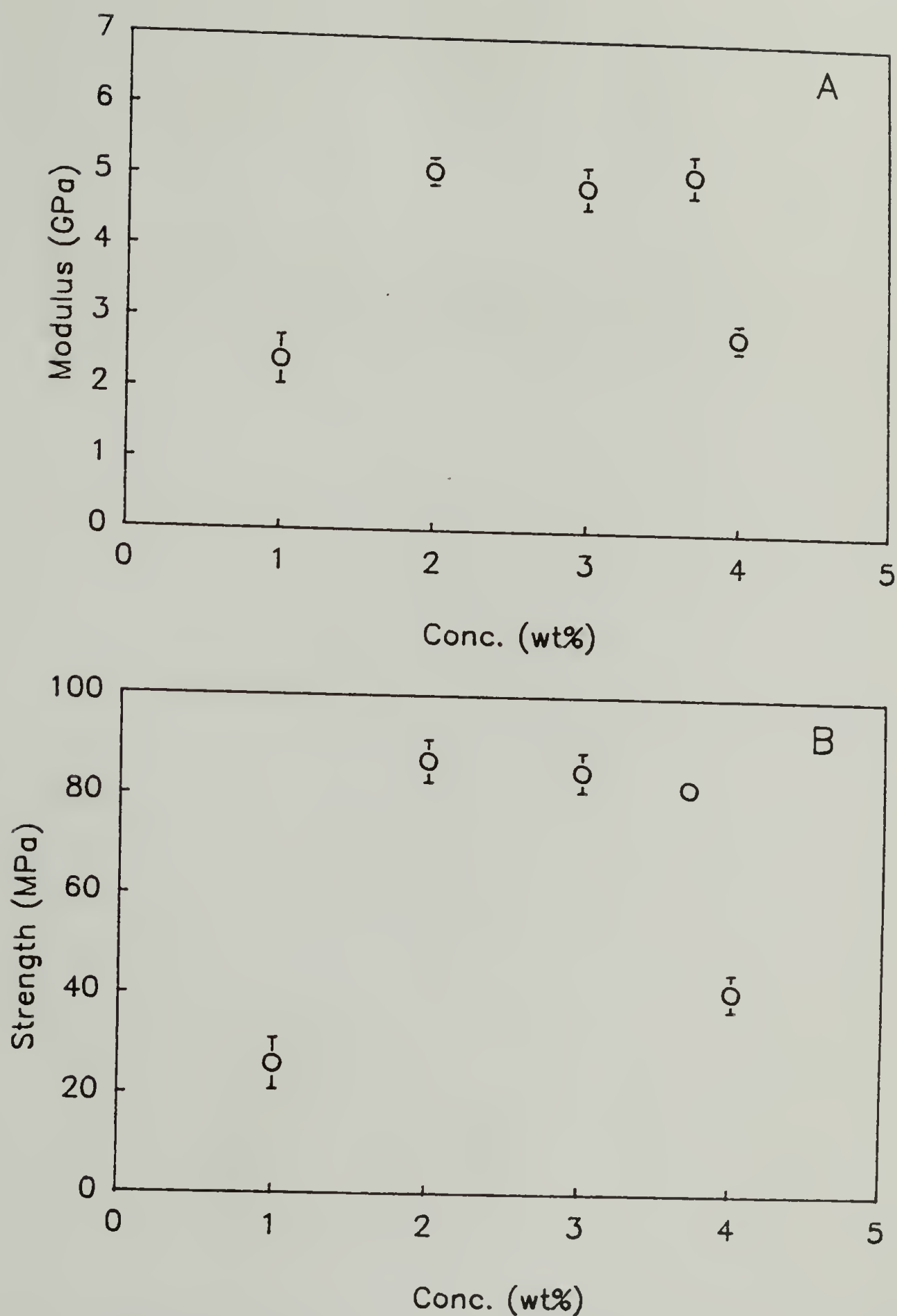


Figure 3.9 Tensile properties for as-spun 75/25 N66/PPBT30 fiber vs. the total polymer concentration in the spinning solution, (a) modulus, (b) strength. Error bars represent the standard deviation from the average calculated from at least five samples, which appears only if greater than the symbol size.

In contrast to the behavior of PEEK/PPBT composites, the fiber spun from the 3.7 wt.% solution has a modulus and strength equivalent to that of a fiber spun from a 2.0 or 3.0 wt% solution. Spinning from a phase separated solution is expected result in a fiber of lower strength and stiffness compared to a fiber spun from an isotropic solution. The fiber spun from an anisotropic solution of 4.0% concentration has a modulus of about half that of one spun from an isotropic solution.

The diameter of the as-spun 75/25 N66/PPBT30 fibers increase with increasing solution concentration, as shown in Figure 3.7. The diameter of the N66/PPBT correlates more closely with the expected diameter calculated from equation 3.1. Scanning electron micrographs of the tensile tested fibers are shown in Figure 3.10. The fibers are seen to have fibrillar surfaces and to be relatively void free. From the solubility studies, the coagulation process for the N66/PPBT/MSA solution can be expected to proceed by the PPBT precipitating out of solution initially, followed by N66. Therefore, N66 would not interfere with the coagulation of the PPBT. For this reason, it would not be expected that a molecular composite of N66 with PPBT would be prepared. From the tensile properties of the as-spun 75/25 N66/PPBT fiber it is evident that effective reinforcement by the PPBT has been achieved. The structure of the PPBT within the N66/PPBT composite fiber is discussed in Chapter 4.

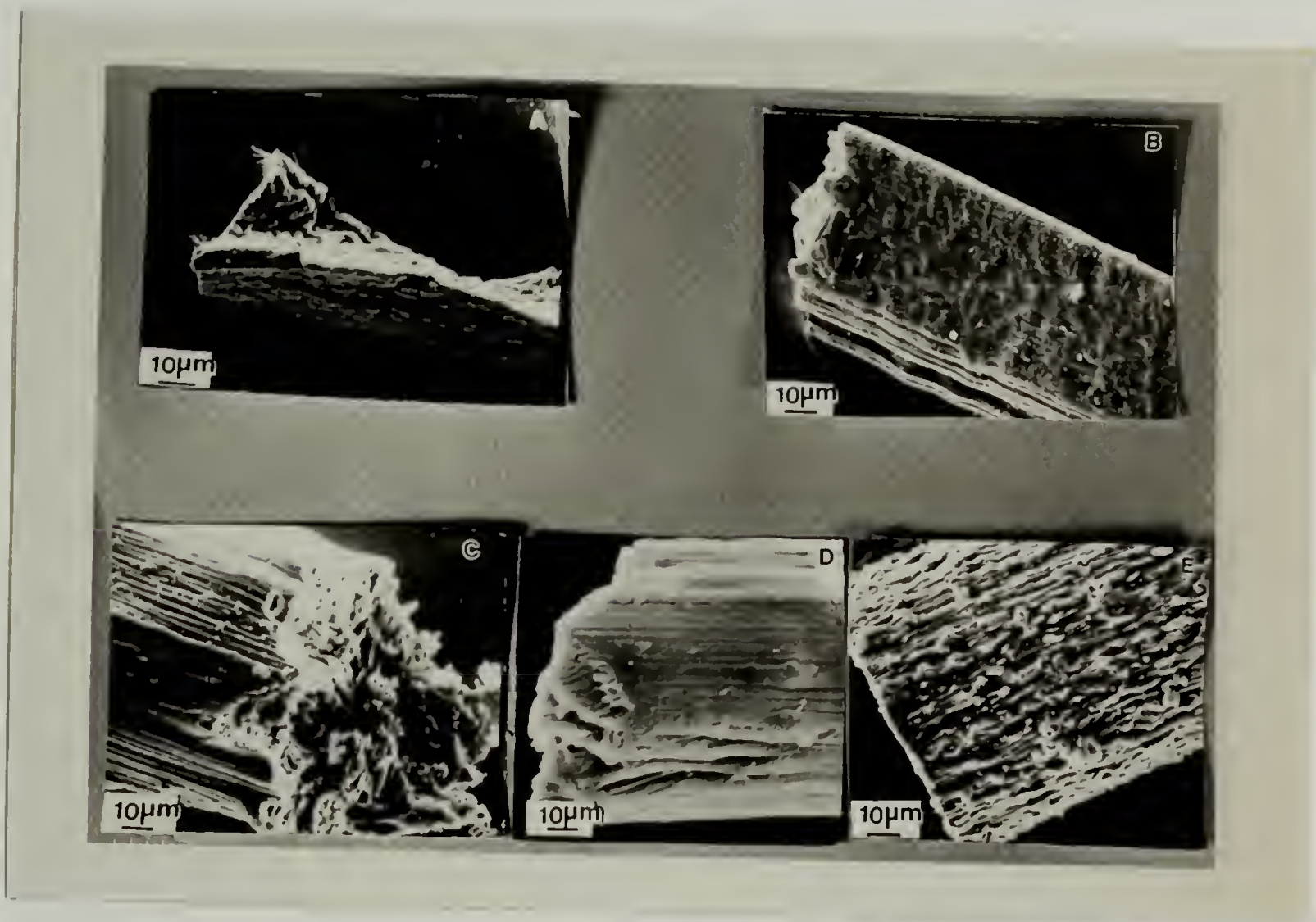


Figure 3.10 Scanning electron micrographs of as-spun 75/25 N66/PPBT30 fibers spun from (a) 1.0% solution, (b) 2.0% solution, (c) 3.0% solution, (d) 3.7% solution, (e) 4.0% solution.

3.5 Summary

The solubility of the matrix has an important effect on the processing of the as-spun composite fiber. If the matrix has approximately the same solubility as the rigid rod polymer, as with PEEK and PPBT, the matrix polymer can interfere with the coagulation of the PPBT. This type of composite system is strongly dependent upon the solution concentration of the processing solution. If, however, the matrix is much more soluble than the rigid rod, as is the case with N66 and PPBT, the matrix does not interfere with the rigid rod polymer during the coagulation process. For the latter system, the fiber properties are relatively insensitive to the concentration of the processing solution. The tensile properties of 75/25 PEEK/PPBT fibers have been shown to strongly depend on the concentration of the processing solution. Isotropic solutions of PEEK/PPBT/MSA close to the critical concentration produce fibers of poor modulus and strength. During the coagulation process, such solutions presumably undergo phase separation. However, by processing from a solution well below the critical concentration, a stiff strong as-spun fiber can be prepared. In contrast, the tensile properties of N66/PPBT fibers are relatively insensitive to the concentration of the isotropic spinning solution except at low concentrations. From the solubility data in Chapter 2, it can be anticipated that the

coagulation of PPBT will not be hindered by the presence of N66. An anisotropic N66/PPBT/MSA spinning solution results in a fiber of approximately half the strength and modulus of a fiber spun from an isotropic solution.

Fibers that are effectively reinforced by PPBT have been prepared. The structure of the PPBT within these composite fibers is the focus of Chapter 4.

CHAPTER 4

PPBT NETWORK STRUCTURE

4.1 Introduction

In this chapter, the structure of the PPBT reinforcing the composite fibers of PEEK/PPBT and N66/PPBT is investigated. The mechanical properties of the wet, as-spun, and heat-treated fibers are investigated to study the effect of post-processing. The thermal properties of the as-spun and heat-treated fibers are investigated.

The presence of the matrix material may hinder the formation of a continuous PPBT phase and result in the formation of discrete domains of PPBT as discussed in Chapter 3. By contrasting the behavior of the PEEK/PPBT30 fibers to those of N66/PPBT30 the effect the matrix polymer has on the structure and properties of the composite fiber is gained.

4.2 Background

Many solution spun fibers form a fibrillar network structures, ⁽⁸³⁾ e.g., nylon 6,6, ⁽⁸⁴⁾ acrylic ⁽⁸⁵⁾, polybenzylglutamate ⁽⁸⁶⁾. Pottick and Farris ⁽⁸⁷⁾ recently presented mechanical property measurements that are consistent with the presence of a network structure in PPBT fibers

prepared by dry-jet wet spinning from anisotropic poly(phosphoric acid) solutions. It was shown that the force to break an as-spun filament of PPBT was equivalent to the force required to break the as-coagulated, wet fiber.

More direct morphological evidence of the network structure was obtained by Cohen and Thomas (88,89). The microfibrils in PPBT fibers are estimated to be approximately $80 - 100 \text{ \AA}$ in diameter.

The morphology of N66/PPBT "molecular" composites was recently investigated using small angle x-ray scattering. (90) This study indicated that phase separation in the composite samples occurred on the scale of approximately 70 \AA which is comparable to the PPBT reported by Cohen and Thomas. (88,89) It was concluded that these composites consists of a microfibrillar PPBT structure in a crystalline N66 phase.

4.3 Experimental Methods

Differential scanning calorimetry, DSC, scans were obtained in a Perkin-Elmer DSC at a heating rate of $10^\circ\text{C}/\text{min}$. A Perkin-Elmer thermal mechanical analyzer, TMA, was also used to obtain the strain versus temperature scans for fiber. The special fiber and film testing attachment was employed. The fiber was crimped between the metal clips and secured in place with a drop of epoxy that was cured for 30 minutes. The fiber was gently placed into the holder,

and subjected to a tensile load of 2.5 grams. The fiber was heated at a rate of 10°C/min while the displacement of the fiber was monitored.

Wet fibers were tested on a Toyo Testing Machine. A mechanical grip immersed in a two liter beaker of water was attached to the crosshead. A loop of wet fiber was secured by the free ends in this mechanical grip. The looped fiber was attached with a wire hook to a 550 g compression and tension load cell and tested at a rate of 0.2 cm/min. The force required to break the fiber was determined; the fibers which failed at the grip or hook due to the stress concentrations were discarded. The wet fiber diameters were measured with an optical microscope.

4.4 PEEK/PPBT Fiber Spun from 2.0% Solutions

4.4.1 Results

In Chapter 3, 2.0 wt% of total polymer was found to be an optimum processing concentration for preparing an as-spun 75/25 PEEK/PPBT fiber. Consequently, fibers of various PEEK/PPBT composition were wet-spun from a 2.0% solution in MSA. This concentration is also convenient, since the entire spectrum of compositions from 0 to 100% PPBT are isotropic. The as-spun fibers were heat-treated with a two minute residence time at 425°C without tension. Figures 4.1a and 4.1b show the tensile modulus and strength for these fibers versus the weight percent of PPBT. The as-spun

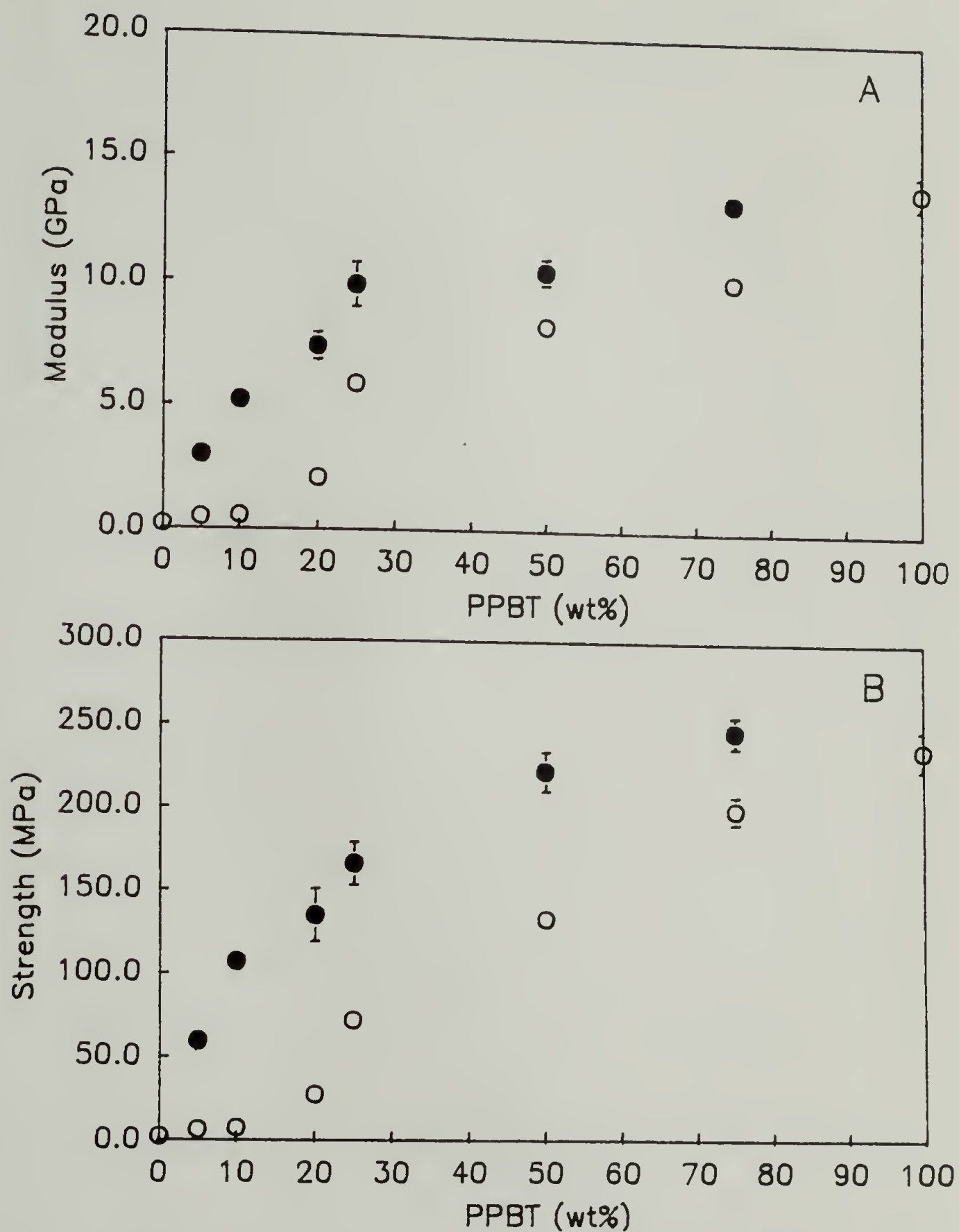


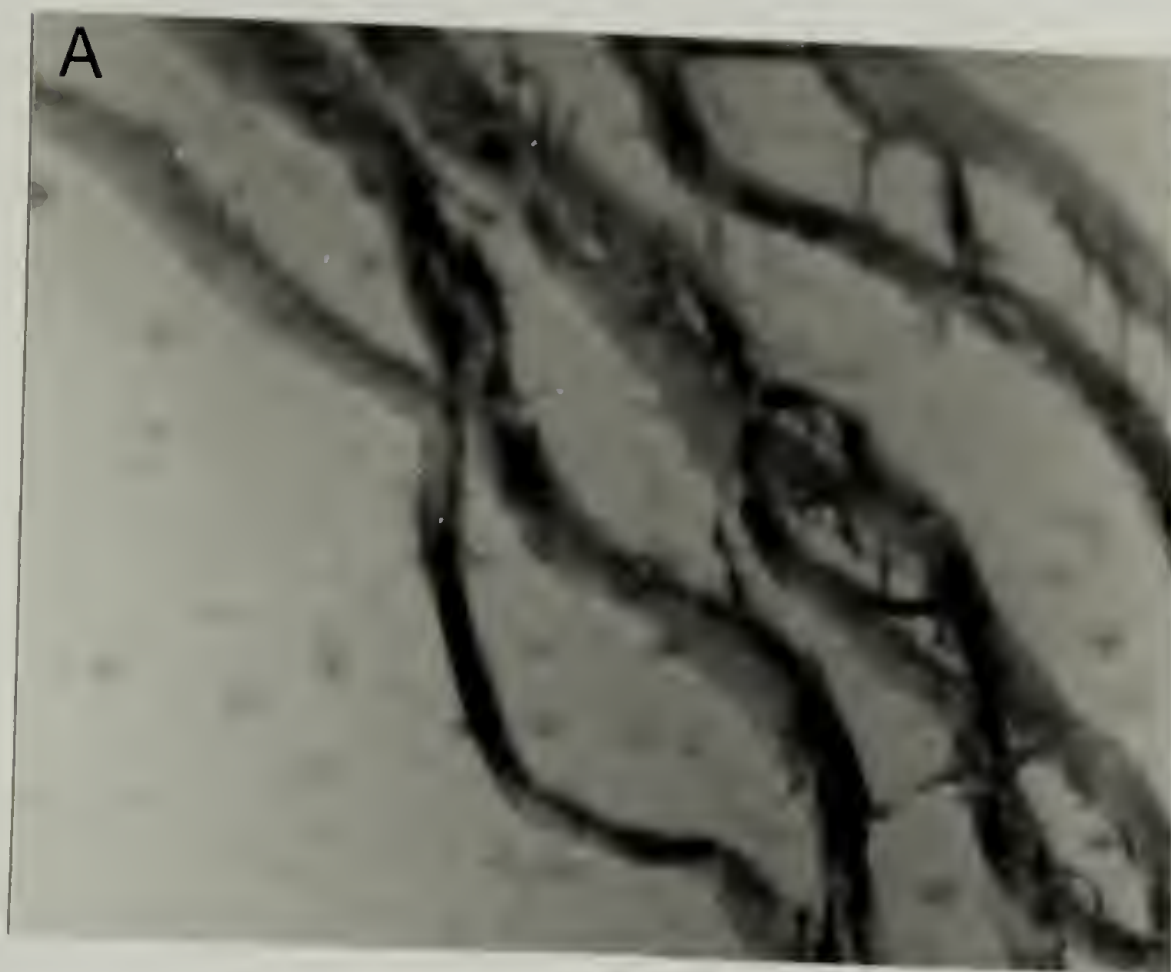
Figure 4.1 Tensile properties for PEEK/PPBT30 fibers, as-spun (○) and heat treated (●) at 425°C with no tension, spun from 2.0% solution in MSA, (a) modulus, (b) strength. Error bars represent the standard deviation from the average calculated from at least five samples, which appears only if greater than the symbol size.

fiber modulus and strength increase with increasing PPBT content. The heat-treated fibers were stiffer and stronger than the corresponding as-spun fibers.

The microstructure of the PPBT reinforcing these composite fibers was examined by selectively removing the PEEK with H_2SO_4 , a solvent for PEEK but a non-solvent for PPBT. Examination of these residual fibers revealed a continuous network-like structure of PPBT. Figure 4.2a shows a typical micrograph of the PPBT structure observed in an as-spun 90/10 PEEK/PPBT fiber. The PPBT is distributed in a fibrillar network that spans the fiber length. Similar network structures of PPBT have been observed for PEEK/PPBT fibers spun from a 2.0% solution with various PPBT contents.

4.4.2 Discussion

A network-like structure of PPBT reinforcing these fibers is consistent with their mechanical properties. First, the dramatic increase in the as-spun modulus and strength when the PPBT content is increased from 20 to 25 wt% may be associated with the onset and perfection of the network continuity. This dramatic increase in tensile modulus and strength is consistent with a percolation-type threshold. Secondly, these fibers were heat-treated at 425°C which is well above the melting point of PEEK ($T_m = 344^\circ\text{C}$). The fiber could only be heat-treated at such



←→
200 μm

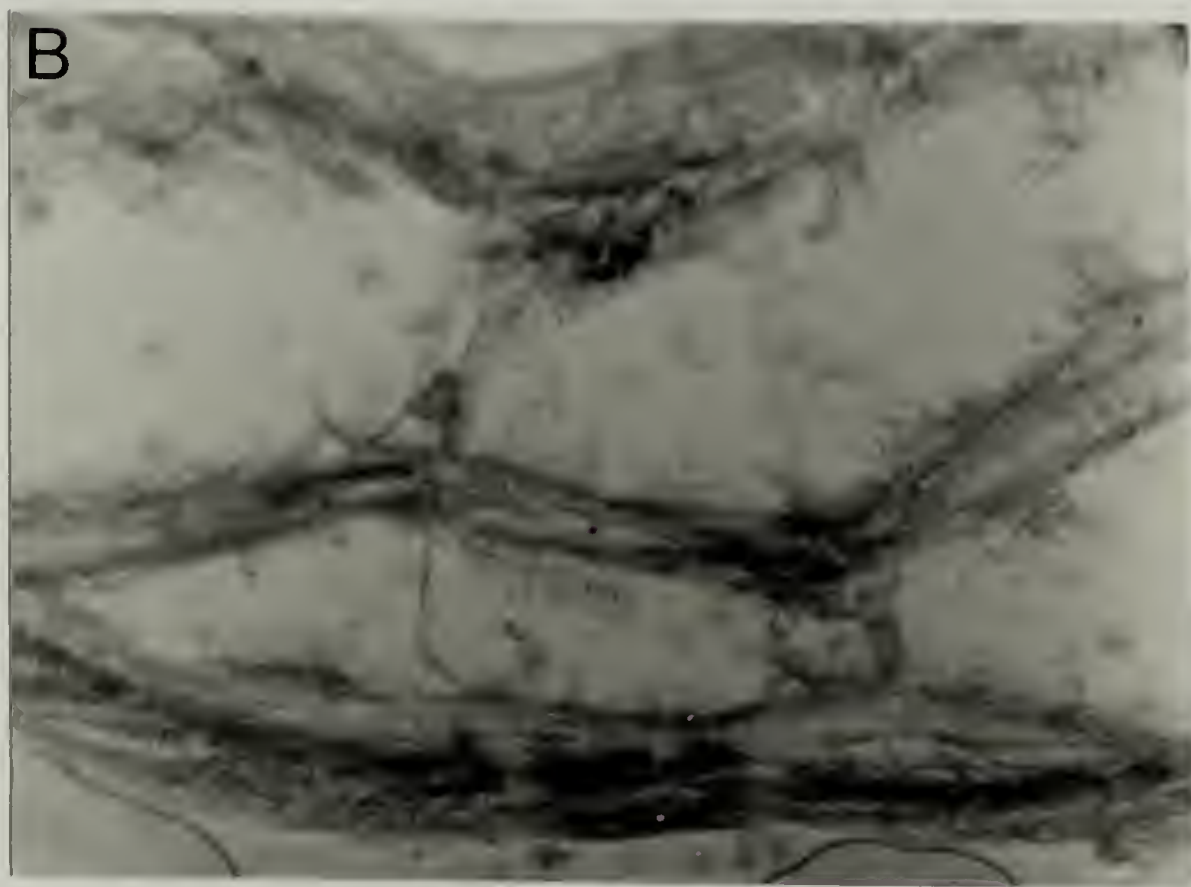


Figure 4.2 Optical micrograph of an (a) as-spun and (b) heat treated at 425°C 90/10 PEEK/PPBT30 fiber spun from a 2.0% concentration solution after being soaked in H_2SO_4 for over four weeks.

extreme temperatures if a network of PPBT acts as a support. After heat-treatment, the modulus and strength of fibers containing less than 25% PPBT are substantially enhanced. As reported by Chauh, (52) when the composite fiber is heated above the melting point of the matrix the mobility of the PPBT would be increases. Thus during heat-treatment, above the melting point of PEEK, it is expected that the PPBT microfibrils may coalesce. It has been shown that heat-treatment of PPBT fibers increases the orientation in the axial direction. (79,80) Therefore, heat-treatment of the composite fibers would be expected to improve the axial orientation of the PPBT phase, aligning the PPBT fibrils. A significant increase in mechanical properties would be expected if the PPBT network continuity is improved during heat-treatment, which is believed to be the case for fibers having less than 25% PPBT. After heat-treatment the modulus and strength appear to be proportional to the percent of PPBT in the fiber contrasting the dramatic increase in tensile properties at 20 -25 wt.% PPBT for the as-spun fiber.

The strain to break of the as-spun and heat-treated fibers is also consistent with a fibrillar microstructure of PPBT that is perfected during the heat-treatment process. (Figure 4.3) The strain of the as-spun fibers with PPBT contents less than 25 wt.% are essentially equivalent to that for the as-spun PEEK fiber. After heat-treatment,

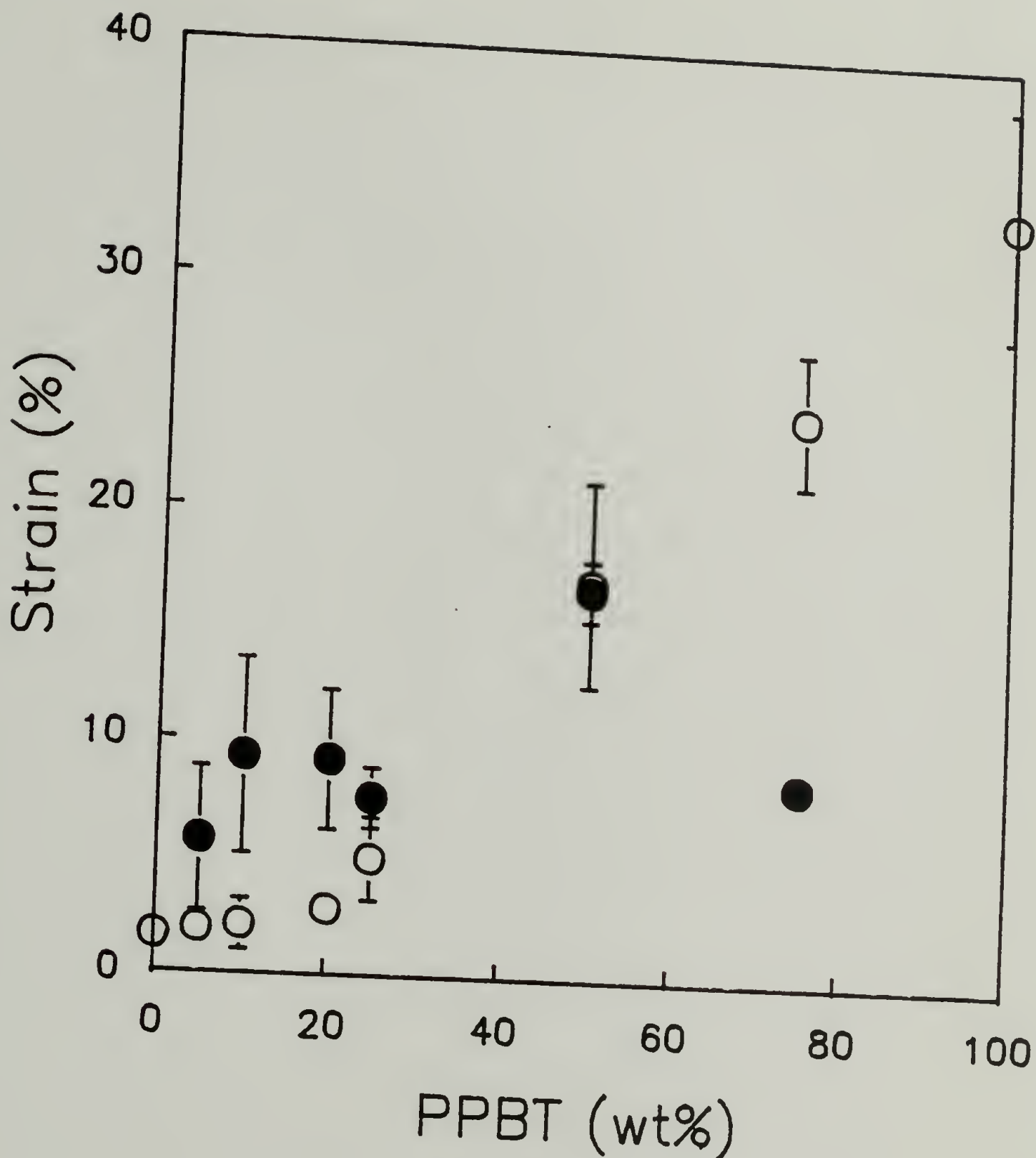


Figure 4.3 Tensile strain at break for PEEK/PPBT30 fibers, as-spun (○) and heat-treated (●) at 425°C with no tension, spun from a 2.0% solution in MSA. Error bars represent the standard deviation from the average calculated from at least five samples, which appears only if greater than the symbol size.

the strain to break of these fibers is greatly increased. Since as-spun PPBT has a higher strain to break than as-spun PEEK, a composite fiber reinforced by a network of PPBT would be expected to have a greater strain to break than as-spun PEEK. Therefore, the increase in strain to break for fibers of less 25 wt.% PPBT after heat-treatment is indicative of the PPBT network being perfected during heat-treatment.

The structure of the PPBT within the as-spun and heat-treated 90/10 PEEK/PPBT30 were examined using optical microscopy as shown in Figure 4.2. After heat-treatment, the PPBT is aggregated into denser fibrils. The PPBT is reorganizing during the heat-treatment process, resulting in improved continuity of the PPBT within the composite fiber. For completeness, a comparison was made of the mechanical properties of a 75/25 PEEK/PPBT as-spun fiber heat-treated at 425°C and 265°C (a good crystallization temperature for PEEK). The tensile properties are summarized in Table 4.1. Fibers heat-treated below the melting of PEEK had inferior properties to those of the fibers heat-treated well above the melting point of PEEK. The greater mobility of the PPBT within a composite fiber heat-treated above the melting point of the matrix polymer, allows the PPBT to form a more perfected network than can be formed by heating above the glass transition temperature of the matrix.

Table 4.1
 Mechanical Properties of 75/25 PEEK/PPBT Heat Treated
 at 265°C and at 425°C

	<u>Modulus (GPa)</u>	<u>Strength (MPa)</u>	<u>Strain (%)</u>
75/25 AS	5.9 ±0.3	72 ±2	5.0 ±1.8
75/25 AS HT 265°C	7.6 ±0.7	110 ± 6	2.7 ±0.4
75/25 AS HT 425°C	9.9 ±0.9	166 ±13	7.6 ±1.3

4.5 The Effect of PPBT Composition

The solution concentration has a strong effect upon the as-spun fiber properties for compositions of less than 30 wt% PPBT. In this section, the effect of concentration is investigated for fibers having a range of PPBT compositions.

It is instructive to consider percolation concept when discussing the effect of PPBT composition. If rods are added to a fixed volume, there is a concentration at which the rods will form a continuous structure that spans the sample. This "percolation limit" or "threshold" depends on the aspect ratio of the rod and the orientation of the rods. The lower bound for the percolation limit can be calculated from chain forming theory as (91)

$$V_f = 1.6 / [3 + 2(L/D)] \quad (4.1)$$

where V_f is the volume fraction of rod and L/D is aspect ratio for rod. (It is interesting to note that the percolation threshold for large L/D is $0.8/(L/D)$, which is an exactly one tenth of the volume fraction calculated by Flory⁽²⁷⁾ for the formation of an anisotropic phase.) The aspect ratio for PPBT30 is approximately 300. From equation 4.1, the percolation threshold for PPBT is 0.265 volume percent.

Figure 4.4 shows the as-spun modulus and strength versus the concentration of the spinning solution for PEEK/PPBT fibers of 25, 50, and 75 % PPBT. The data for the 25% PPBT fiber was shown in Figure 3.6. The modulus and strength for the 1% 75/25 PEEK/PPBT30 fiber is low compared to that for the fiber spun from a 2.0 or 2.5% solution. The PPBT concentration in the 1.0 % solution is only 0.25 wt%. According to the statistical estimate for the percolation limit, this solution would not have the PPBT spanning the solution phase which would result in a poorly-connected PPBT network. Below the percolation limit, the continuity of the PPBT in solution with PEEK present is not enough to result in the formation of a strong-well connected PPBT phase in the coagulated fiber, although a PPBT fiber may be spun from a 0.01% solution of PPBT30 in MSA.

The structure of the PPBT within these fibers was examined by removing the PEEK with H_2SO_4 , as previously described. Typical optical micrographs for these fibers are shown in Figure 4.5. The PPBT structure in the 75/25 PEEK/PPBT fiber spun from a 1.0% solution, shown in Figure 4.5a, is not fibrillar. In fact, if the coverglass is sheared slightly, the PPBT structure is observed to break up into short lengths.

The PPBT in the fiber spun from a 2.0% solution was distributed in a continuous fibrillar structure as shown in

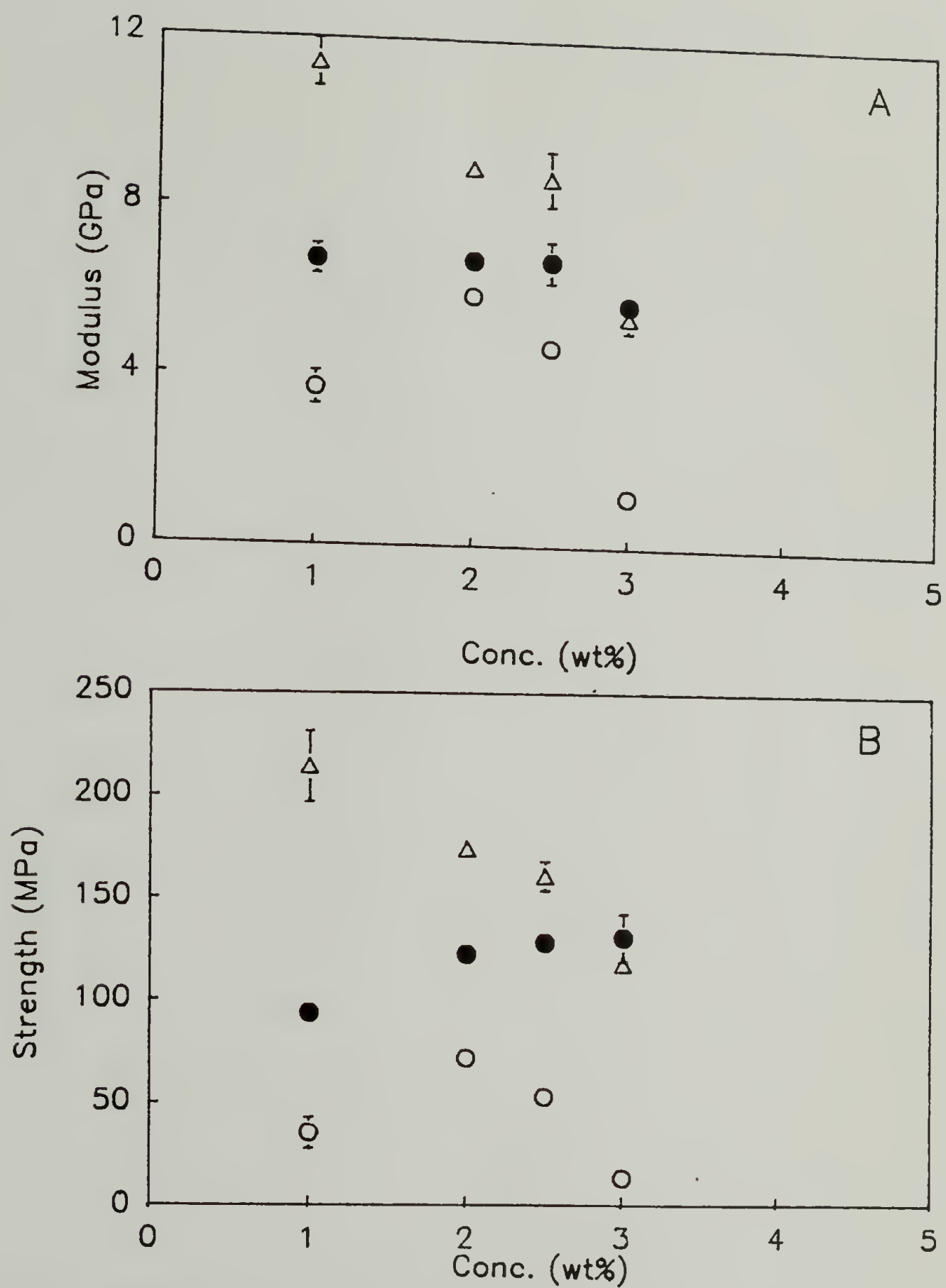


Figure 4.4 Tensile properties for as-spun 75/25 (○), 50/50 (●), 25/75 (△) PEEK/PPBT30 fibers vs. the total polymer concentration, (a) modulus, (b) strength. Error bars represent the standard deviation from the average calculated from at least five samples, which appears only if greater than the symbol size.

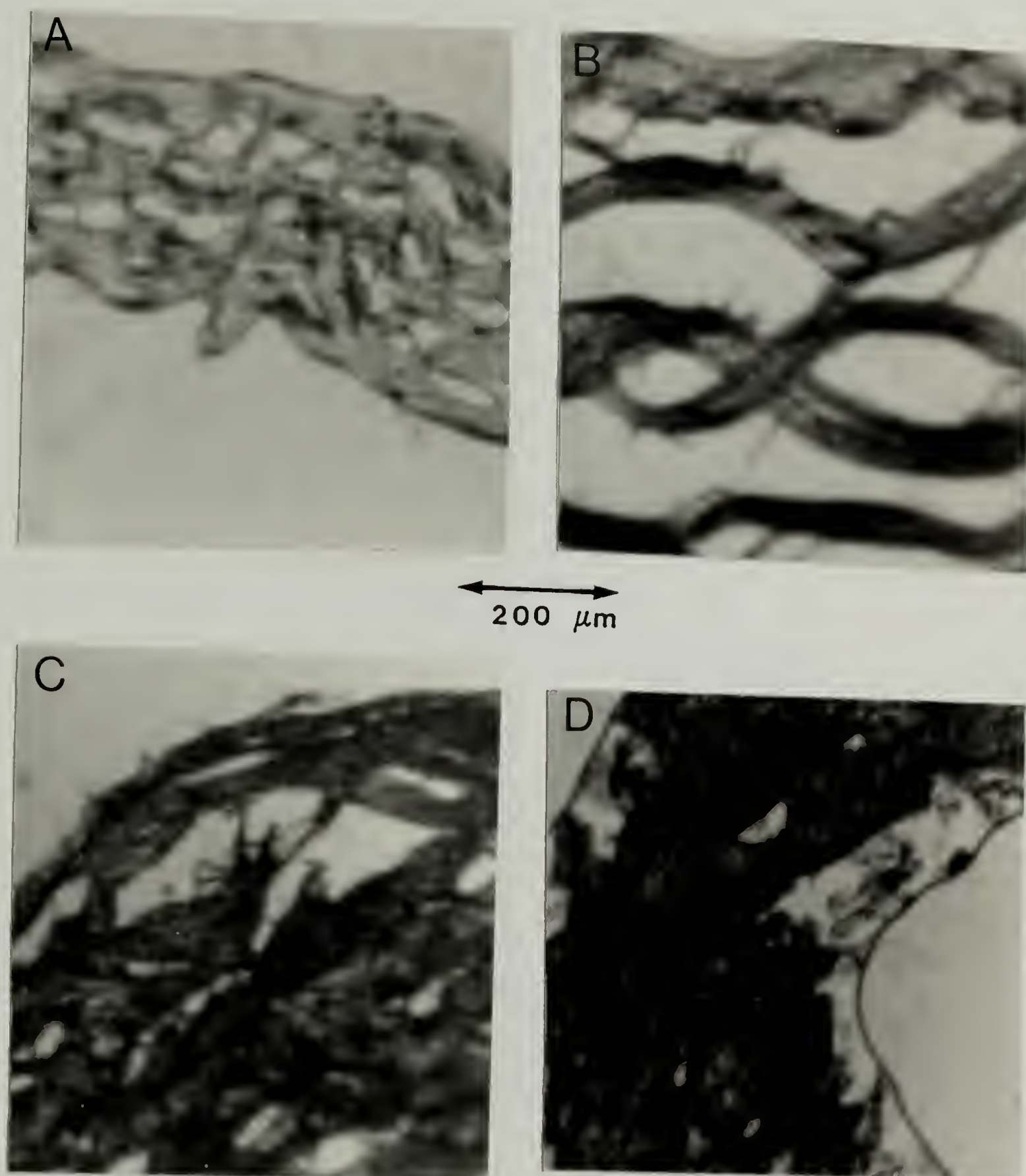


Figure 4.5 Optical micrographs of a single as-spun 75/25 PEEK/PPBT fiber soaked in H_2SO_4 for several weeks (a) spun from a 1.0% solution, (b) spun from a 2.0% solution, (c) spun from a 3.0% solution, (d) spun from a 4.0% solution.

Figure 4.5b. Many PPBT fibrils are interconnected across the fiber diameter and this is actually a three dimensional structure which has been collapsed into a two dimensional image.

As the solution concentration was increased to 3.0%, the PPBT formed the denser fibrillar structure seen in Figure 4.5c. The fibrils are loosely connected. The fiber spun from a 4.0% solution has the PPBT distributed in dense isolated domains, similar to those seen in Figure 3.5. In contrast to the strong dependence of the 75/25 PEEK/PPBT fiber properties on solution concentration, the mechanical properties for an as-spun 50/50 fibers are insensitive to the solution concentration. The processing solutions have enough PPBT to result in the formation a continuous phase of PPBT in the coagulated fiber. Similarly, fibers having 75 wt% PPBT were insensitive to the concentration of the processing solution. In fact, a fiber spun from an anisotropic solution of 3.0% had a stiffness and strength about half that of a fiber spun from an isotropic solution. Apparently, in the case of the higher composition PPBT fibers (greater than 25 wt% PPBT) there is enough PPBT form a continuous phase in the presence of PEEK, regardless of the processing concentration.

4.6 Thermal Characterization

4.6.1 Differential Scanning Calorimetry

DSC scans of all compositions of the composite fibers were obtained. If the PPBT was dispersed on a molecular level throughout the PEEK, then a single T_g and T_m , higher than that of PEEK would be expected. If, however, the composites had the same T_g and T_m as the neat matrix, which would be indicative of matrix domains with a characteristic size of at least 300 . Thus, DSC was used to provide further evidence for the presence of a PPBT network reinforcing these composite fibers.

DSC scans of as-spun 75/25 PEEK/PPBT fibers spun from 2.0, 3.0, and 4.0% solution are compared to that for a 3.0% as-spun PEEK fiber in Figure 4.6. The composite fibers have essentially the same thermal transitions as the PEEK fiber. The glass transition of PEEK is observed at about 143°C, after which crystallization occurs. The crystallization exotherm is a few degrees lower for the composite fibers; a consequence of the PPBT which may act as a nucleating site for crystallization of the PEEK. The characteristic two peak melting endotherm is observed.^(87,88) The lower melting (at about 320°C) is associated with smaller, less perfect crystallites. The higher melt endotherm ($T_m = 344^\circ\text{C}$) corresponds to larger, more perfect crystals.

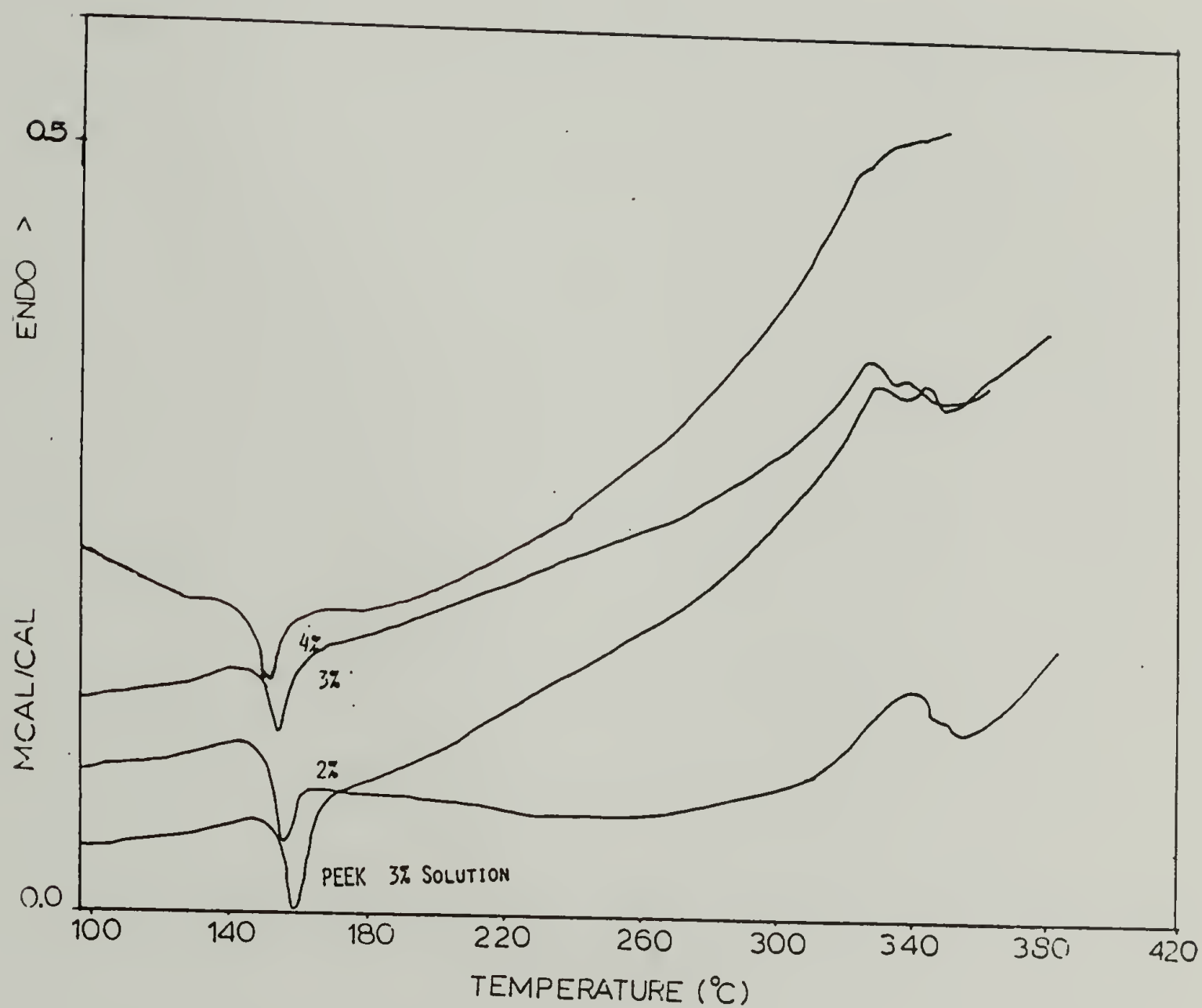


Figure 4.6 DSC scans for as-spun 75/25 PEEK/PPBT30 spun from 2.0%, 3.0%, and 4.0% solutions in MSA and for as-spun PEEK fiber spun from a 3.0% solution.

Figure 4.7 shows the DSC scan for an as-spun and heat-treated (425°C) 95/5 PEEK/PPBT. The as-spun fiber undergoes recrystallization and exhibits characteristic melting endotherm. A second scan exhibits only a single higher melting point, associated with the crystals perfected during crystallization. Similarly, after heat-treatment, a single higher melting endotherm is observed as seen in Figure 4.6.

All compositions of as-spun PEEK/PPBT fibers were analyzed with DSC, and found to exhibit essentially the same thermal transitions as an as-spun PEEK fiber. Phase transitions with the DSC are indicative of the existence of PEEK with characteristic domains of at least 300 .

4.6.2 Thermal Mechanical Analysis

The thermal expansion of the PEEK/PPBT30 composite fibers was investigated using a thermal mechanical analyzer, TMA, using a tension of approximately 20 MPa. If a continuous phase of PPBT is reinforcing the composite fibers, little deformation would be expected as the composite is heated above the T_g of PEEK and the thermal expansion behavior of PPBT should dominate the composite response.

Figure 4.8a shows the elongation vs. temperature curve for a 2.0% as-spun PPBT fiber. Essentially no dimensional changes result upon heating from 50°C to 100°C and subsequent cooling to 50°C. The fiber is then heated up to 200°C, and some elongation occurs above 100°C. Subsequent

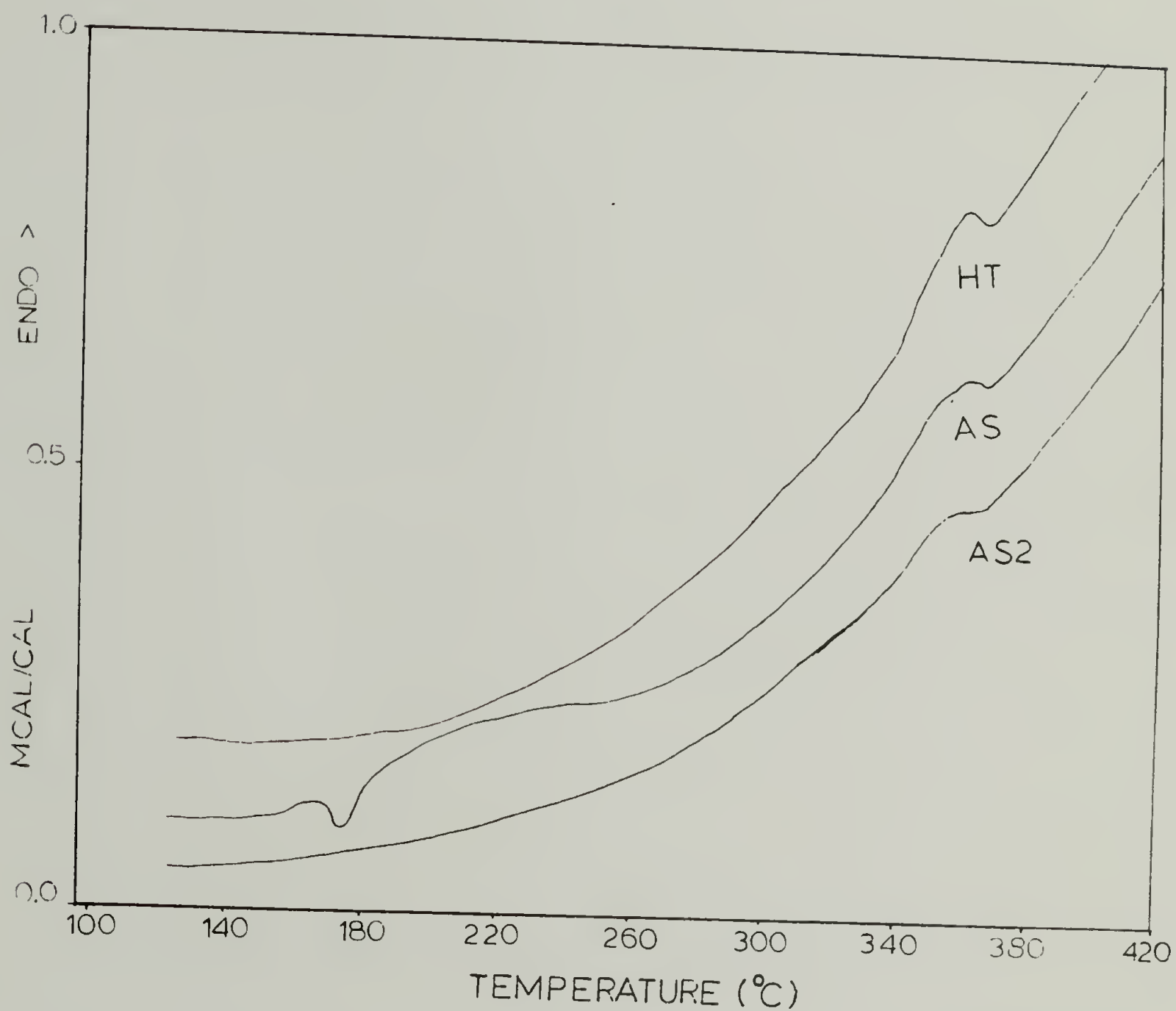


Figure 4.7 DSC scans for as-spun first run, AS, as-spun second run, AS2, and heat-treated, HT, at 425°C, 90/10 PEEK/PPBT30 fiber.

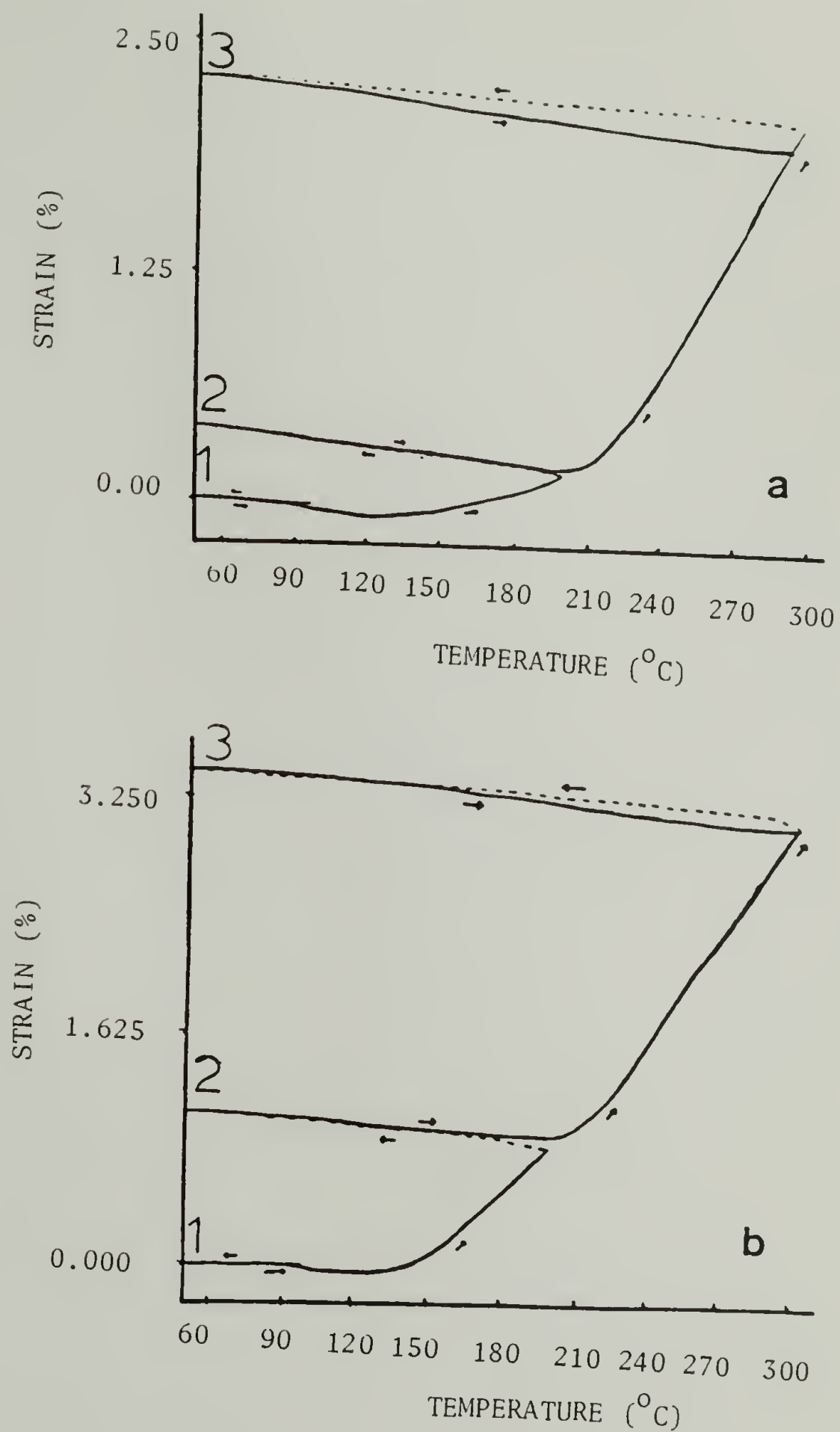


Figure 4.8 TMA curves for an as-spun fiber of (a) PPBT30 spun from 2.0% solution, (b) 75/25 PEEK/PPBT30 spun from a 2.0% solution.

cooling to 50°C results in a slight shrinkage of the fiber. Upon reheating to 300°C, the fiber is dimensionally stable to temperatures it has been previously exposed. Cooling to 50°C and reheating to 300°C, the fiber exhibits a negative thermal expansion coefficient, which is consistent with reported force-temperature for PPBT dry-jet wet spun from an anisotropic polyphosphoric acid solution.(94)

The elongation versus temperature curve for a 2.0% 75/25 PEEK/PPBT as-spun fiber is shown in Figure 4.8b. The first heating through the T_g of PEEK, about 140°C, results in elongation of the fiber. Cooling the fiber from 200 to 50°C, caused only a slight shrinkage of the fiber. Heating to 300°C, it is apparent that the composite fiber, as with the neat PPBT fiber spun from a 2.0% solution, is dimensionally stable to temperatures it which it has been exposed. Cooling to 50°C, and reheating to 300°C shows the thermal expansion behavior of PPBT dominates the composite fiber. This behavior is consistent with the concept of a continuous phase of PPBT propagating throughout the fiber.

4.6.3 Thermal Removal of the Matrix

Nylon 6,6 was thermally degraded to allow the residual PPBT structure to be tensile-tested. If a continuous phase of PPBT is present, then the residual structure should be able to sustain a significant fraction of the the composite fiber's breaking load. From thermal gravimetric analysis,

Nylon 6,6 degrades at 400°C. By placing a 50/50 N66/PPBT fiber in an oven at 425°C for four hours the N66 was thermally removed from the composite fiber. The residual fiber was tensile tested and the properties are compared to those for the as-spun fiber in Table 4.2. The decrease in fiber diameter corresponds to a 50% loss in volume.

The residual fiber has a higher strength and modulus than the as-spun fiber. The fiber is very brittle, the strain to break is very low, as a result of the extensive heat-treatment. It is important to note that the burned fiber can carry two thirds of the force carried by the as-spun fiber. This observation indicates that the structure of PPBT within the composite fiber bears a significant portion of the load and is consistent with a network of PPBT reinforcing the composite fiber.

4.7 Fiber Wet Strength

4.7.1 Results

Pottick and Farris gave evidence for a continuous network microstructure in PPBT fibers by demonstrating that the force to break of the wet fiber was equivalent to that of the dry fiber. (87) Similar measurements have been made of the breaking force for wet composite fibers. A composite fiber reinforced by a continuous PPBT phase should have a

Table 4.2
 Mechanical Properties of As-spun and Extended Heat-treatment
 50/50 N66/PPBT36 Fiber

	<u>Diam (μm)</u>	<u>Modulus (GPa)</u>	<u>Strength (MPa)</u>	<u>Breaking Force (g)</u>
AS	69	7.0 ± 0.3	151 ± 5	58.2 ± 2.6
425°C 4 hr.	49	16.2 ± 0.8	205 ± 14	39.0 ± 2.5

wet breaking force which is a significant fraction of its dry breaking force.

PEEK/PPBT30 and N66/PPBT30 fibers of various weight percent PPBT30 were spun from 2.0% total polymer solutions. The ratio of the breaking force for the wet fiber to that of the as-spun fiber versus wt.% of PPBT is shown in Figure 4.9. The breaking force of the all of the as-spun fibers is greater than the corresponding wet fibers. The ratio of the breaking force for the as-spun fiber to that for the wet fiber is seen to decrease with increasing PPBT content for the N66/PPBT30 fibers as shown in Figure 4.9. The ratio of dry to wet breaking force for the PEEK/PPBT fibers is a maximum at about 20% PPBT. The behavior at 20% PPBT and higher follows that of N66/PPBT.

4.7.2 Discussion

All the wet fibers spun with a 330 μm die had diameters of 320 μm , except the 90/10 N66/PPBT fiber which had a wet diameter of about 220 microns. The small diameter for the 90/10 N66/PPBT fiber is a consequence of the 2.0% 90/10 N66/PPBT solution containing only 0.2 wt% PPBT and N66 being very soluble in MSA and water mixtures. Apparently before the solution coagulates, it is drawn down significantly by gravity during the spinning process. The other composite fibers having a wet diameter of 320 microns are coagulated very near the entrance of the 330 micron die.

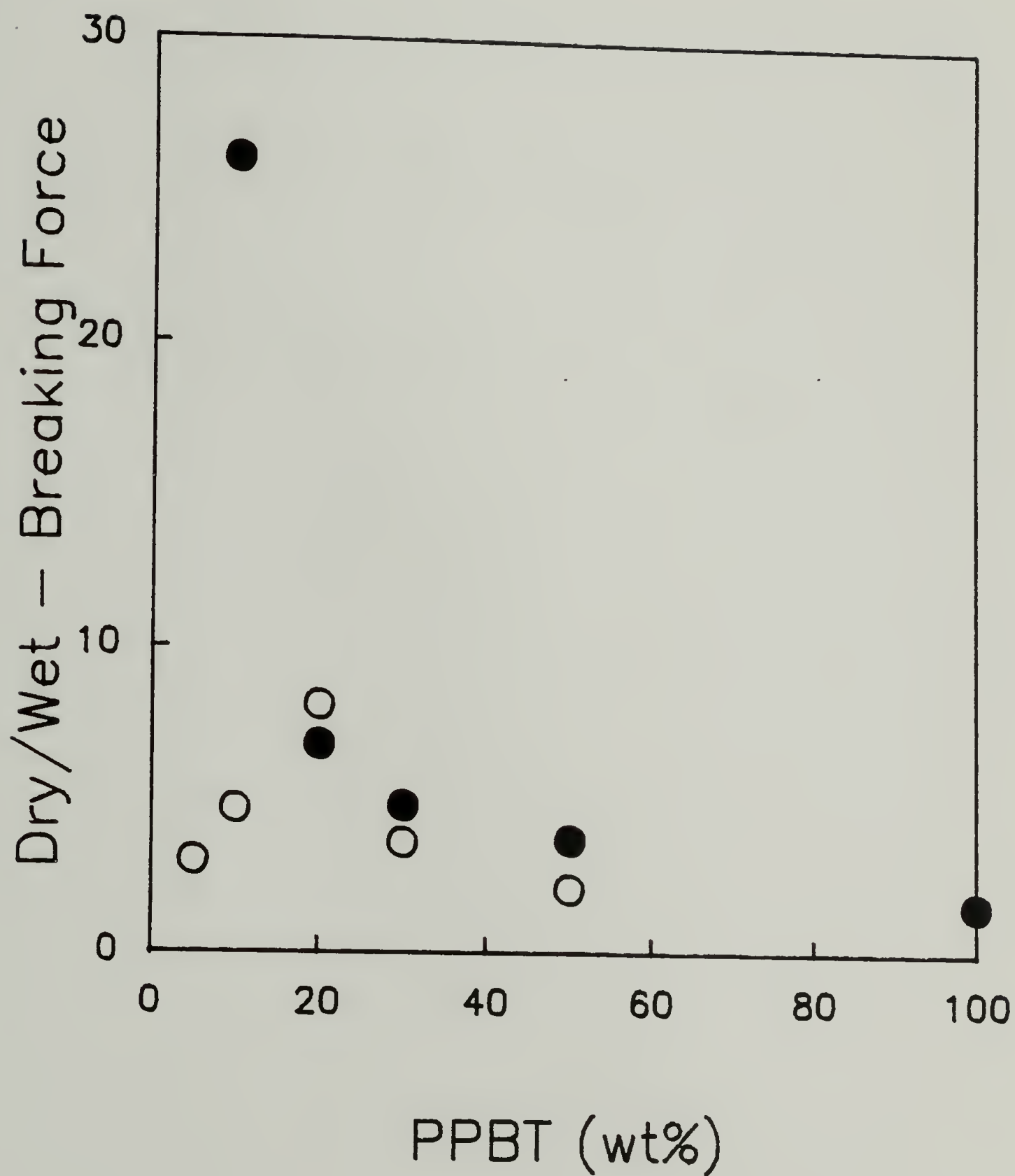


Figure 4.9 Ratio of the dry to wet breaking force for N66/PPBT30 (●) and PEEK/PPBT30 (○) fibers spun from 2.0% solution.

Upon drying the fiber diameter decreases by about 75% which results in the PPBT fibrils within the wet fiber collapsing upon each other and orienting. Thus, drying perfects the continuity of the PPBT network structure in the wet composite fiber which increasing the load bearing ability of the resultant as-spun fiber.

For the N66/PPBT fibers, the ratio of the wet to as-spun fiber breaking force increasing with increasing PPBT. At high PPBT contents the ratio of the wet to dry fiber breaking force approaches one, which is the ratio reported for dry-jet wet spun PPBT.⁽⁸⁷⁾ As the PPBT content is increased the network structure in the wet fiber is improved and load bearing ability of the wet fiber approaches that of the as-spun fiber.

The behavior of the PEEK/PPBT30 fibers differs from that of the N66/PPBT fiber with less than 20% PPBT. From Figure 4.1, the modulus and strength of as-spun PEEK/PPBT fibers increased dramatically between 20 and 25% PPBT content, corresponding to a percolation threshold. The strength of as-spun PEEK/PPBT fibers of less than 25% PPBT content was essentially the same as the strength of as-spun PEEK. The PPBT within the PEEK/PPBT fibers having a PPBT content below 20% PPBT was prevented from forming a continuous phase in the wet fiber because of the competitive coagulation rate of PEEK, and a continuous phase of PEEK formed in the wet and as-spun fiber. At less than 20% PPBT, the

properties of PEEK dominate the composite fibers of PEEK/PPBT. When there is more than 20% PPBT present, the PPBT forms a continuous phase during coagulation and this network is perfected during drying, and the PEEK/PPBT fibers behave like the N66/PPBT fibers as seen from Figure 4.9.

4.8 Post-Processing

4.8.1 Results

The properties for 90/10, 80/20, 70/30, 50/50 PEEK/PPBT30 and N66/PPBT30 composite fibers spun from MSA solutions of 2.0% total polymer concentration. The 70/30 and 50/50 fibers were wet-stretched; fibers of less than 30% PPBT were not amenable to wet-stretching due to their poor wet strengths. The N66/PPBT30 and PEEK/PPBT30 fibers were heat-treated for 2 minutes with tension at 305°C and 425°C, respectively. The motivation for preparing these fibers was to obtain the "best" fiber properties and investigate the effect of post-processing for PEEK/PPBT versus N66/PPBT fibers.

Figure 4.10 shows the as-spun modulus and strength for N66/PPBT fibers and PEEK/PPBT fibers spun 2.0% total polymer concentration solutions as a function of wt% PPBT. The tensile properties for PEEK/PPBT fibers containing less than 30% PPBT are inferior to N66/PPBT fibers of the same PPBT content, but the modulus and strength for the PEEK/PPBT30

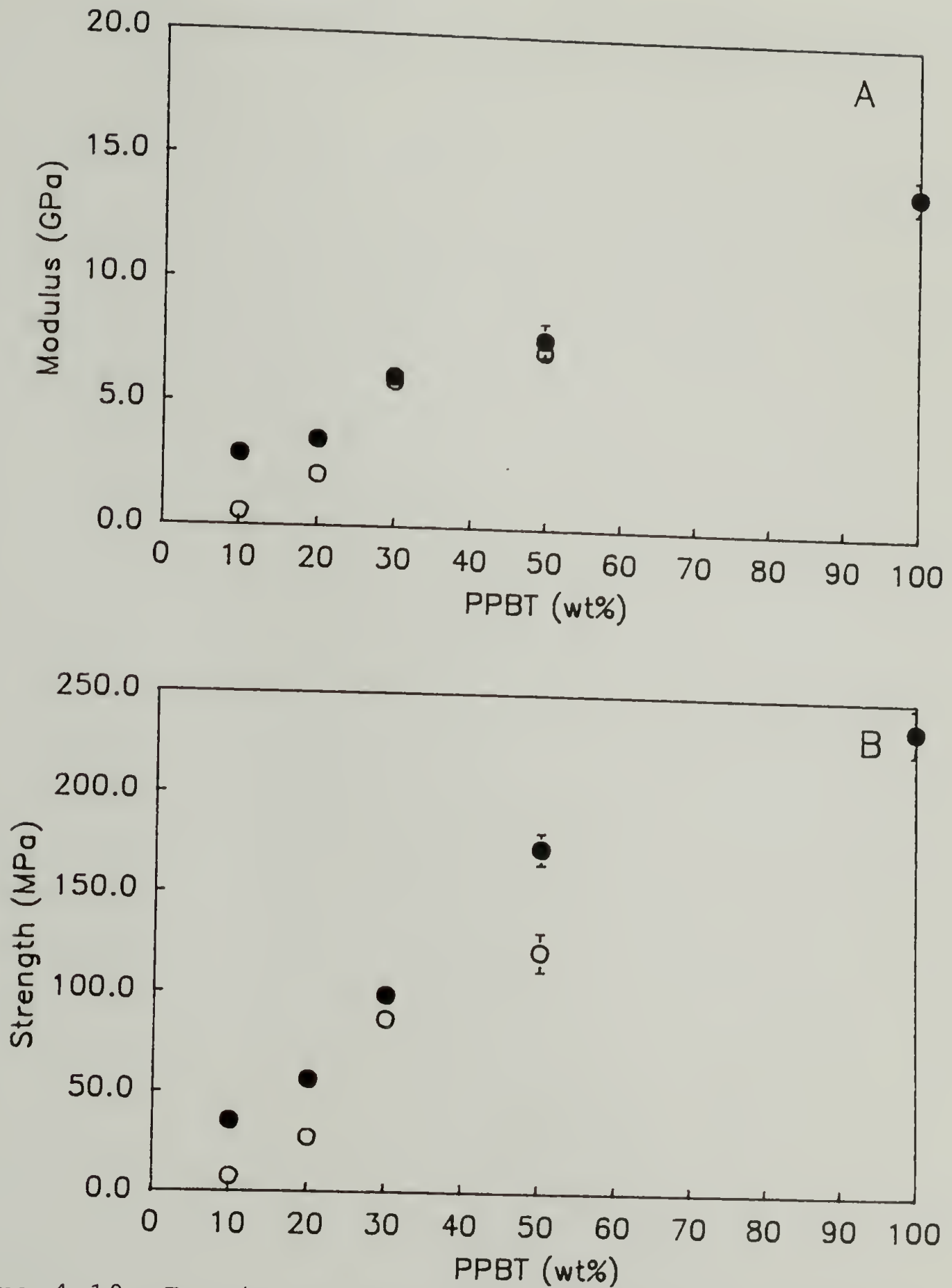


Figure 4.10 Tensile properties for as-spun PEEK/PPBT30 (○) and N66/PPBT30 (●) fibers vs. the wt% of PPBT, a) modulus, b) strength. Error bars represent the standard deviation from the average calculated from at least five samples, which appears only if greater than the symbol size.

and N66/PPBT30 fibers of 30 and 50% PPBT are essentially the same.

In Figure 4.11 the modulus and strength of the post-processed N66/PPBT and PEEK/PPBT fibers are plotted. The modulus and strength of PEEK/PPBT fibers are approximately equivalent to those of N66/PPBT fibers after post-processing. Typical stress-strain curve for an as-spun and heat-treated 90/10 and 50/50 PEEK/PPBT fibers are shown in Figure 4.12.

4.8.2 Discussion

The as-spun modulus and strength of the N66/PPBT30 fibers are superior to those of PEEK/PPBT30 containing 10 and 20% PPBT, since the N66 does not interfere with the coagulation of the PPBT, as a result of their different solubilities in MSA/water mixtures. In contrast, PEEK does restrict PPBT during the coagulation process, due to their similar solubilities. If there is enough PPBT present in the solution (above 20%) a PPBT network spanning the fiber length will be formed regardless of the solubility of the matrix; the properties of PEEK/PPBT and N66/PPBT are essentially equivalent for 30 and 50% PPBT.

Heat-treatment of the 90/10 and 80/20 PEEK/PPBT30 and N66/PPBT30 fibers perfects and improves the PPBT network. The structure of the PPBT in the as-spun fibers can be

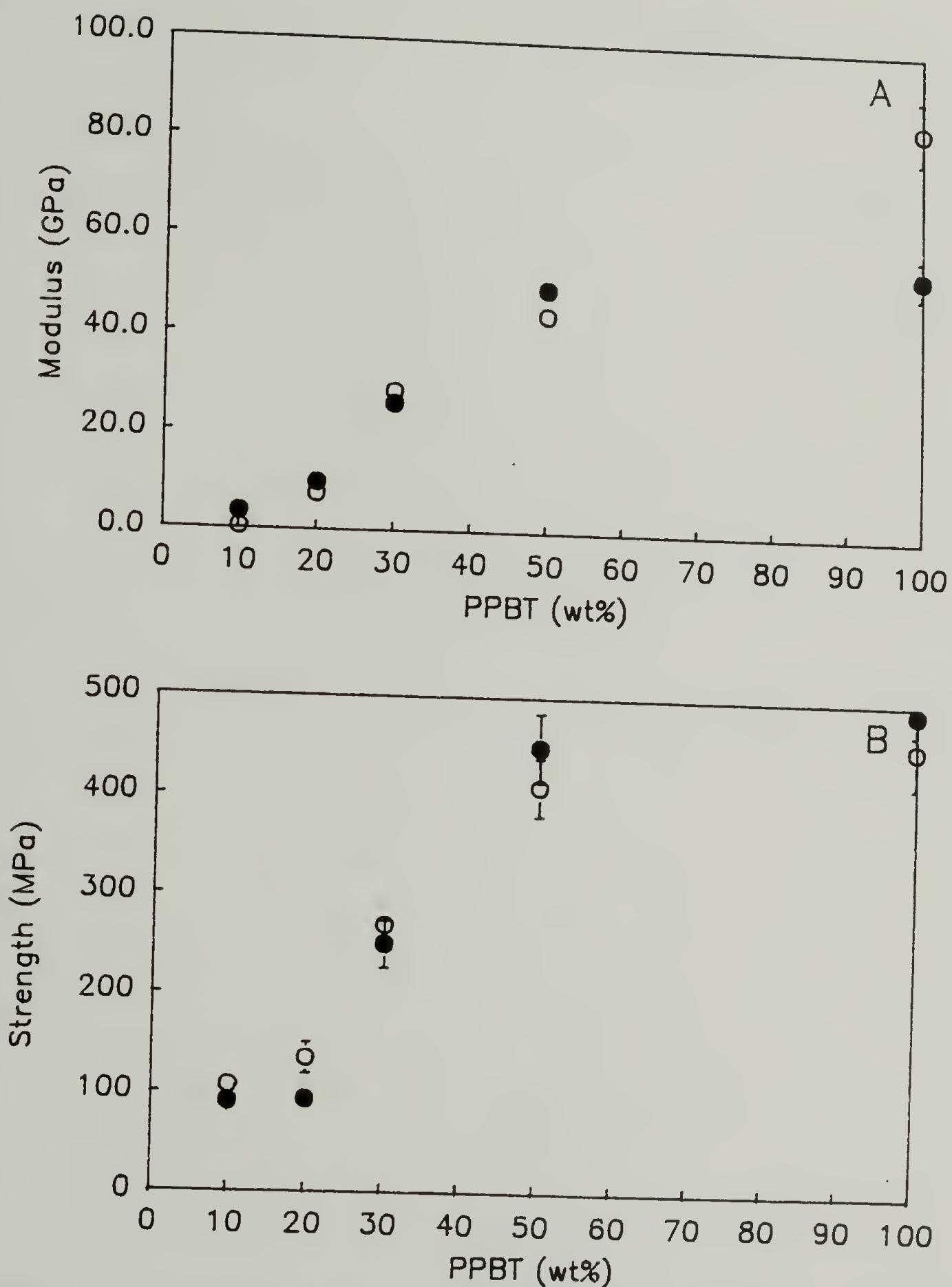


Figure 4.11 Tensile properties for heat-treated PEEK/PPBT30 (○) and N66/PPBT30 (●) fibers vs. the wt% for PPBT, a) modulus, b) strength. Error bars represent the standard deviation from the average calculated from at least five samples, which appears only if greater than the symbol size.

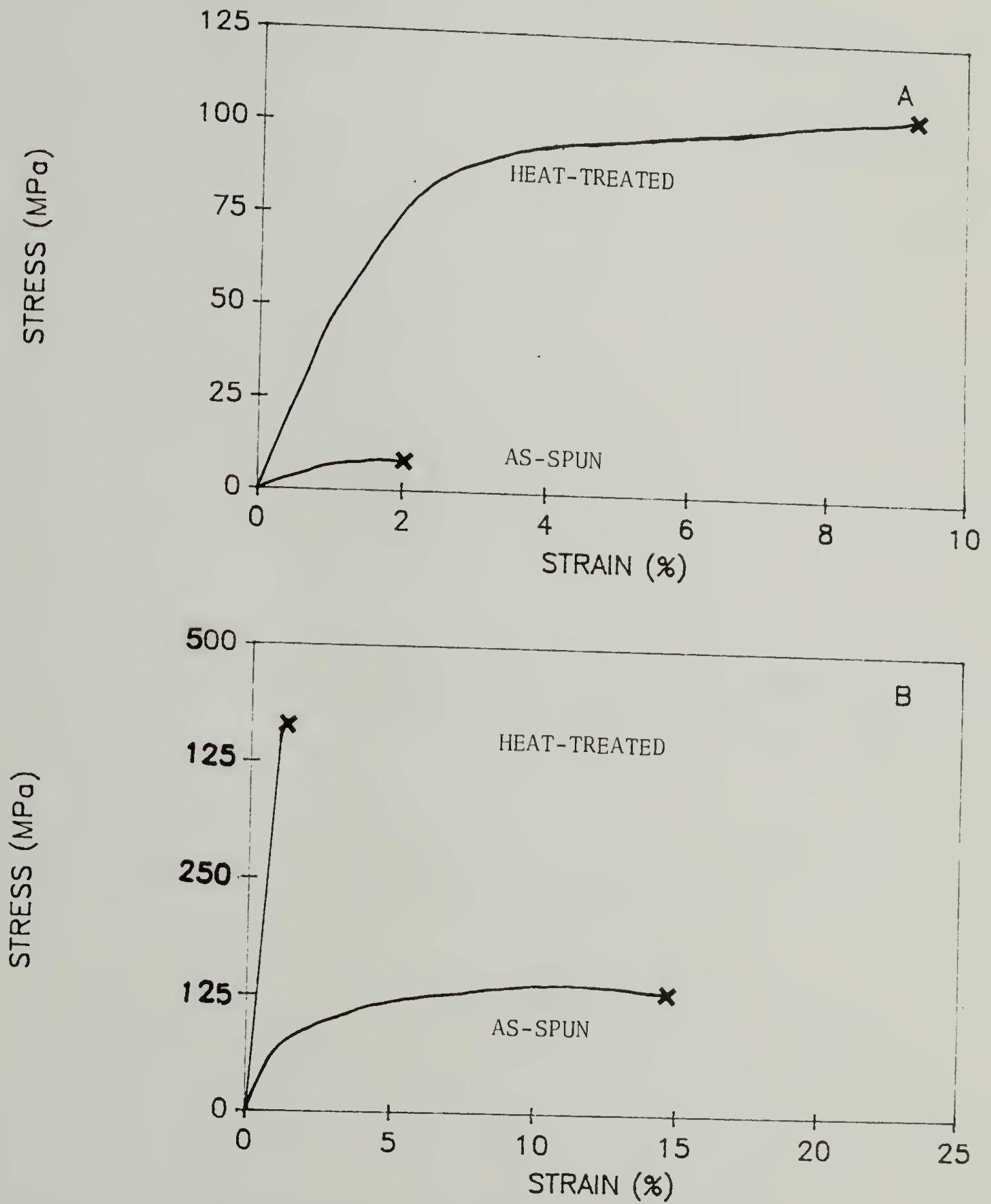


Figure 4.12 Typical stress-strain curve for as-spun and heat-treated (a) 90/10 and (b) 50/50 PEEK/PPBT fibers.

modified with post-processing, erasing differences seen in the as-spun fiber properties.

The tensile properties of conventional PEEK/chopped carbon fiber composites and N66/chopped glass fiber composites are listed in Table 4.3. The modulus and strength of the heat-treated N66/PPBT30 and PEEK/PPBT30 composite fibers of also included in Table 4.3. The composite fibers prepared are superior to the conventional chopped fiber composite materials. It should, however, be noted that the 70/30 is wt/wt ratio and the densities of carbon, glass, and PPBT are 1.8-2.1, 2.55, and 1.44 g/cm³, respectively.

4.9 Summary

In this chapter, the structure of the PPBT reinforcing the composite fibers was investigated. There is a hierarchy of structure in these types of composite materials. The resultant structure is controlled by the relative solubilities of the PPBT and the matrix, and the time required for coagulation versus the time required for phase separation.

A solution, which is composed of a molecular dispersion of a flexible coil matrix polymer and a rigid rod molecule may be coagulated to form a structure having a) the matrix (flexible coil polymer) as the continuous phase, b) a molecular dispersion of the rigid rod through out the flexible coil matrix, or c) a continuous phase of the rigid

Table 4.3

Tensile Properties of 70/30 PEEK/Graphite and N66/Glass
Chopped Fiber Composites

	<u>Modulus (GPa)</u>	<u>Strength (MPa)</u>
PEEK/Carbon Fiber (95)	13	190
N66/Glass Fiber (96)	9.7	172
PEEK/PPBT30	28	269
N66/PPBT30	26	249

rod, reinforcing polymer. This concept is summarized in Figure 4.13.

If the time required for phase separation, t_{ps} , is less than the time required for the coagulation process, t_c , then the molecular composite solution will phase separate into an anisotropic solution during the coagulation process. Such a process results in a composite fiber having discrete domains of rigid rod within a continuous matrix phase. This structure is depicted in Figure 4.13a. This structure results when PEEK/PPBT fibers having less than 30 weight percent PPBT are spun from solutions close to the critical concentration. The fiber was found to have a continuous PEEK phase with discrete islands of PPBT.

The idealized molecular composite structure, depicted in Figure 4.13b, could result only if the time required for the solution to solidify is significantly less than the time required for phase separation and if the matrix and the rigid rod have similar solubilities. The ternary systems investigated (PEEK/PPBT/MSA and N66/PPBT/MSA) are not suitable for preparing a molecular composite.

If the solubility of the matrix in the solvent/ coagulant mixture is much greater than that of the rigid rod, then the rigid rod molecules are free to find one another during the solidification process, and form a continuous phase. This type of composite structure is illustrated

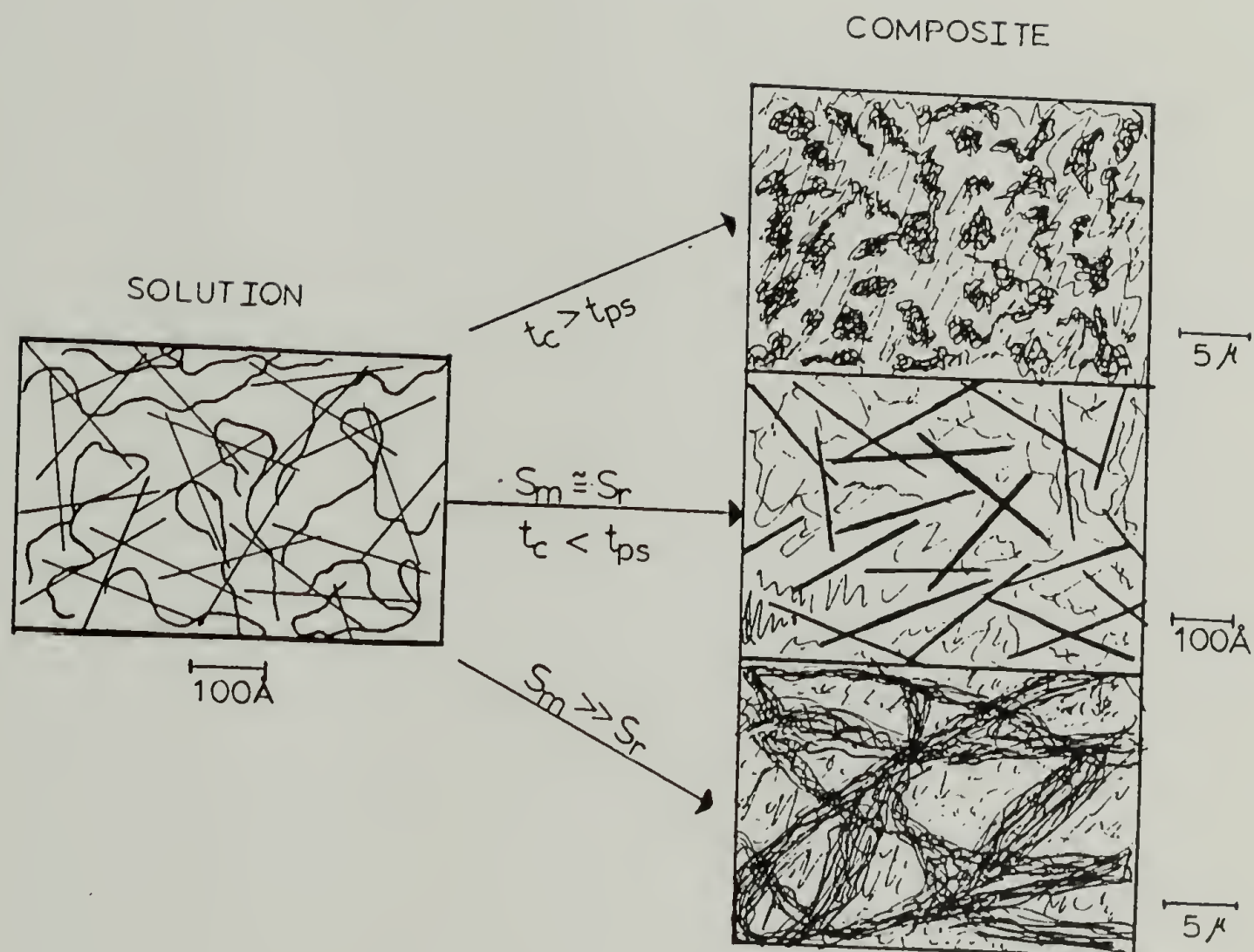


Figure 4.13 Dependence of composite morphology for ternary solution of flexible coil/rigid rod/solvent on the t_c , time for coagulation, t_{ps} , time for phase separation, S_m , solubility of the matrix, S_r , solubility of the rigid rod.

in Figure 4.13c. The solubility of N66 in MSA/water mixtures is much greater than that for PPBT.

Accordingly, N66/PPBT fibers were found to be reinforced with a continuous PPBT structure. PEEK/PPBT fibers processed well below the critical concentration or which had a PPBT content greater than 30 weight percent showed evidence of the continuous network-like PPBT structure.

The PPBT effectively reinforces the N66 and PEEK matrices in the form of a continuous network structure. Macrofibrils of PPBT were observed microscopically to be 2-7 μm in diameter as from optical micrographs. Post-processing techniques such as heat-treatment and wet-stretching are simply a means of perfecting the network structure, thereby enhancing the tensile properties of the composite fibers.

CHAPTER 5

CONCLUSIONS AND SUGGESTIONS FOR FUTURE WORK

In this dissertation, it was concluded that the relatively solubility of two polymers being spun from a common solvent is important to the morphology and tensile properties of the coagulated product. If the solubilities are largely different, the polymer with the lower solubility will coagulate first and have the freedom of motion to form its preferred structure, i.e., a continuous fibrillar network for PPBT. If the solubilities of the two polymers are similar then they will precipitate on the same time scale which may hinder the formation of the individual polymers preferred structure. In this case, solution concentration is an important processing variable.

Specifically it was concluded that the solution concentration and PPBT composition are important processing variables for the PEEK/PPBT/MSA system and not such important processing variables for the N66/PPBT/MSA system. This is a consequence of MSA being a much better solvent for N66 than for PEEK. It was shown that PPBT will form a network-like structure spanning the entire composite sample during the coagulation process if sufficient PPBT is

present, and the matrix material does not hinder PPBT's freedom motion. Such composite fibers reinforced with a continuous PPBT phase have been shown to have good tensile properties; a 50/50 PEEK/PPBT and 50/50 N66/PPBT fibers had moduli of 44.2 and 49.5 GPa and strengths of 410 and 450 MPa, respectively.

A composite fiber of PEEK/PPBT displays hysteresis in its strain-temperature behavior. Therefore, a dimensionally stable material results after annealing.

The phase behavior of PEEK/PPBT/MSA has been experimentally determined and can be fit to Flory's theory for rigid rod/flexible coil/solvent, if the aspect ratio for the flexible polymer is chosen to be much smaller than the actual value for PEEK. This is indicative of PEEK being a stiff molecule in solution. The N66/PPBT/MSA system solution behavior, however, is more closely predicted by Flory's theory, since N66 is a flexible molecule in solution.

Dynamic rheological data shows that 1.0, 2.0 and 3.0 75/25 N66/PPBT solutions have larger viscosities and longer relaxation times than corresponding PEEK/PPBT solutions. This may be a consequence of the well solvated N66 molecule hindering the mobility of PPBT molecule in solution.

The author suggests that if the preparation of a "molecular composite" is to be pursued, suggestions for the processing system can be inferred from this dissertation.

It is desirable that the solubility in the coagulant/solvent mixture of the matrix polymer be poor and equivalent to that of the rigid rod polymer. This would presumably allow the molecular dispersion present in solution to be "frozen-in" during the coagulation process. Also, the chemical structure of the rigid rod molecule and the flexible coil should be similar. This would aid in the blending of the two polymers being thermodynamically favorable.

In general, the author feels it would be of interest to investigate the rheological behavior of the ternary solutions. The rheological behavior (relaxation times and viscosities) of the solutions provide an understanding of the molecular interactions in solution, which dictates the morphology of the coagulated composite. The rheological behavior and the processing of a highly entangled matrix would be interesting, particularly if the viscosity of the solution allows it to be dry-jet wet spun. A matrix material that is amorphous would be interesting because the precipitation from solution for an amorphous polymer is less complex than that of a semi-crystalline polymer. An investigation of the coagulation of the composite in various coagulants may be useful as a means of adjusting the relative solubilities of the polymers.

REFERENCES

1. W. Worthy, "Wide Variety of Applications Spark Polymer Composites Growth," Chem. Engr. News, 65, (11), 7 (1987).
2. G.R. Belbin, "Thermoplastic Structural Composites - A Challenging Opportunity," Proc. Inst. Mech. Engr., 198B (6), 71 (1984).
3. R.B. Seymour, "Reinforced Plastics: Yesterday, Today and Tomorrow," Polym. News, 9, 9 (1983).
4. T.E. Helminiak, C.L. Benner, F.E. Arnold, G.E. Husman, "Aromatic Heterocyclic Polymer Alloys and Product Produced Therefrom," U.S. Patent Appl. SN 902,525 (1978) Patent No. 4,207,407 (1980).
5. G.E. Husman, T.E. Helminiak, W. Adams, D. Wiff, C. Benner, "Molecular Composites: Rodlike Polymer Reinforcing an Amorphous Polymer Matrix," ACS, Org. Coat. Plas. Prpts., 40, 797 (1979).
6. G.E. Husman, T.E. Helminiak, W. Adams, D. Wiff, C. Benner, "Molecular Composites: Rodlike Polymer Reinforcing an Amorphous Polymer Matrix," ACS, Symp. Ser., 132, 203 (1979).
7. M. Takayanagi, T. Ogata, M. Mirikawa, T. Kai, "Polymer Composites of Rigid and Flexible Molecules: System of Wholly Aromatic and Aliphatic Polyamides," J. Macromol. Sci. - Phys., B17 (4), 591 (1980).
8. W.B. Black, "High Modulus/High Strength Organic Fibers," Ann. Rev. Mater. Sci., 10, 311 (1980).
9. W.B. Black, "Stiff-Chain Aromatic Polymer Solutions, Melts, and Fibers," in Flow-Induced Crystallization, R.L. Miller, Ed., Gordon and Breach, New York (1979).
10. A. Zwijnenburg, A.J. Pennings, "Longitudinal Growth of Polymer Crystals from Flowing Solutions. IV. The Mechanical Properties of Fibrillar Polyethylene Crystals," J. Polym. Sci., Polym. Letters Ed., 14, 339 (1976).
11. N.E. Weeks, R.S. Porter, "Mechanical Properties of Ultra-Oriented Polyethylene," J. Polym. Sci., Polym. Phys. Ed., 12, 635 (1974).

12. G. Capaccio, I.M. Ward, "Properties of Ultra-High Modulus Linear Polyethylenes," Nature Phys. Sci., 243, 143 (1973).
13. J.B. Donnet, R.C. Bansal, "Carbon Fibers," International Fiber Science and Technology Series, Vol. 3, Marcel Dekker, Inc., NY, NY (1984).
14. S. L. Kwolek, "Optically Anisotropic Aromatic Polyamide Dopes," U.S. Patent 3671542 assigned to E.I. DuPont de Nemours & Co. (1972).
15. P.R. Langston, "Overview of Kevlar Composites: Properties and Uses," Kevlar Composites, SPE (1980)
16. T.E. Helminiak, "The Air Force Ordered Polymers Research Program: An Overview," ACS Org. Coat. and Plast. Prepts., 40, 475 (1979).
17. S.R. Allen, A.G. Fillippov, R.J. Farris, E.L. Thomas, "Structure-Property Relations in Poly(p-Phenylene Benzobisthiazole) Fibers," in The Strength and Stiffness of Polymers, A.E. Zachariades, R.S. Porter, Ed., Marcel Dekker, N.Y. (1983).
18. H.F. Kuhfus, W.J. Jackson, U.S. Patent 3,804,805, assigned to Eastman Kodak Co. (1974).
19. P.W. Morgan, U.S. Patent 4,048,148, assigned to E.I. DuPont de Nemours & Co. (1977).
20. G.W. Calundann and M. Jaffe, "Anisotropic Polymers, Their Synthesis and Properties," Proceedings of the Robert A. Welch Conferences on Chemical Research XXVI. Synthetic Polymers, 247 (1982).
21. H. Chanzy, A. Peguy, S. Chauis, P. Monzie, "Oriented Cellulose Films and Fibers from a Mesophase System", J. Polym. Sci., Phys., 18, 1137 (1980).
22. W.G. Miller, J.H. Rai, E.L. Wee, "Liquid Crystal-Isotropic Phase Equilibria in Stiff Chain Polymers", Liquid Crystals and Ordered Fluids, Vol. II, R. Porter, I. Johnson, Eds.; Plenum Press: New York, (1975).
23. J. Preston, 'Synthesis of Ultra-High Strength and High Modulus Fibers from Wholly Aromatic Polymers', pp. 155, Ultra High Modulus Polymers, A. Ciferri, I. M. Ward, Eds.; Applied Science Publishers: London (1979).

24. J.F. Wolfe, and F.E. Arnold, " Rigid-Rod Polymers. 2. Synthesis and Thermal Properties of Para-Aromatic Polymers with 2,6-Benzobisthiazole Units in the Main Chain", Macromolecules, 14, 915 (1981).
25. E.W. Choe, S.N. Kim, "Synthesis, Spinning, and Fiber Mechanical Properties of Poly(p-phenylene benzobisoxazole)", Macromolecules, 14, 920 (1981).
26. L. Onsager, "The Effects of Shapes on the Interaction of Colloidal Particles," Ann. N.Y. Acad. Sci., 51, 627 (1949).
27. Flory, P.J., "Phase Equilibria in Solutions of Rod-like Particles", Proc. Roy. Soc. London Ser A, 234, 73 (1956).
28. A. Yu Groşber, A.R. Khokhlov, "Statistical Theory of Polymeric Liquid Crystals", Adv. Polym. Sci., 41, 53 (1981).
29. T. Odijk, "Theory of Lyotropic Polymer Liquid Crystals," Macromolecules, 19, 2313 (1986).
30. H.H. Tsai, Phase Equilibrium and Rheological Studies of Solutions of Rodlike Articulated Polymers and Their Mixtures, Ph.D. Thesis, Carnegie-Mellon University (1983)
31. S.G. Chu, S. Venkatraman, G.C. Berry, Y. Einaga, "Rheological Properties of Rodlike Polymers in Solution, 1. Linear and Nonlinear Steady State Behavior," Macromolecules, 14, 939, (1981).
32. S. Venkatraman, G.C. Berry, Y. Einaga, "Rheological Properties of Rodlike Polymers in Solution, 2. Linear and Nonlinear Transient Behavior," J. Polym. Sci., Polym. Phys. Ed., 23, 1275 (1985).
33. Y. Einaga, G.C. Berry, S.G. Chu, "Rheological Properties of Rodlike Polymers in Solution, 3. Transient and Steady State Studies on Nematic Solutions," Polym. J., 17, 239 (1985).
34. H.H. Frost, Microstructure and Phase Behavior of Poly(p-phenylene benzobisthiazole)/Methane-sulfonic Acid Crystal Solvates, M.S. Thesis, Polymer Science and Engineering Department, University of Massachusetts, (1984).

- 35a. P.J. Flory, A. Abe, "Statistical Thermodynamics of Mixtures of Rodlike Particles. 1. Theory for Polydisperse Systems", Macromolecules, 11, 1119 (1978).
- 35b. P.J. Flory, A. Abe, "Statistical Thermodynamics of Mixtures of Rodlike Particles. 2. Ternary System", Macromolecules, 11, 1122 (1978).
- 35c. P.J. Flory, R.S. Frost, "Statistical Thermodynamics of Mixtures of Rodlike Particles. 3. The Most Probable Distribution", Macromolecules, 11, 1126 (1978).
- 35d. P.J. Flory, R.S. Frost, "Statistical Thermodynamics of Mixtures of Rodlike Particles. 4. The Poisson Distribution", Macromolecules, 11, 1134 (1978).
- 35e. P.J. Flory, "Statistical Thermodynamics of Mixtures of Rodlike Particles. 5. Mixtures with Random Coils", Macromolecules, 11, 1138 (1978).
- 35f. P.J. Flory, "Statistical Thermodynamics of Mixtures of Rodlike Particles. 6. Rods Connected by Flexible Joints", Macromolecules, 11, 1141 (1978).
36. E. Bianchi, A. Ciferri, "Liquid Crystal Solutions. Ternary Systems Involving a Nematogenic and a Nonnematogenic Polymer", Macromolecules, 15, 1268 (1982).
37. W. F. Hwang, D.R. Wiff, C. Verschoore, "Phase Relationships of Rigid Rod Polymer/Flexible Coil Polymer/Solvent Ternary Systems", Polym. Engr. and Sci., 23 (14) 789 (1983).
38. S. M. Aharoni, "Rigid Backbone Polymers: 6. Ternary Phase Relationships of Polyisocyanates", Polymer, 21, 21 (1981).
39. H. Ishida, J.L. Koenig, Ed., Composite Interfaces, Elsevier, N.Y., N.Y. (1986).
40. W.F. Hwang, D.R. Wiff, T.E. Helminiak, G. Price, W.W. Adams, "Solution Processing and Properties of Molecular Composite Fibers and Films," Polym. Eng. and Sci., 23 (14) 784 (1983).
41. J.R. Wolfe, B.H. Loo, F.E. Arnold, "Thermally Stable Rodlike Polymers: Synthesis of an All-Para Poly(benzobisthiazole)," Polym. Prept. 19, (2) 1 (1978).

42. C.R. Crosby, W.C. Ford, F.E. Karasz, K.H. Langley, "Depolarized Light Scattering of a Rigid Macromolecule Poly(p-phenylene benzobisthiazole)," J. Chem. Phys., 75, 4298 (1981).
43. W.F. Hwang, D.R. Wiff, C.L. Benner, T.E. Helminiak, "Composites on a Molecular Level: Phase Relationships, Processing and Properties," J. Macro. Sci., B22, (2) 231 (1983)
44. W.F. Hwang, D.R. Wiff, "Molecular Composites of Rigid Rod Poly-p-phenylenebenzobisthiazole (PPBT) in Thermoplastic Matrices", Org. Coat. and Plas. Chem. Preps., 48, 929, (1982).
45. S.J. Krause, T. Haddock, G.E. Price, P.G. Lenhert, J.F. O'Brien, T.E. Helminiak, W.W. Adams, "Morphology of a Phase-Separated and a Molecular Composite PBT/ABPBI Polymer Blend," J. Polym. Sci., B24, 1991 (1986).
46. T. Nishihara, H. Mera, K. Matsuda, "Molecular Composite of Poly(p-phenylenebenzobisthiazole) and Aromatic Copolyamide," ACS, PMSE Proc., 55, 821 (1986).
47. J. Halpin, Primer on Composite Materials: Analysis, (Revised), Technomic Publishing Co., Inc., Lancaster, PA (1984).
48. J.C. Halpin, J.L. Kardos, "The Halpin-Tsai Equations: A Review," Polym. Engr. Sci., 16, 344 (1976).
49. J.L. Kardos, J. Raison, "The Potential Mechanical Response of Macromolecular Systems--A Composite Analogy," Polym. Engr. Sci., 15, 185 (1975).
50. S. Wickliffe, "Processing and Properties of Poly(p-phenylene Benzobisthiazole)/Nylon Fiber", Masters Thesis, Chem. Engr. Dept., Univ. of Mass. (1985) Also; AFWAL-TR-86-4126(1986) and Submitted to J. Appl. Polym. Sci. with M.F. Malone, R.J. Farris (1986).
51. M. Takayanagi, "Molecular Composites," Proc. of 28th IUPAC Microsymp. Macrom., Polymer Composites, Ed. B. Sedláček, Walter de Gruyter & Co., NY, NY (1985).
52. H.H. Chuah, T.Kyu, T.E. Helminiak, "The Kinetics of Phase Separation of PBT/Nylon 66 Molecular Composite," PMSE Preps., 56, 58 (1987).

53. G. Kiss, "In Situ Composites: Blends of Isotropic Polymers and Thermotropic Liquid Crystalline Polymers," Polym. Engr. Sci., 27, 410 (1987).
54. A. Siegmann, A. Dagan, S. Kenig, "Polyblends Containing a Liquid Crystalline Polymer," Polymer, 26, (1985).
55. A. Apicella, P. Iannelli, L. Nicodemo, L. Nicolais, A. Roviello, A. Sirigu, "Dimensional Stability of Polystyrene/Polymeric Liquid Crystal Blends," Polym. Engr. Sci., 26, 600 (1986).
56. S.R. Allen, A.G. Fillippov, R. J. Farris, E.L. Thomas, "Microstructure and Mechanical Behavior of Fibers of Poly (p-phenylene benzobisthiazole)," J. Appl. Polym. Sci., 26, 291 (1981)
57. J.R. Minter, K. Shimamura, E.L. Thomas, "Microstructural Study of As-Extruded and Heat Treated Ribbons of Poly (p-phenylene benzobisthiazole)," J. Matl. Sci., 16, 3303, (1981).
58. G.C. Berry, P.C. Metzger, S. Venkatraman, D.B. Cotts, "Properties of Rodlike Polymers in Solution", Polymer Preprints, 20 (1), 42 (1979).
59. G.C. Berry, E.F. Casassa, P. Metzger, S. Venkatraman, "Physical - Chemical Properties of Complex Aromatic Heterocyclic Polymers," AFML-TR-78-164 (1979).
60. O.B. Searle, R.H. Pfeiffer, "Vitrex^R Poly(ether sulfone) (PES) and Vitrex^R Poly(etheretherketone) (PEEK)" Polym. Engr. and Sci., 25 (8) 404 (1985).
61. D.J. Blundell, B.N. Osborn, "The Morphology of Poly(aryl-ether-ether-ketone)," Polymer, 24, 953 (1983).
62. R. Rigby, Adv. Polym. Tech., 2, 163 (1983).
63. D.P. Jones, D.C. Leach, D.R. Moore, "Mechanical Properties of Poly(ether-ether-ketone) for Engineering Applications," Polymer, 26, 1385 (1985).
64. R.B. Rigby, "Polyetheretherketone PEEK," Polymer News, 9, 325 (1984).
65. T.E. Attwood, P.C. Dawson, J.L. Freeman, L.R.J. Hoy, J.B. Rose, P.A. Staniland, "Synthesis and Properties of Polyarylketones", Polymer, 22, 1096 (1981).
66. Private communication with P.A. Staniland.

67. M.T. Bishop, F.E. Karasz, P.S. Russo, "Solubility and Properties of a Poly(aryl ether ketone) in Strong Acids", Macromolecules, 18, 86 (1985).
68. N.T. Wakelyn, "On the Structure of Poly(ether etherketone) (PEEK)" Polymer Comm., 25, 306, Oct (1984)
69. A. Tager, Physical Chemistry of Polymers, translated by D. Sobolev, N. Bobrov, Mir Publishers, Moscow (1978).
70. P.R. Saunders, J. Polym. Sci., Part A, 2, 3765 (1964).
71. M.E. Epstein, A.J. Rosenthal, "Spinning of Polyamides from Sulfuric Acid Solutions", Textile Research Journal, 813, (1966).
72. W.W. Graessley, S.F. Edwards, "Entanglement Interactions in Polymers and the Chain Contour Concentration," Polymer, 22, 1329 (1981).
73. P.C. Dawson, D.J. Blundell, "X-ray Data for Poly(aryl ether ketones)," Polymer Letts., 21, 577 (1980)
74. C.W. Bunn, E.V. Garner, "The Crystal Structures of Two Polyamides ('Nylons')," Proc. Roy. Soc., A189, 39 (1949).
75. F.W. Billmeyer, Jr., Textbook of Polymer Science, 2nd Ed., John Wiley and Sons, New York, (1971).
76. D.R. Wiff, S. Timms, T.E. Helminiak, W.F. Hwang, "Molecular Entanglement for Rigid Rod Molecular Composites: Poly(p-Phenylene-2,6-Benzobisthiazole)/Poly(Hexamethylene Adipamide)," Polym. Engr. Sci., 27, 424 (1987).
77. J.D. Ferry, Viscoelastic Properties of Polymers, John Wiley & Sons, Inc. (1961).
78. G.C. Berry, R. Furukawa, S. Mohan, C. Wei, C. Kim, "Physical-Chemical Properties of Articulated Rodlike Polymers," AFWAL-TR-86-4035 (1986).
79. S.R. Allen, "Mechanical and Morphological Correlations in Poly(p-phenylenebenzobisthiazole) Fibers," Ph.D. Dissertation, Polymer Science and Engineering Dept., Univ. Of Mass. (1985)

80. S.R. Allen, R.J. Farris, E.L. Thomas, "High Modulus/High Strength Poly(p-phenylene benzobisthiazole) Fibers Part 1. Heat Treatment Processing," J. Matl. Sci., 20, 2727 (1985).
81. J.A. Duiser, J.A. Copper, "Matrix/Fibril Fibers from Cellulose Acetate and Acrylonitrile Copolymer," Fibre Sci. Tech., 6, 119 (1973).
82. M.Takayanagi, T. Ogata, M. Mirikawa, T. Kai, "Polymer Composites of Rigid and Flexible Molecules: System of Wholly Aromatic and Aliphatic Polyamides," J. Macromol. Sci. - Phys., B17 (4), 591 (1980).
83. A. Ziabicki, Fundamentals of Fiber Formation: The Science of Fibre Spinning and Drawing, Wiley, London;NY (1976) .
84. T.A. Hancock, J.E. Spruiell, J.L. White, "Wet Spinning of Aliphatic and Aromatic Polyamides," J. Appl. Polym. Sci., 21, 1227 (1977).
85. J.P. Craig, J.P. Knudsen, V.F. Holland, "Characterization of Acrylic Fiber Structure," J.Text. Res., 32, 435 (1962).
86. K.Tohyama, W.G. Miller, "Network Structure in Gels of Rodlike Polypeptides," Nature, 289, 813 (1981).
87. L.A. Pottick, R.J. Farris, "Alterations in the Structure and Mechanics of Poly(p-phenylene benzobisthiazole) Fibers Due to the Collapse Process During Drying," TAPPI Nonwovens Symposium Proceedings, 65 (1985)
88. Y. Cohen, E.L. Thomas, "Structure Formation During Spinning of Poly(p-phenylenebenzobisthiazole) Fiber", Polym. Engr. Sci., 25, 1093 (1985)
89. Y. Cohen, "Structure Formation in Solutions of Rigid Polymers Undergoing a Phase Transition," AFWAL-TR-87-4030 (1987)
90. O. Nehme', C. Gabriel, M.F.Malone, R.J. Farris, E.L. Thomas, "Microfibrillar Morphology of Nylon 6,6/ PPBT Composite Fibers," to be published
91. D.E. Davenport, "Metalloplastics - The Art of Infinite Chains," Paper Presented at the 55th Annual Meeting of the Society of Rheology (1983)

92. S.Z.D. Cheng, M.Y. Cao, B. Wunderlich, "Glass Transition and Melting Behavior of Poly(oxy-1,4-phenyleneoxy 1,4-phenylenecarbonyl-1,4-phenylene)," Macromolecules, 19, 1868 (1986)
93. O. Yoda, "The Radiation Effect on Non-Crystalline Poly(aryl-ether-ketone) as Revealed by X-ray Diffraction and Thermal Analysis," Polym. Comm., 25, 238 (1984).
94. L.A. Pottick, S.R. Allen, R.J. Farris, " Force-Temperature Behavior of Rigid Rod Polymeric Fibers," J. Appl. Polym. Sci., 29, 3915 (1984)
95. R.B. Rigby, "High Temperature Thermoplastic Matrices for Advanced Composites," 27th SAMPE Symp., 747 (1982).
96. J.G. Mohr, S.S. Oleesky, G.D. Shook, L.S. Meyer, SPI Handbook of Technology and Engineering of Reinforced Plastics/Composites, 2nd Ed., Van Nostrand Reinhold Co., NY, (1973).

APPENDIX A

The persistence length (equal to twice the length of the Kuhn segment, L) of Nylon 6,6 was estimated from (r_0^2/M) . A good basis for this discussion is provided by Tager(69). The unperturbed end to end distance, r_0 is related to the length of a Kuhn segment, L , and the number of Kuhn segments, N , by

$$r_0^2 = NL^2 \quad (A.1)$$

The number of Kuhn segments, N , is related to the number of repeat units, n , in a polymer chain, by

$$N = n/S \quad (A.2)$$

where S is the number of repeat units per Kuhn segment, which is equal to

$$S = L/l \quad (A.3)$$

The parameters n and S may be written in terms of the molecular weight of the repeat unit, M_r , the molecular weight of the chain, M , and the molecular weight of the Kuhn segment, M_s ,

$$n = M/M_r \quad (A.4)$$

$$S = M_s/M_r \quad (A.5)$$

Combining equations 2-5, results in

$$r_o^2 = (MLL)/M_r \quad (A.6)$$

Then the Kuhn length L is related to (r_o^2/M) by

$$L = (M_r/l) (r_o^2/M) \quad (A.7)$$

This relation was used to determine L for N66, $M_r = 226$ g/mole, $(r_o^2/M)^{1/2} = 0.96 \text{ \AA}/\text{mole}^{1/2}\text{g}^{-1/2}$, and $l = 17.2 \text{ \AA}$ from crystal dimensions, giving $L = 12.1 \text{ \AA}$ equal to twice the persistence length.

APPENDIX B

Tensile Properties for As-Spun PEEK/PPBT36, $C \leq C_{cr}$

<u>PPBT (% Wt)</u>	<u>E (GPa)</u>	<u>σ (MPa)</u>	<u>ϵ (%)</u>
0	0.169 +0.005 -0.005	3.4 +0.2 -0.2	14.2 +7.6 -7.6
5	0.119 +0.003 -0.003	2.9 +0.8 -0.8	43.6 +2.5 -2.5
10	0.074 +0.007 -0.007	2.0 +0.06 -0.06	30.7 +3.7 -3.7
15	0.076 +0.005 -0.005	1.7 +0.1 -0.1	17.9 +5.8 -5.8
20	0.058 +0.004 -0.004	1.0 +0.036 -0.036	8.9 +2.1 -2.1
30	0.110 +0.005 -0.005	1.6 +0.2 -0.2	4.2 +0.9 -0.9

Tensile Properties for Hot-Drawn (265°C) PEEK/PPBT36, $C \leq C_{cr}$

<u>PPBT (% Wt)</u>	<u>E (GPa)</u>	<u>σ (MPa)</u>	<u>ϵ (%)</u>
0	1.24 +0.06 -0.06	30.3 +3.8 -3.8	4.6 +1.7 -1.7
5	1.06 +0.09 -0.09	22.9 +2.1 -2.1	6.1 +1.2 -1.2
10	1.01 +0.05 -0.05	21.0 +0.7 -0.7	4.2 +0.7 -0.7
15	0.91 +0.03 -0.03	15.3 +0.9 -0.9	2.5 +0.3 -0.3
20	0.64 +0.03 -0.03	8.7 +0.4 -0.4	1.9 +0.2 -0.2
25	0.51 +0.03 -0.03	6.7 +0.8 -0.8	1.6 +0.3 -0.3

Tensile Properties for As-Spun 75/25 PEEK/PPBT30

<u>Total Polym. Conc. (wt%)</u>	<u>D (μm)</u>	<u>E (GPa)</u>	<u>σ (MPa)</u>	<u>ϵ (%)</u>
1.0	40.7 +1.8 —	3.7 +0.4 —	35 +8 —	1.6 +1.0 —
2.0	63.4 ± 0.9	5.9 ± 0.3	72 ± 2	5.0 ± 1.8
2.5	70.7 +0.8 —	4.7 ± 0.2	53 ± 3	2.2 ± 0.7
3.0	137.8 +7.3 —	1.1 ± 0.1	14 ± 2	1.8 ± 0.4
4.0	250 +12 —	0.23 ± 0.04	1.8 ± 0.2	1.3 ± 0.4

Tensile Properties for As-Spun 75/25 N66/PPBT30

<u>Total Polym. Conc. (wt%)</u>	<u>D (μm)</u>	<u>E (GPa)</u>	<u>σ (MPa)</u>	<u>ϵ (%)</u>
1.0	35 +1.5 —	2.4 +0.3 —	26 +5 —	1.2 ± 0.3
2.0	57 ± 5	5.1 ± 0.2	87 ± 4	14.6 ± 5.3
3.0	84 ± 1	4.9 ± 0.3	85 ± 4	9.3 ± 2.5
3.7	87 ± 1	5.1 ± 0.3	82 ± 2	1.9 ± 0.3
4.0 (> Ccr)	100 +7 —	2.8 ± 0.2	41 ± 4	2.6 ± 0.8

Tensile Properties for As-Spun PEEK/PPB30 Fibers

<u>Total Polym. Conc. (wt%)</u>	<u>E (GPa)</u>	<u>σ (MPa)</u>	<u>ϵ (%)</u>
50/50 PEEK/PPBT30			
1.0	6.7 ± 0.4	94 ± 5	6.8 ± 2.0
2.0	6.7 ± 0.3	123 ± 2	19.1 ± 3.2
2.5	6.7 ± 0.5	129 ± 5	19.5 ± 4.6
3.0	5.7 ± 0.3	131 ± 12	27.2 ± 5.9
25/75 PEEK/PPBT30			
1.0	11.4 $\pm .6$	214 ± 17	23.6 ± 6.1
2.0	8.9 ± 0.3	174 ± 5	19.9 ± 1.6
2.5	8.7 ± 0.7	162 ± 7	17.5 ± 3
3.0	5.5 ± 0.4	118 ± 5	25.1 ± 2.8

Tensile Properties for As-Spun PEEK/PPBT30 Fibers Spun From
2.0% Total Polymer Solution

<u>PPBT (wt%)</u>	<u>E (GPa)</u>	<u>σ (MPa)</u>	<u>ϵ (%)</u>
0	0.200 ± 0.014	2.3 ± 0.3	1.6 ± 0.1
5	0.49 ± 0.05	6.4 ± 1.0	1.9 ± 0.3
10	0.56 ± 0.03	7.5 ± 1.7	2.1 ± 1.1
20	2.08 ± 0.24	27.4 ± 3.4	2.8 ± 0.8
25	5.9 ± 0.3	72 ± 2	5.0 ± 1.8
50	8.33 ± 0.30	132.9 ± 5.4	17.0 ± 4.4
75	10.2 ± 0.53	198.6 ± 8.4	24.4 ± 2.9
100	14.0 ± 0.7	236 ± 12	33.3 ± 5.0

Tensile Properties for PEEK/PPBT30 Fibers Heat-Treated at 425°C with No Tension for 2.0 Minutes

<u>PPBT (wt%)</u>	<u>E (GPa)</u>	<u>σ (MPa)</u>	<u>ϵ (%)</u>
5	3.0 +0.5 —	59 +6 —	5.7 +3.1 —
10	5.2 +0.2 —	107 +6 —	9.3 +4.2 —
20	7.4 +0.6 —	135 +16.0 —	9.2 +3.0 —
25	9.9 +0.9 —	166 +13 —	7.6 +1.3 —
50	10.5 +0.5 —	222 +12 —	16.7 +0.3 —
75	13.4 +0.3 —	246 +10 —	8.5 +0.7 —

Tensile Properties for As-Spun PEEK/PPBT30 Fibers Spun from 2.0% Total Polymer Solution

<u>PPBT (wt%)</u>	<u>E (GPa)</u>	<u>σ (MPa)</u>	<u>ϵ (%)</u>
10	0.56 +0.03 —	7.5 +1.7 —	2.1 +1.1 —
20	2.1 +0.2 —	27 +3 —	2.8 +0.8 —
30	5.9 +0.2 —	87 +2 —	10.7 +0.7 —
50	7.2 +0.3 —	121 +10 —	14.8 +3.2 —
100	14.0 +0.7 —	236 +12 —	33.3 +5.0 —

Tensile Properties for Wet-Stretched PEEK/PPBT30 Fibers Spun from 2.0% Total Polymer Solution

<u>PPBT (wt%)</u>	<u>E (GPa)</u>	<u>σ (MPa)</u>	<u>ϵ (%)</u>
Draw Ratio = 1.2			
30	6.85 +0.40 —	89.5 +6.2 —	4.7 +2.4 —
Draw Ratio = 1.3			
50	11.7 +1.4 —	182 +9 —	10.2 +4.5 —
Draw Ratio = 1.4			
100	23.3 +1.6 —	-- -- --	-- -- --

Tensile Properties for PEEK/PPBT30 Fibers Spun from 2.0% Total Polymer Solution Heat-Treated at 425°C; 2 Min. Res.

<u>PPBT (wt%)</u>	<u>E (GPa)</u>	<u>σ (MPa)</u>	<u>ϵ (%)</u>
No Tension During Heat-Treatment of As-Spun Fiber			
10	5.2 +0.2 —	107 +5 —	9.3 +4.2 —
20	7.4 +.6 —	135 +16 —	9.2 +3.0 —
17 MPa Tension During Heat-Treatment of Wet-Stretched Fiber			
30	28.3 +1.4 —	269 +10 —	1.6 +0.3 —
38 MPa Tension During Heat-Treatment of Wet-Stretched Fiber			
50	44.2 +1.8 —	410 +30 —	1.2 +0.2 —
40 MPa Tension During Heat-Treatment of Wet-Stretched Fiber			
100	84.3 +6.5 —	455 +38 —	1.1 +0.7 —

Tensile Properties for As-Spun N66/PPBT30 Fibers Spun from
2.0% Total Polymer Solution

<u>PPBT (wt%)</u>	<u>E (GPa)</u>	<u>σ (MPa)</u>	<u>ϵ (%)</u>
10	2.9 ± 0.3	35 ± 6	1.6 ± 0.5
20	3.5 ± 0.1	56 ± 5	2.3 ± 0.4
30	6.1 ± 0.1	99 ± 4	13.5 ± 1.9
50	7.7 ± 0.7	173 ± 8	38 ± 5
100	14.0 ± 0.7	236 ± 12	33.3 ± 5.0

Tensile Properties for Wet-Stretched N66/PPBT30 Fibers Spun
from 2.0% Total Polymer Solution

<u>PPBT (wt%)</u>	<u>E (GPa)</u>	<u>σ (MPa)</u>	<u>ϵ (%)</u>
Draw Ratio = 1.6 30	7.7 ± 0.9	139 ± 9	19.4 ± 1.5
Draw Ratio = 1.3 50	11.9 ± 1.1	212 ± 20	18.5 ± 5.8
Draw Ratio = 1.4 100	23.3 ± 1.6	--	--

Tensile Properties for N66/PPBT30 Fibers Spun from 2.0%
Total Polymer Solution Heat-Treated at 305°C; 2 Min. Res.

<u>PPBT (wt%)</u>	<u>E (GPa)</u>	<u>σ (MPa)</u>	<u>ϵ (%)</u>
No Tension During Heat-Treatment of As-Spun Fiber			
10	3.6 ± 0.3	90 ± 7	40 ± 14
20	9.6 ± 0.4	93 ± 3	14.4 ± 3.0
27 MPa Tension During Heat-Treatment of Wet-Stretched Fiber			
30	25.8 ± 1.9	250 ± 24	3.3 ± 2
42 MPa Tension During Heat-Treatment of Wet-Stretched Fiber			
50	47.0 ± 0.8	450 ± 35	1.0 ± 0.1
40 MPa Tension During Heat-Treatment of Wet-Stretched Fiber			
100	54.0 ± 4.1	492 ± 21	1.3 ± 0.5

Force to Break for N66/PPBT30 Fibers Spun From 2.0% Solution

<u>PPBT (wt%)</u>	<u>Wet Fiber(g)</u>	<u>Dry Fiber(g)</u>	<u>Ratio Wet to Dry</u>
10	0.6 +0.08 —	15.5 +1.6 —	26
20	3.2 +0.4 —	21.8 +2.2 —	6.8
30	6.6 +1.0 —	31.6 +2.9 —	4.8
50	15.9 +1.1 —	59.2 +1.5 —	3.7
100	41.8 +4.6 —	68.7 +7.8 —	1.6

Force to Break for PEEK/PPBT30 Fibers Spun From 2.0% Solution

<u>PPBT (wt%)</u>	<u>Wet Fiber(g)</u>	<u>Dry Fiber(g)</u>	<u>Ratio Wet to Dry</u>
5	1.5 +0.2 —	4.5 +0.6 —	3
10	1.6 +0.1 —	7.5 +0.7 —	4.7
20	2.3 +0.2 —	18.7 +0.9 —	8.1
30	8.5 +0.9 —	30.5 +2.9 —	3.6
50	18.7 +2.0 —	39.9 +1.9 —	2.1
100	41.8 +4.6 —	68.7 +7.8 —	1.6

BIBLIOGRAPHY

- Aharoni S.M., "Rigid Backbone Polymers: 6. Ternary Phase Relationships of Polyisocyanates", Polymer, 21, 21 (1981).
- Allen S.R., Filippov A.G., Farris R.J., Thomas E.L., "Structure-Property Relations in Poly(p-Phenylene Benzobisthiazole) Fibers," in The Strength and Stiffness of Polymers, A.E. Zachariades, R.S. Porter, Ed., Marcel Dekker, N.Y. (1983).
- Allen S.R., Fillippov A.G., Farris R.J., Thomas E.L., "Microstructure and Mechanical Behavior of Fibers of Poly (p-phenylene benzobisthiazole)," J. Appl. Polym. Sci., 26, 291 (1981)
- Allen S.R., Farris R.J., Thomas E.L., "High Modulus/High Strength Poly(p-phenylene benzobisthiazole) Fibers Part 1. Heat Treatment Processing," J. Matl. Sci., 20, 2727 (1985).
- Allen S.R., "Mechanical and Morphological Correlations in Poly(p-phenylenebenzobisthiazole) Fibers," Ph.D. Dissertation, Polymer Science and Engineering Dept., Univ. Of Mass. (1985)
- Apicella A., Iannelli P., Nicodemo L., Nicolais L., Roviello A., Sirigu A., "Dimensional Stability of Polystyrene/Polymeric Liquid Crystal Blends," Polym. Engr. Sci., 26, 600 (1986).
- Attwood T.E., Dawson P.C., Freeman J.L., Hoy L.R.J., Rose J.B., Staniland P.A., "Synthesis and Properties of Polyarylktones", Polymer, 22, 1096 (1981).
- Belbin G.R., "Thermoplastic Structural Composites - A Challenging Opportunity," Proc. Inst. Mech. Engr., 198B (6), 71 (1984).
- Berry G.C., Casassa E.F., Metzger P., Venkatraman S., "Physical - Chemical Properties of Complex Aromatic Heterocyclic Polymers," AFML-TR-78-164 (1979).
- Berry G.C., Metzger P.C., Venkatraman S., Cotts D.B., "Properties of Rodlike Polymers in Solution", Polymer Preprints, 20 (1), 42 (1979).

- Berry G.C., Furukawa R., Mohan S., Wei C., Kim C., "Physical-Chemical Properties of Articulated Rodlike Polymers," AFWAL-TR-86-4035 (1986).
- Bianchi E., Ciferri A., "Liquid Crystal Solutions. Ternary Systems Involving a Nematogenic and a Nonnematogenic Polymer", Macromolecules, 15, 1268 (1982).
- Billmeyer F.W.Jr., Textbook of Polymer Science, 2nd Ed., John Wiley and Sons, New York, (1971).
- Bird R.B., Armstrong R.C., Hassager O., Dynamics of Polymeric Fluids, Vol. 1, John Wiley & Sons, NY (1977).
- Bishop M.T., Karasz F.E., Russo P.S., "Solubility and Properties of a Poly(aryl ether ketone) in Strong Acids", Macromolecules, 18, 86 (1985).
- Black W.B., "High Modulus/High Strength Organic Fibers," Ann. Rev. Mater. Sci., 10, 311 (1980).
- Black W.B., "Stiff-Chain Aromatic Polymer Solutions, Melts, and Fibers," in Flow-Induced Crystallization, R.L. Miller, Ed., Gordon and Breach, New York (1979).
- Blundell D.J., Osborn B.N., "The Morphology of Poly(aryl-ether-ether-ketone)," Polymer, 24, 953 (1983).
- Bunn C.W., Garner E.V., "The Crystal Structures of Two Polyamides ('Nylons')," Proc. Roy. Soc., A189, 39 (1949).
- Calundann G.W., Jaffe M., "Anisotropic Polymers, Their Synthesis and Properties," Proceedings of the Robert A. Welch Conferences on Chemical Research XXVI. Synthetic Polymers, 247 (1982).
- Capaccio G., Ward I.M., "Properties of Ultra-High Modulus Linear Polyethylenes," Nature Phys. Sci., 243, 143 (1973).
- Chanzy H., Peguy A., Chauis S., Monzie P., "Oriented Cellulose Films and Fibers from a Mesophase System", J. Polym. Sci., Phys., 18, 1137 (1980).
- Cheng S.Z.D., Cao M.Y., Wunderlich B., "Glass Transition and Melting Behavior of Poly(oxy-1,4-phenyleneoxy 1,4-phenylenecarbonyl-1,4-phenylene)," Macromolecules, 19, 1868 (1986)

- Choe E.W., Kim S.N., "Synthesis, Spinning, and Fiber Mechanical Properties of Poly(p-phenylene benzobisoxazole)", Macromolecules, 14, 920 (1981).
- Chu S.G., Venkatraman S., Berry G.C., Einaga Y., "Rheological Properties of Rodlike Polymers in Solution, 1. Linear and Nonlinear Steady State Behavior," Macromolecules, 14, 939, (1981).
- Chuah H.H., Kyu T., Helminiak T.E., "The Kinetics of Phase Separation of PBT/Nylon 66 Molecular Composite," PMSE Preps., 56, 58 (1987).
- Cohen Y., "Structure Formation in Solutions of Rigid Polymers Undergoing a Phase Transition," AFWAL-TR-87-4030 (1987)
- Cohen Y., Thomas E.L., "Structure Formation During Spinning of Poly(p-phenylenebenzobisthiazole) Fiber", Polym. Engr. Sci., 25, 1093 (1985)
- Craig J.P., Knudsen J.P., Holland V.F., "Characterization of Acrylic Fiber Structure," J.Text. Res., 32, 435 (1962).
- Crosby C.R., Ford W.C., Karasz F.E., Langley K.H., "Depolarized Light Scattering of a Rigid Macromolecule Poly(p-phenylene benzobisthiazole)," J. Chem. Phys., 75, 4298 (1981).
- Davenport D.E., "Metalloplastics - The Art of Infinite Chains," Paper Presented at the 55th Annual Meeting of the Society of Rheology (1983)
- Dawson P.C., Blundell D.J., "X-ray Data for Poly(aryl ether ketones)," Polymer Letts., 21, 577 (1980)
- Donnet J.B., Bansal R.C., "Carbon Fibers," International Fiber Science and Technology Series, Vol. 3, Marcel Dekker, Inc., NY, NY (1984).
- Duiser J.A., Copper J.A., "Matrix/Fibril Fibers from Cellulose Acetate and Acrylonitrile Copolymer," Fibre Sci. Tech., 6, 119 (1973).
- Einaga Y., Berry G.C., Chu S.G., "Rheological Properties of Rodlike Polymers in Solution, 3. Transient and Steady State Studies on Nematic Solutions," Polym. J., 17, 239 (1985).

- Epstein M.E., Rosenthal A.J., "Spinning of Polyamides from Sulfuric Acid Solutions ", Textile Research Journal, 813, (1966).
- Ferry J.D., Viscoelastic Properties of Polymers, John Wiley & Sons, Inc. (1961).
- Flory P.J., "Phase Equilibria in Solutions of Rod-like Particles", Proc. Roy. Soc. London Ser A, 234, 73 (1956).
- Flory P.J., "Statistical Thermodynamics of Mixtures of Rodlike Particles. 5. Mixtures with Random Coils", Macromolecules, 11, 1138 (1978).
- Flory P.J., "Statistical Thermodynamics of Mixtures of Rodlike Particles. 6. Rods Connected by Flexible Joints", Macromolecules, 11, 1141 (1978).
- Flory P.J., Abe A., "Statistical Thermodynamics of Mixtures of Rodlike Particles. 1. Theory for Polydisperse Systems", Macromolecules, 11, 1119 (1978).
- Flory P.J., Abe A., "Statistical Thermodynamics of Mixtures of Rodlike Particles. 2. Ternary System", Macromolecules, 11, 1122 (1978).
- Flory P.J., Frost R.S., "Statistical Thermodynamics of Mixtures of Rodlike Particles. 3. The Most Probable Distribution", Macromolecules, 11, 1126 (1978).
- Flory P.J., Frost R.S., "Statistical Thermodynamics of Mixtures of Rodlike Particles. 4. The Poisson Distribution", Macromolecules, 11, 1134 (1978).
- Frost H.H., Microstructure and Phase Behavior of Poly(p-phenylene benzobisthiazole)/Methane-sulfonic Acid Crystal Solvates, M.S. Thesis, Polymer Science and Engineering Department, University of Massachusetts, (1984).
- Graessley W.W., Edwards S.F., "Entanglement Interactions in Polymers and the Chain Contour Concentration," Polymer, 22, 1329 (1981).
- Halpin J.C., Kardos J.L., "The Halpin-Tsai Equations: A Review," Polym. Engr. Sci., 16, 344 (1976).
- Halpin J., Primer on Composite Materials: Analysis, (Revised), Technomic Publishing Co., Inc., Lancaster, PA (1984).

- Hancock T.A., Spruiell J.E., White J.L., "Wet Spinning of Aliphatic and Aromatic Polyamides," J. Appl. Polym. Sci., 21, 1227 (1977).
- Helminiak T.E., "The Air Force Ordered Polymers Research Program: An Overview," ACS Org. Coat. and Plast. Prepts., 40, 475 (1979).
- Helminiak T.E., Benner C.L., Arnold F.E., Husman G.E., "Aromatic Heterocyclic Polymer Alloys and Product Produced Therefrom," U.S. Patent Appl. SN 902,525 (1978) Patent No. 4,207,407 (1980).
- Helminiak T.E., Wellman M., Hwang W.F., Wiff D.R., Rodgers V., Benner C., "Critical Processing Conditions of a Specific Ternary System - Molecular Composites," AFWAL-TR-80-4163 (1980).
- Husman G.E., Helminiak T.E., Adams W., Wiff D., Benner C., "Molecular Composites: Rodlike Polymer Reinforcing an Amorphous Polymer Matrix," ACS, Org. Coat. Plas. Prpts., 40, 797 (1979).
- Husman G.E., Helminiak T.E., Adams W., Wiff D., Benner C., "Molecular Composites: Rodlike Polymer Reinforcing an Amorphous Polymer Matrix," ACS, Symp. Ser., 132, 203 (1979).
- Hwang W.F., Wiff D.R., "Molecular Composites of Rigid Rod Poly-p-phenylenebenzobisthiazole (PPBT) in Thermoplastic Matrices," Org. Coat. and Plas. Chem. Preps., 48, 929, (1982).
- Hwang W.F., Wiff D.R., Verschoore C., "Phase Relationships of Rigid Rod Polymer/Flexible Coil Polymer/Solvent Ternary Systems," Polym. Engr. and Sci., 23 (14) 789 (1983).
- Hwang W.F., Wiff D.R., Benner C.L., Helminiak T.E., "Composites on a Molecular Level: Phase Relationships, Processing and Properties," J. Macro. Sci., B22, (2) 231 (1983).
- Hwang W.F., Wiff D.R., Helminiak T.E., Price G., Adams W.W., "Solution Processing and Properties of Molecular Composite Fibers and Films," Polym. Eng. and Sci., 23 (14) 784 (1983).

- Hwang W.F., Benner C.L., Wiff D.R., Helminiak T.E.,
"Molecular Composite: Phase Relationship, Processing
and Properties," Proceeding, IUPAC MACRO 82, 827
(1982).
- Hwang W.F., Wiff D.R., Price G.E., Helminiak T.E.,
Adams W.W., "Solution Processing and Properties of
Molecular Composite Fibers and Films from Rigid Rod-
like/Flexible Coil-like Polymer Blends in Methane
Sulfonic Acid," SPE: Polymer Alloys, Blends and
Composites, National Technical Conference Proceedings
(1982).
- Hwang W.F., Helminiak T.E., Wiff D.R., Benner C., Price G.,
"Molecular Level Composite of PBT/ABPBI: Phase
Relationship, Properties and Processing," AFWAL-TR-82-
4039 (1982).
- Ishida H., Koenig J.L., Ed., Composite Interfaces, Elsevier,
N.Y., N.Y. (1986).
- Jones D.P., Leach D.C., Moore D.R., "Mechanical Properties
of Poly(ether-ether-ketone) for Engineering
Applications," Polymer, 26, 1385 (1985).
- Kardos J.L., Raison J., "The Potential Mechanical Response
of Macromolecular Systems--A Composite Analogy," Polym.
Engr. Sci., 15, 185 (1975).
- Kiss G., "In Situ Composites: Blends of Isotropic Polymers
and Thermotropic Liquid Crystalline Polymers,"
Polym. Engr. Sci., 27, 410 (1987).
- Krause S.J., Haddock T., Price G.E., Lenhert P.G.,
O'Brien J.F., Helminiak T.E., Adams W.W., "Morphology
of a Phase-Separated and a Molecular Composite
PBT/ABPBI Polymer Blend," J. Polym. Sci., B24, 1991
(1986).
- Kuhfus H.F., Jackson W.J., U.S. Patent 3,804,805, assigned
to Eastman Kodak Co. (1974).
- Kwolek S.L., "Optically Anisotropic Aromatic Polyamide
Dopes," U.S. Patent 3671542 assigned to E.I. DuPont de
Nemours & Co. (1972).
- Langston P.R., "Overview of Kevlar Composites: Properties
and Uses," Kevlar Composites, SPE (1980)

- Miller W.G., Rai J.H., Wee E.L., "Liquid Crystal-Isotropic Phase Equilibria in Stiff Chain Polymers", Liquid Crystals and Ordered Fluids, Vol. II, R. Porter, I. Johnson, Eds.; Plenum Press: New York, (1975).
- Minter J.R., Shimamura K., Thomas E.L., "Microstructural Study of As-Extruded and Heat Treated Ribbons of Poly (p-phenylene benzobisthiazole)," J. Matl. Sci., 16, 3303, (1981).
- Mohr J.G., Oleesky S.S., Shook G.D., Meyer L.S., SPI Handbook of Technology and Engineering of Reinforced Plastics/Composites, 2nd Ed., Van Nostrand Reinhold Co., NY, (1973).
- Morgan P.W., U.S. Patent 4,048,148, assigned to E.I. DuPont de Nemours & Co. (1977).
- Nehme' O.A., Gabriel C.A., Farris R.J., Thomas E.L., Malone M.F., "Microstructural Investigations of PBT/N66 Composites," submitted to J. Appl. Polym. Sci., June 1987.
- Nishihara T., Mera H., Matsuda K., "Molecular Composite of Poly(p-phenylenebenzobisthiazole) and Aromatic Copolyamide," ACS, PMSE Proc., 55, 821 (1986).
- Odiijk T., "Theory of Lyotropic Polymer Liquid Crystals," Macromolecules, 19, 2313 (1986).
- Onsager L., "The Effects of Shapes on the Interaction of Colloidal Particles," Ann. N.Y. Acad. Sci., 51, 627 (1949).
- Pottick L.A., Farris R.J., "Alterations in the Structure and Mechanics of Poly(p-phenylene benzobisthiazole) Fibers Due to the Collapse Process During Drying," TAPPI Nonwovens Symposium Proceedings, 65 (1985)
- Pottick L.A., Allen S.R., Farris R.J., " Force-Temperature Behavior of Rigid Rod Polymeric Fibers," J. Appl. Polym. Sci., 29, 3915 (1984)
- Preston J., 'Synthesis of Ultra-High Strength and High Modulus Fibers from Wholly Aromatic Polymers', pp. 155, Ultra High Modulus Polymers, A. Ciferri, I. M. Ward, Eds.; Applied Science Publishers: London (1979).
- Rigby R.B., "High Temperature Thermoplastic Matrices for Advanced Composites," 27th SAMPE Symp., 747 (1982).

- Rigby R.B., "Polyetheretherketone PEEK," Polymer News, 9, 325 (1984).
- Saunders P.R., "The Unperturbed Dimensions of Nylon 66," J. Polym. Sci., Part A, 2, 3765 (1964).
- Searle O.B., Pfeiffer R.H., "Vitrex^R Poly(ether sulfone) (PES) and Vitrex^R Poly(etheretherketone) (PEEK)" Polym. Engr. and Sci., 25 (8) 404 (1985).
- Seymour R.B., "Reinforced Plastics: Yesterday, Today and Tomorrow," Polym. News, 9, 9 (1983).
- Siegmann A., Dagan A., Kenig S., "Polyblends Containing a Liquid Crystalline Polymer," Polymer, 26, 1325 (1985).
- Stober E.J., Seferis J.C., Keenan J.D., "Characterization and Exposure of Polyetheretherketone(PEEK) to Fluid Environments," Polymer, 25, 1849 (1984).
- Tager A., Physical Chemistry of Polymers, translated by D. Sobolev, N. Bobrov, Mir Publishers, Moscow (1978).
- Takayanagi M., "Molecular Composites," Proc. of 28th IUPAC Microsymp. Macrom., Polymer Composites, Ed. B.Sedl cek, Walter de Gruyter & Co., NY, NY (1985).
- Takayanagi M., Ogata T., Mirikawa M., Kai T., "Polymer Composites of Rigid and Flexible Molecules: System of Wholly Aromatic and Aliphatic Polyamides," J. Macromol. Sci. - Phys., B17 (4), 591 (1980).
- Takayanagi M., Ogata T., Mirikawa M., Kai T., "Polymer Composites of Rigid and Flexible Molecules: System of Wholly Aromatic and Aliphatic Polyamides," J. Macromol. Sci. - Phys., B17 (4), 591 (1980).
- Tohyama K., Miller W.G., "Network Structure in Gels of Rodlike Polypeptides," Nature, 289, 813 (1981).
- Tsai H.H., Phase Equilibrium and Rheological Studies of Solutions of Rodlike Articulated Polymers and Their Mixtures, Ph.D. Thesis, Carnegie-Mellon University (1983)
- Venkatraman S., Berry G.C., Einaga Y., "Rheological Properties of Rodlike Polymers in Solution, 2. Linear and Nonlinear Transient Behavior," J. Polym. Sci., Polym. Phys. Ed., 23, 1275 (1985).

- Wakelyn N.T., "On the Structure of Poly(ether etherketone) (PEEK)" Polymer Comm., 25, 306, Oct (1984)
- Weeks N.E., Porter R.S., "Mechanical Properties of Ultra-Oriented Polyethylene," J. Polym. Sci., Polym. Phys. Ed., 12, 635 (1974).
- Wickliffe S., "Processing and Properties of Poly(p-phenylene Benzobisthiazole)/Nylon Fiber", Masters Thesis, Chem. Engr. Dept., Univ. of Mass. (1985) Also; AFWAL-TR-86-4126(1986) and Submitted to J. Appl. Polym. Sci. with M.F. Malone, R.J. Farris (1986).
- Wiff D.R., Timms S., Helminiak T.E., Hwang W.F., "Molecular Entanglement for Rigid Rod Molecular Composites: Poly(p-Phenylene-2,6-Benzobisthiazole)/Poly(Hexamethylene Adipamide)," Polym. Engr. Sci., 27, 424 (1987).
- Wolfe J.F., Arnold F.E., "Rigid-Rod Polymers. 2. Synthesis and Thermal Properties of Para-Aromatic Polymers with 2,6-Benzobisthiazole Units in the Main Chain", Macromolecules, 14, 915 (1981).
- Wolfe J.R., Loo B.H., Arnold F.E., "Thermally Stable Rodlike Polymers: Synthesis of an All-Para Poly(benzobisthiazole)," Polym. Prept. 19, (2) 1 (1978).
- Worthy W., "Wide Variety of Applications Spark Polymer Composites Growth," Chem. Engr. News, 65, (11), 7 (1987).
- Yoda O., "The Radiation Effect on Non-Crystalline Poly(aryl-ether-ketone) as Revealed by X-ray Diffraction and Thermal Analysis," Polym. Comm., 25, 238 (1984).
- Yu Grosber A., Khokhlov A.R., "Statistical Theory of Polymeric Liquid Crystals", Adv. Polym. Sci., 41, 53 (1981).
- Ziabicki A., Fundamentals of Fiber Formation: The Science of Fibre Spinning and Drawing, Wiley, London;NY (1976).
- Zwijnenburg A., Pennings A.J., "Longitudinal Growth of Polymer Crystals from Flowing Solutions. IV. The Mechanical Properties of Fibrillar Polyethylene Crystals," J. Polym. Sci., Polym. Letters Ed., 14, 339 (1976).

